

Philipps



Universität
Marburg

An experimental approach to probe conformational changes in protein structure using a biotin derivative followed by mass spectrometry

Dissertation
zur Erlangung des Doktorgrades
der Naturwissenschaften
(Dr. rer. nat.)

dem Fachbereich Biologie
der Philipps-Universität Marburg
vorgelegt von

Omid Azimzadeh
aus Teheran

Marburg/ Lahn 2008

The following paper was published by the date of the present thesis:

Azim-Zadeh O, Hillebrecht A, Linne U, Marahiel MA, Klebe G, Lingelbach K, Nyalwidhe J. (2007). Use of biotin derivatives to probe conformational changes in proteins. *J Biol Chem.* 282(30):21609-17.

For my wife Maryam

I Table of Contents

II List of Figures	4
III List of Tables	6
IV List of Abbreviations	7
1. Introduction	8
1.1. Erythrocyte membrane structure	8
1.1.1. Membrane lipids	8
1.1.2. Membrane proteins	8
1.1.3. Erythrocyte surface proteins	10
1.1.4. Membrane transporters and channels	10
1. 2. The membrane of the <i>P. falciparum</i> infected erythrocytes	11
1.2.1. The malaria parasite <i>Plasmodium falciparum</i>	11
1.2.1.1. Parasite Life Cycle	11
1.2.1.2. Alteration of the host plasma membrane	12
1.2.1.3. Novel Permeation Pathways (NPPs)	15
1.3. Biotinylation of proteins	19
1.4. Mass spectrometry	21
1.5. Study of conformational changes in model protein	24
1.5.1. The structure and properties of bovine serum albumin (BSA)	24
1.5.2. The structure and properties of Carbonic anhydrase II (CA II)	28
1.6. The structure and properties of Band III protein (Anion Exchanger 1, AE1)	31
1.7. Objectives	37
2. Materials and Methods	38
2.1. Materials	38
2.1.1. Equipments	38
2.1.2. Disposable Materials	39
2.1.3. Chemicals and reagents	39

I Table of Contents

2.1.4. Solutions and buffers	41
2.1.5. Host cells and parasite isolates	44
2.1.6. Antibodies and working concentrations	44
2.1.7. Software	44
2.2. Methods	45
2.2.1. Parasite Cultures	45
2.2.2. Biotin labelling of bovine serum albumin and carbonic anhydrase II	45
2.2.3. Biotinylation of erythrocyte membrane protein Band III	46
2.2.4. Affinity purification of biotinylated peptides	46
2.2.5. Gel Electrophoresis (Laemmli, 1970)	47
2.2.6. Western Blot Analysis (Towbin et al., 1979)	47
2.2.7. Sample preparation for mass spectrometry	47
2.2.8. Mass spectrometry analysis and protein identification	49
3. Results	51
3.1. Biotinylation pattern of BSA is saturable	51
3.2. Biotinylated lysine residues in BSA are uniformly distributed in the protein	54
3.3. Not all lysine residues of BSA can be detected by mass spectrometry	55
3.4. The modified lysine residues are identified by MS and MS/MS analysis	58
3.5. Biotinylated peptides can be effectively affinity purified using streptavidin sepharose beads	60
3.5.1. Affinity purification of intact biotinylated BSA	61
3.5.2. Affinity purification of biotinylated BSA peptides	62
3.6. Biotinylated lysine residues are resistant to trypsin cleavage	64
3.7. Elevated temperatures expose novel lysine residues in the biotinylation pattern of BSA	65
3.8. Reduction has no effect on the biotinylation pattern of BSA	70
3.9. The biotinylation reaction does not induce structural changes in the biotinylated protein, as detected by circular dichroism	71
3.10. Involvement of lysine residues in hydrogen bonding may decrease their capacity to be biotinylated	74

I Table of Contents

3.11. Analysis of biotinylated and non-biotinylated CA II by MS	78
3.12. Band III is biotinylated in infected and non-infected erythrocytes	81
3.13. MS analysis identifies Band III	84
3.14. The peaks found in non-biotinylated samples are falsely identified by database searches as corresponding to a biotinylated peptide	88
3.15. Biotinylated Band III peptides were rarely detected	91
3.16. Biotinylation does not affect the ionization efficiency of peptides	97
4. Discussion	99
4.1. Biotinylated lysine residues can be detected by MS and MS/MS analysis	100
4.2. The biotinylation of protein is reproducible but incomplete	100
4.3. The conformational changes are reflected in the biotinylation pattern	103
4.4. The biotinylated lysine residues are resistant to trypsin cleavage	104
4.5. Involvement of lysine residues in H bonding may prevent the biotinylation	104
4.6. Only few biotinylated lysine residues in Band III structure are detected	105
4.7. The biotinylation pattern of Band III is different in RBC and IRBC	107
4.8. Future directions and implications of this study	109
5. Literture	111
V Summary	125
VI Zusammenfassung	126
Acknowledgements	127
Declaration	128
Appendix	129

II List of Figures

Figure 1. The erythrocyte membrane organization_____	9
Figure 2. Parasite induced alterations in infected erythrocytes_____	15
Figure 3. The sulfo-NHS-LC biotin derivative reacts with primary amines forming an amide bond_____	21
Figure 4. The comparison of primary structure of HAS and BSA_____	26
Figure 5. The secondary structure of bovine CA II_____	29
Figure 6. Proposed topology model for Band III protein with 12-14 transmembrane domains_____	34
Figure 7. Biotinylation with sulfo-NHS-LC-Biotin increases the mass of peptides by a specific value_____	51
Figure 8. Analysis of the mass of BSA after biotinylation using increasing concentrations of sulfo-NHS-LC-Biotin_____	52
Figure 9. Effect of the increase in the concentration of sulfo-NHS-LC-biotin on the biotinylation and mass of BSA_____	53
Figure 10. Comparison of the detected sequence coverage in biotinylated and non-biotinylated BSA_____	56
Figure 11. Comparison of biotinylated and non-biotinylated BSA_____	59
Figure 12. MS/MS spectra of peptide 1329.694 which was detected in the biotinylated BSA_____	60
Figure 13. Schematic representation of the experimental methodology for the affinity purification of biotinylated intact BSA or biotinylated BSA peptides using streptavidin beads_____	61
Figure 14. Comparison of bound and unbound fraction of biotinylated BSA_____	62
Figure 15. Comparison of generated peptides from starting, bound and unbound fractions of biotinylated BSA_____	63
Figure 16. Comparison of the biotinylation pattern of BSA after exposure to different temperatures_____	66

II List of Figures

Figure 17. Sections of the MALDI mass spectra for BSA biotinylated at RT and after exposure to an elevated temperature of 80°C	67
Figure 18. MS/MS analysis of peptide 1979.09 that is only biotinylated after exposure to a temperature of 80°C	68
Figure 19. MS/MS analysis of peptide 2810.253	69
Figure 20. Far-UV CD spectra for different samples of BSA	73
Figure 21. Position of biotinylated lysine residues in the primary structure of BSA	75
Figure 22. Analysis of the mass of biotinylated CA II after exposure to different temperature	78
Figure 23. Comparison of biotinylated and non-biotinylated CA II	80
Figure 24. Analysis of biotinylation of membrane protein from infected (IRBC) and non-infected erythrocytes (RBC) with elevated concentration of biotin derivative	83
Figure 25. MS analysis of biotinylated and non-biotinylated RBC	85
Figure 26. Comparisons of the detected peptides in biotinylated and non-biotinylated Band III	87
Figure 27. Zoom of section of MS spectra of biotinylated and non-biotinylated RBC including peak with m/z 1934	89
Figure 28. MS/MS analysis of peaks with m/z 1877.34 and 1934.24 from non-biotinylated RBC	90
Figure 29. The distribution of lysine residues in the Band III sequence	91
Figure 30. Zoom of sections MS spectra for Band III from infected erythrocytes and non-infected erythrocytes	94
Figure 31. MS/MS analysis of peptide 1612.81 that is found only in the biotinylated Band III in RBC	95
Figure 32. MS/MS analysis of peptide 1028.54 that is found in the biotinylated Band III in RBC and IRBC	96
Figure 33. Biotinylation of synthetic Band III peptide using sulfo-NHS-LC-biotin	97
Figure 34. Structure of cross-linkers was Bis (sulfosuccinimidyl) substrate	101
Figure 35. Biotinylation pattern of the highly flexible domain of the Band III molecule	107

III List of Tabela

Table 1. The differences in the physical properties of BSA and CA II_____	31
Table 2. Effect of the increase in the molar ratio of sulfo-NHS-LC-biotin to BSA on the mass of BSA_____	53
Table 3. Biotinylation of individual lysine residues follows a concentration dependent specific order_____	55
Table 4. List of detected lysine residues in biotinylated and non-biotinylated BSA_____	57
Table 5. Biotinylated lysine residues are resistant to trypsin_____	65
Table 6. List of biotinylated lysine residues in all five different experiments of labelling BSA under different conditions_____	71
Table 7. Positions of biotinylated lysine residues in the BSA structure_____	76
Table 8. Analysis of all lysines of BSA for surface accessibility and H bonding_____	77
Table 9. Effect of temperature on the biotinylation pattern of CA II_____	79
Table 10. Analysis of all lysines of CA II for surface accessibility and H bonding_____	81
Table 11. Listing of identified lysine residues of Band III in non-infected erythrocytes (RBC) and infected erythrocytes (IRBC) after biotinylation_____	92
Table 12. The comparison of identified labelled lysine residues in current study and Huang <i>et al.</i> , (2004) study_____	102

IV List of Abbreviations

AE1	Anion Exchanger 1
AP	Alkaline phosphotase
ATP	Adenosine triphopshate
Da	Dalton
ECL	Enhanced Chemiluminescence
<i>et al.</i>	Together with
HRP	Horse Raddish Peroxidase
IRBC	Infected Red Blood Cell
kDa	Kilodalton
MALDI	Matrix assisted laser desorption ionization
Min	minute
μg	microgram
μl	microliter
MS	Massenspectrometry
Mw	Molecular weight
NC-Membran	Nitrocellulose-Membrane
Nm	Nanometer
NPPs	Novel Permeation Pathways
PMF	Peptide Mass Fingerprinting
ppm	parts per million
RBC	Red Blood Cell
Rpm	Revolutions per minute
RT	Room temperature
SAV	Streptavidin
SDS-PAGE	SDS-polyacrylamide gel electrophoresis
SNT	Supernatant
Tab.	Table
TOF	Time of flight
TM	Transmembrane
v/v	volume/volume
w/v	weight/volume

1. Introduction

1.1. Erythrocyte membrane structure

The main function of human erythrocytes is the transport of oxygen from the lungs to the tissues. The efficiency of this function depends on different factors specially the activity and the structure of membrane erythrocytes. The erythrocyte membrane contains approximately equal molar amounts of lipids and proteins. The composition and organization of the human erythrocyte membrane shown in figure 1, is briefly described in the following sections (Tse and Lux, 1999; De Rosa *et al.*, 2007; Daniels, 2007).

1.1.1. Membrane lipids

Membrane lipids include phospholipids, glycolipids and cholesterol, which are arranged as a bilayer. The glycolipids and choline phospholipids are mostly oriented towards the outer surface of membrane while amino-phospholipids are more concentrated on the cytoplasmic surface. Cholesterol is found between the phospholipid molecules. The relative amounts of cholesterol and phospholipids are responsible for the fluid properties of the erythrocyte membrane (Deuticke, 1982).

1.1. 2. Membrane proteins

Erythrocyte membrane proteins are divided into two classes of integral and peripheral proteins depending on their relation to the lipid bilayer.

The peripheral proteins which are, termed membrane cytoskeleton, are located below the cytoplasmic surface of lipid bilayer and play an important role to stabilize of bilayer integrity and control the cell shape of erythrocytes. The most prominent component of the erythrocyte cytoskeleton is spectrin. Two isoforms of spectrin, alpha (260 kDa) and beta (225 kDa) have been identified. These two form a loosely wound helix which form a tetramer. The spectrin tetramers are organized into a meshwork that is fixed to the

1. Introduction

membrane by the protein ankyrin (Branton *et al.*, 1981). Ankyrin (215 kDa) binds to spectrin in the membrane skeleton and a site on the cytoplasmic domain of Band III (Davis and Bennett, 1990).

Glycophorin A is the major contact or receptor membrane polypeptide that also spans the lipid bilayer (Anderson and Lovrien, 1984; Chasis *et al.*, 1985). It is suggested that the blood group determinants and possibly other biological receptor sites have been localized on the extracellular portion of glycophorin A. The other glycophorins (B and C) are present in smaller amounts on the erythrocyte membrane and are suggested to be associated with the membrane skeleton (Mueller and Morrison, 1981).

Protein 4.1 has been shown to associate with cytoplasmic domains of glycophorin A (Anderson and Lovrien, 1984; Anderson and Marchesi, 1985), the Band III (Pasternack *et al.*, 1985), and phosphatidylserine in the lipid bilayer (Cohen *et al.*, 1988).

Integral proteins contain a quite high number of membrane transporters and channels, the major species being the anion exchange protein, Band III. All of the integral proteins share a typical structure with 6 to 13 transmembrane domains, with both termini inside the cytosol and with an N-glycan on one of the external loops. Most other major membrane transporters are apparently essential for maintaining a stable erythrocyte cell shape and flexibility via a functional membrane cytoskeleton (Van Dort *et al.*, 2002).

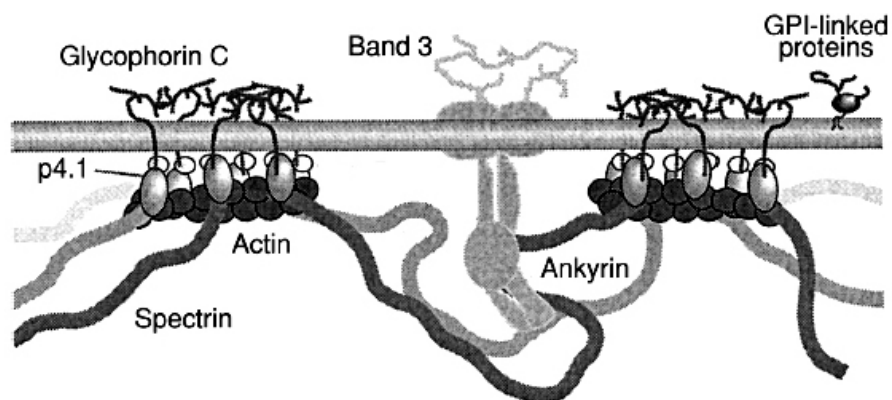


Figure 1. The erythrocyte membrane organization. The integral membrane proteins like Band III and glycophorin are connected to the spectrin skeleton network via the bridging proteins, ankyrin, and protein 4.1. (Modified from De Roza *et al.*, 2007).

1.1.3. Erythrocyte surface proteins

The external membrane of the human erythrocytes contains the proteins which either cross the lipid bilayer or are anchored to it through a lipid tail. These proteins are divided into different categories based on their functions: membrane transporters; adhesion molecules and receptors; enzymes; blood groups and structural proteins which link the membrane with the membrane skeleton (Viitala and Järnefelt, 1985; Daniels, 2007).

1.1.4. Membrane transporters and channels

Membrane transport proteins are integral proteins which facilitate the transfer of ions and molecules across the biological membranes. These proteins play key roles in cell life including the uptake of nutrients and removal of metabolic waste products as well as maintenance of electrochemical gradients (Deuticke, 2003).

The membrane transport proteins are divided into two major classes: transporters and channels. Transporter proteins, also referred to as carrier proteins, bind to the specific solute and undergo a series of conformational changes in order to transfer the bound solute across the membrane. In contrast, protein channels do not bind the solute; they provide the pores across the lipid bilayer which allow the specific solute pass through the membrane. All channels and most of the transporters facilitate the transport of solutes passively based on the concentration or electrical gradient, while active transport which is always mediated by transporters needs a source of metabolic energy like ATP hydrolysis.

Different types of membrane transporters have been identified on the erythrocyte membrane including the $\text{Cl}^-/\text{HCO}_3^-$ exchanger (Band III ; AE1), water and glycerol channels(Aquaporin 1 and 2); the Na^+ and Ca^{2+} pump, the Na^+ (K^+)/ H^+ exchanger, the $\text{Na}^+\text{K}^+\text{2Cl}^-$ and KCl co-transporter, choline, monocarboxylate, glucose, different amino acid and nucleoside carriers (Ginsburg and Kirk, 1998; Kirk , 2001; Bernhardt and Ellory, 2003). All membrane transporters detected in mature erythrocytes are synthesized early in erythrocyte differentiation, as the mature erythrocyte lacks the necessary machinery for protein synthesis.

1. 2. The membrane of the *P. falciparum* infected erythrocytes

The erythrocytic stage of the life cycle of the malaria parasite is responsible for the most important clinical symptoms and pathology of acute and severe malaria disease. As the infected red blood cells ruptures and releases parasites, the patient typically develops a shaking chill followed by a high fever, the classical signs of the uncomplicated malaria which is directly associated with the intracellular development of the parasite in erythrocytes (Miller *et al.*, 2002; Weatherall *et al.*, 2002). Because of the high metabolic activity of the parasite during the intra-erythrocytic stage of the life cycle, the parasite carries out various alterations and conformational changes relating to the uptake of nutrients or survival in the host cell.

1. 2.1. The malaria parasite *Plasmodium falciparum*

P. falciparum is the causative agent of the most lethal form of human malaria which is estimated to be responsible for more than 300 million cases of clinical disease and more than 1 million deaths per year (Carter and Mendis, 2002; Snow *et al.*, 2005). About 80% of malaria deaths are in sub-sahara Africa and among children under five years and pregnant women (WHO, 2005). In addition, malaria endemic countries have lower rates of economic growth (Sachs and Malaney, 2002, Malaney *et al.*, 2004).

1.2.1.1. Parasite Life Cycle

Plasmodium species have a complex life cycle that alternates between a vertebrate host and an insect vector. The parasites are injected into the bloodstream of the human host by the bite of an infected female *Anopheles* mosquito. The parasites rapidly disappear from the bloodstream and invade hepatocytes in the liver. During the next 10-15 days, the parasite matures, and differentiates within hepatocytes, and undergoes several rounds of asexual division which produce thousands of infective merozoites that are released into the bloodstream. These merozoites invade host red blood cells where they undergo a process of growth followed by shizogony (asexual division) to form 6–32

daughter merozoites over a period of 48–72 h depending on the species. When the daughter merozoites are fully mature (the schizont stage), the infected red blood cell (IRBC) ruptures and the cycle begins again with the invasion of erythrocytes. A small proportion of the intracellular parasites undergo differentiation into male and female gametocytes, which may then be taken up in a mosquito blood meal, where they are released from the erythrocytes and fuse to form a zygote. The zygote then develops into a motile form, called the ookinete; this penetrates the mosquito's gut wall and develops into an oocyst which undergoes sporogony and produces a large number of infective sporozoites in the salivary glands of the mosquito (Miller et al., 2002; Bannister and Mitchell, 2003).

1. 2.1. 2. Alteration of the host plasma membrane

During the intra-erythrocytic development, the parasite induces a number of alterations in the host cell including the rearrangement and modification of host membrane proteins and lipids, insertion of the parasite proteins into the cell membrane of erythrocytes, an increase in the rigidity of the cell, increased permeability and alterations in metabolite transport (Reviewed by: Craig and Scherf, 2001). These alterations enable parasites to survive within the erythrocytes; they facilitate the acquisition of nutrients by the parasites and the release of waste products to the surrounding environment. Some of the induced changes protect the parasite against the immune system of the host by adhesion, sequestration and antigenic variation (Deitsch and Wellems, 1996).

One of the most prominent ultra structural changes of the surface of infected erythrocytes is the electron-dense protrusions structures called knobs (Figure 2). It has been shown that knobs on the surface of infected erythrocytes act as attachment points of parasitized cells to the vascular endothelium (Aikawa, 1971 and 1996). During the first 24 h of the *P. falciparum* asexual cycle, infected erythrocytes are found in the peripheral circulation, but during the second 24 h, the parasitized cells adhere to the endothelial cells and can sequester in capillary and post-capillary venules of different organs (Turner *et al.*, 1998; Deitsch and Wellems, 1996). It has been reported that

1. Introduction

cytoadherence is a parasite response to the ability of the host spleen to destroy infected erythrocytes (Deitsch and Wellems, 1996). Cytoadherence has an important role in parasite survival and pathology of the disease.

It has been shown that parasite proteins are associated with the knobs (Deitsch and Wellems, 1996). The *P. falciparum* erythrocyte membrane protein-1 (*PfEMP1*) which mediates adhesion of infected erythrocytes to host endothelial cells is one of the parasite proteins which are found in knobs structure (Su *et al.*, 1995; Smith *et al.*, 1995; Kyes *et al.*, 2001). Duffy binding ligand (DBL) domains of *PfEMP1* molecules are able to attach to different specific receptors on the surface of endothelial cells including thrombospondin (TSP) (Roberts *et al.*,1985), ICAM-1 (Berendt *et al.*, 1989), VCAM-1 (Ockenhouse *et al.*, 1992), E-selectin, Chondroitin sulphate A (Rogerson *et al.*, 1995), CD31 (Treutiger *et al.*, 1997), and CD36 (Barnwell *et al.*, 1989). It has been shown that *PfEMP1* is localized to the Maurer's clefts (Wickham *et al.*, 2001), the knobs (Roberts *et al.*, 1992; Su *et al.*, 1995; Smith *et al.*, 1995; Kyes *et al.*, 2001) and associates with the infected erythrocyte membrane (Waterkeyn *et al.*, 2000). Mechanism of trafficking (Newbold and Marsh,1990; Baruch *et al.*,1995; Su *et al.*,1995; Smith *et al.*,1995; Wickham *et al.*, 2001; Marti *et al.*, 2005 ; Knupfer *et al.*, 2005), insertion and topology of *PfEMP1* have been well studied (Kriek *et al.*, 2003; Papakrivos *et al.*, 2005). The C terminal domain (ATS domain) interacts with the binding motif of KAHRP (Waller *et al.*, 1999 and 2000), actin, spectrin and band 4.1 to anchor the protein in the red blood cell membrane (Oh *et al.*, 2000; Voigt *et al.*, 2000).

Further parasite proteins inserted into the membrane of the host cell, possibly also playing a role in antigenic variation, and thus can be classified as major virulence factors. Some of these proteins which are exposed on the surface of infected erythrocytes are briefly described in the following sections.

RIFINS. The repetitive interspersed family of genes (*rif*), expressed at early trophozoite stage, were characterized as encoding potential variant antigens (Cheng *et al.*, 1998; Kyes *et al.*, 1999). They encode a group of 30-45 kDa proteins which were initially identified as “rosettin” because they are associated with the rosetting phenotype (Helmbj, *et al.*, 1993). The exposure of RIFINS on the surface of infected erythrocytes was studied using surface radiolabelling of infected erythrocytes (Fernandez *et al.*, 1999) antibody detection and immunofluorescence data (Kyes *et al.*, 1999).

STEVOR. The sub-telomeric variant open reading frame (*stevor*) encodes a family of 30-40 kDa proteins. These proteins have been shown to be localized in Maurer’s clefts (Kavirante *et al.*, 2002; Przyborski *et al.*, 2005) and on the surface of the infected erythrocyte (Blythe *et al.*, 2004). It is proposed that STEVOR proteins based on the structure, cellular localization and expression patterns in different stages of parasite development have a multifunctional role in the parasite lifecycle (Blythe *et al.*, 2004).

SURFIN. The proteomic analysis of released peptides after trypsination of exposed protein on the surface of infected erythrocytes identified a new high molecular mass (286 kDa) protein encoded by *surfin* genes. Surfin is a polymorphic antigen that colocalizes with *PfEMP1* and RIFINS and is present at both the infected erythrocytes and merozoite surface. SURFIN is suggested to be involved in the invasion of merozoites into erythrocytes (Winter *et al.*, 2005).

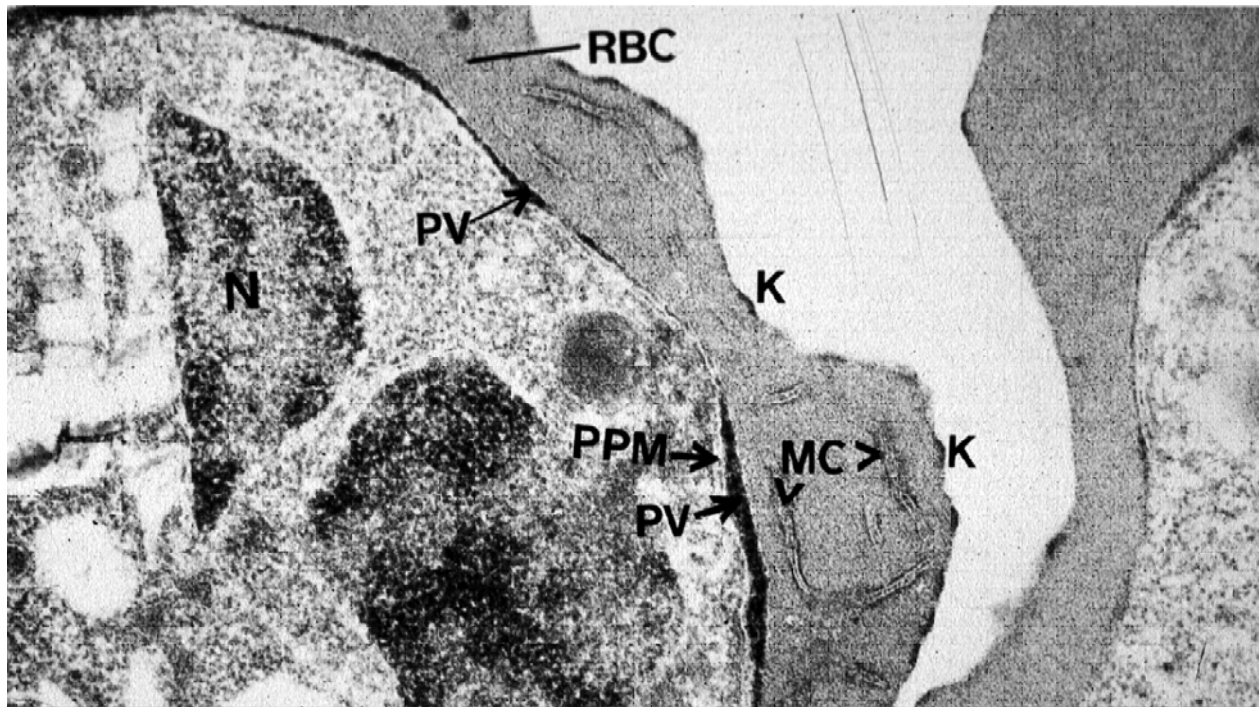


Figure 2. Parasite induced alterations in infected erythrocytes. During the erythrocytic development, the malaria parasite induces significant alterations in the cytosol and on the surface of the host cell that enable it to survive and proliferate in the host. RBC, red blood cell; PV, Parasitophorous vacuole; MC, Maurer's clefts; K, Knobs; PPM, Parasite plasma membrane (Nyalwidhe *et al.*, 2003).

1. 2.1. 3. Novel Permeation Pathways (NPPs)

Upon infection of the erythrocytes, the membrane of infected cells shows an unusually high permeability to a variety of solutes which are normally excluded from intact erythrocytes (Kunter *et al.*, 1983, Ginsburg *et al.*, 1985). The phenomenon which is referred to as "novel permeation pathways" (NPPs) (Ginsburg *et al.*, 1983; Kirk *et al.*, 1999) is induced 10-20 hours after erythrocyte invasion and is detectable through the parasite development (Kunter *et al.*, 1983, 1985; Saliba and Kirk, 2001).

The NPPs are responsible for the increased permeability of infected erythrocytes membrane to the low molecular weight solutes including monosaccharides (Ginsburg *et al.*, 1983, 1985; Kirk *et al.*, 1994, 1996), amino acids (Erfold *et al.*, 1985; Ginsburg *et al.*, 1985; Kirk *et al.*, 1994, 1996) peptides (Atamna and Ginsburg, 1997; Saliba and Kirk,

1. Introduction

1998), nucleosides (Upston and Gero, 1995), anions (Cranmer *et al.*, 1995; Kirk *et al.*, 1993), cations (Staines *et al.*, 2000) vitamin pantothenic acid (Cranmer *et al.*, 1995; Kirk *et al.*, 1993) and monovalent organic ions like choline (Kirk *et al.*, 1991; Staines and Kirk, 1998). The NPPs act as a channel with a general preference for anions and solutes over cations (Desai *et al.*, 2000; Kirk, 2001). The typical anion channel blockers like furosomide, 5-nitro-2-(3-phenylpropylamino)benzoic acid (NPPB) (Kirk *et al.*, 1994), 4,4'-Di-isothiocyanatostilbene-2,2'-disulfonic acid (DIDS) (Kirk and Horner, 1995a and b) and 4,4'-diisothiocyano-2,2'-dihydrostilbene disulfonic acid (H2DIDS) (Breuer *et al.*, 1987) can inhibit the pathway. It has been shown that infected erythrocytes are permeable to the different membrane impermeable biotin derivatives and that permeability can be inhibited by these biotin derivatives (Nyalwidhe *et al.*, 2002; Baumeister *et al.*, 2003).

The function and morphological characterization of NPPs has been well studied, but the origins and numbers of induced NPPs on erythrocyte are still under investigation (Kirk, 2004; Staines *et al.*, 2007).

Different electrophysiological studies including whole-cell patch-clamp and hemolysis experiments on infected cells indicated the increased conductance of parasitized erythrocytes (Desai *et al.*, 2000; Egee *et al.*, 2002; Huber *et al.*, 2002a and b; Duranton *et al.*, 2003, 2004; Staines *et al.*, 2003, 2004), but it is still unclear, whether the NPPs are mediated by the parasite-derived proteins which are inserted into the erythrocyte membrane or they are endogenous protein which induced on the host membrane proteins upon infection. The current proposed models for the NPPs are composed of several channel types and pores (Staines *et al.*, 2007).

The first direct physiological evidence for the involvement of a novel anion channel in NPPs activity was provided by the data from whole and single channel recording of infected and non-infected erythrocytes. In this study a voltage-dependent small ion channel on the surface of infected RBC (plasmodium surface anion channel (PSAC)) was identified which presents at about 1000-2000 copies on trophozoite stage of infected erythrocytes and suggested to account for the increased permeability of infected erythrocytes (Desai *et al.*, 2000; Alkhalil *et al.*, 2004). Failure to induce PSAC-like activity in non-infected erythrocytes does not definitively exclude a modified host

protein which may be involved in NPPs. Several studies have reported that some stresses (like oxidation) can induce NPP-like pathway in non-infected erythrocytes. Based on these findings, the investigators suggested that possible NPP pathways are derived from host cell proteins (Duranton *et al.*, 2002; Egee *et al.*, 2002; Huber *et al.*, 2002; Verloo *et al.*, 2004, Bouyer *et al.*, 2006).

To investigate this possibility, the malaria-induced anion channel was compared with an endogenous anion channel in infected erythrocytes using the patch clamp approach, the data provided evidences for existence of three distinct anion channels including an intermediate, a small and an outwardly rectifying large anion channel (Egge *et al.*, 2002, Boyer *et al.*, 2006) which can be activated by either, protein kinase A (PKA)/ATP or membrane deformation. Based on these findings, it is thought that the mechanism which the parasite uses to induce the NPPs in host membrane may involve phosphorylation (Egg *et al.*, 2002; Descherf *et al.*, 2004).

Furthermore, since the parasite induces high oxidative stress in the host erythrocyte (Atamna and Ginsburg, 1993, 1997), increased membrane permeability is suggested to result from oxidative alteration of the host cell membrane upon infection. To confirm this, the membrane permeability in infected erythrocytes and in non-infected erythrocytes that were oxidised were measured using whole-cell patch recording and iso-osmotic lysis (Huber *et al.*, 2002). At least four parasite induced channels were reported including 3 endogenous anion channels which can be activated in the host cell by oxidation (Huber *et al.*, 2002, 2004; Staines *et al.*, 2003). In accordance with these previous experiments, a previous study has shown that NPP activity can be inhibited by protease treatment of infected cells, suggesting that a protein within the erythrocyte plasma membrane mediates NPP activity. However, this activity recovered upon reintroducing the infected erythrocytes to cell culture, and reappearance could be blocked by treatment of the infected erythrocytes with the fungal metabolite brefeldin A (BFA), which blocks secretion of parasite encoded proteins to the host cell (Baumeister *et al.*, 2006). These data, whilst supporting the notion that an erythrocyte plasma membrane protein is involved in NPP activity however also show that parasite encoded protein also play an important role in NPP, either by directly transporting NPP substrates, or by activating endogenous erythrocyte membrane channels.

1. Introduction

A variety of membrane transporters have been identified on the erythrocyte membrane such as the $\text{Cl}^-/\text{HCO}_3^-$ exchanger (Band III; AE1), the Na^+ and Ca^{2+} pump, the Na^+ (K^+)/ H^+ exchanger, the $\text{Na}^+\text{K}^+2\text{Cl}^-$ and KCl co-transporter, choline, monocarboxylate, glucose, amino acid and nucleoside carriers (Ginsburg and Kirk, 1998), of which Band III, as a major anion exchanger shares some properties with NPPs anion channels and it has been proposed to be one of the candidate proteins for the NPPs (In: Kirk, 2001) (Huber *et al.*, 2002; Thomas *et al.*, 2004). Band III acts as anion channel with permeability to a range of anionic and electroneutral organic solutes (Fievet *et al.*, 1995). Moreover, the specific NPPs inhibitor like DIDS and H_2DIDS can block the anion transport function of Band III (Okubo *et al.*, 1994; Winograd *et al.*, 2004). It has been reported that oxidative stress induces a variety of modification in the structure of Band III; these include phosphorylation (Zipser *et al.*, 1997), clustering (Dumaswala *et al.*, 1999; Hornig and Lutz, 2000) and methyl esterification (Ingrosso *et al.*, 2000). Similar alterations on Band III also occur upon malaria infection (Giribaldi *et al.*, 2001).

It has been shown that Band III undergoes cleavage in the infected erythrocytes (Sherman and Wingorad, 1990; Crandall and Sherman, 1991,1994) and this modified form of Band III protein is suggested to be involved in NPPs (Kirk, 1994). Baumeister *et al.*, 2006 studied the effect of protease treatment on the Band III protein and on NPP activity in infected erythrocytes. The data showed that both Band III and putative NPPs were resistant to trypsin treatment and susceptible to chymotrypsin cleavage but the effect of chymotrypsin on the NPPs activity was concentration and time dependent. Chymotrypsin treatment of intact erythrocytes at 37°C for more than 10 min resulted in the complete cleavage of Band III but has no effect on NPPs activity under same the conditions. Based on these findings the authors concluded that induced NPPs activity cannot be entirely dependent on the Band III (Baumeister *et al.*, 2006).

1. 3. Biotinylation of proteins

Since parasite induced alterations (due to exposed parasite proteins on the surface of infected erythrocytes or conformational changes of erythrocytes membrane protein upon infection) can be expected to be in low amounts in order to avoid of host immune system, a sensitive method has to be established and used to detect them. Biotin labelling is one of the most commonly used tools for proteins study. Because of its small molecular weight and steric volume, biotin residues can react with many different molecules (Wilchek and Bayer, 1988 and 1990) without inducing any alteration in their biological activity. The labelled molecule can be effectively affinity purified using avidin or its bacterial alternative streptavidin. The biotin-avidin complex is the strongest known non-covalent interaction between protein and ligand with extraordinary affinity ($K_a = 10^{15} \text{ M}^{-1}$).

Biotinylation has been used to characterize cell wall proteins of different organisms such as *Borrellia burgdorfi* (Luft *et al.*, 1989), *Saccharomyces cerevisiae* (Cappellaro *et al.* 1998), *Candida albicans* (Casanova *et al.*, 1992), *Helicobacter pylori* (Sabarth *et al.*, 2002), *Shistosoma mansoni* (Braschi and Wilson, 2006) and *Cryptosporidium neoformans* (Foster *et al.*, 2007). Scheurer *et al.*, (2005) used different biotinylation reagents and 2D peptide mapping to identify and quantify the membrane proteins of human umbilical vein endothelial cells cultured in normoxic and hypoxic condition.

Different biotin derivatives have been used to label the proteins on the surface of *P. falciparum* infected erythrocytes (Nyalwidhe *et al.*, 2002; Baumeister *et al.*, 2003; Florens *et al.*, 2004; Winter *et al.*, 2003, 2005; Sharling *et al.*, 2007; Azimzadeh *et al.*, 2007). It has been shown that the membrane impermeable sulfo-NHS-LC biotin derivative is internalized by infected erythrocyte probably through NPPs and that their uptake and subsequent biotinylation of internal proteins can be prevented using NPPs inhibitors (Nyalwidhe *et al.*, 2002; Baumeister *et al.*, 2003). Sulfo-NHS-LC-biotin was used to biotinylate permeabilized infected erythrocytes to specifically label soluble proteins in the parasitophorous vacuole (Nyalwidhe *et al.*, 2002; Nyalwidhe and Lingelbach, 2006). Recently, sulfo-NHS-LC-biotin was used to probe the protein

structure and conformational changes of Band III on the surface of infected erythrocytes (Azimzadeh *et al.*, 2007).

The structure of sulfo-NHS-LC-biotin, which has been used in this current study, consists of an active ester group, N-hydroxysuccinimydyl (NHS), which reacts in aqueous solution with primary amines of proteins, particularly with the N terminus and the epsilon amino group of lysine residues at a neutral pH or higher. A novel stable amide bond is formed and the biotin moiety is covalently attached to the respective amino group (Figure 3). In addition, the sulfo-NHS-LC-biotin contains a sulfonyl moiety (NaSO_3) which is hydrophilic and this group inhibits the ability of these derivatives to permeate biological membranes. These derivatives are used to selectively label surface proteins in different organisms. The sulfonyl group permits the solubilisation of biotin derivative in aqueous buffers and the experiments can be conducted under physiological conditions. The biotin and reactive ester group are linked by a spacer arm. The spacer in LC-biotin is a hexanoate link (LC=long chain) 22.4 Angstroms in length. This spacer reduces steric hinderance and facilitates binding of biotinylated proteins to avidin to increase the sensitivity of detection.

Although amino acid residue modifications by specific tags or cross-linkers in combination with mass spectrometry have been used as tools for probing the tertiary structure of proteins (Bennet *et al.*, 2000; Young *et al.*, 2000; Back *et al.*, 2002), the use of biotin derivatives has additional advantages: the labelled proteins can be readily visualized before analysis; the labelled peptides can be affinity-enriched; and several membrane-impermeant derivatives exist, allowing the selective labelling of cell-surface proteins.

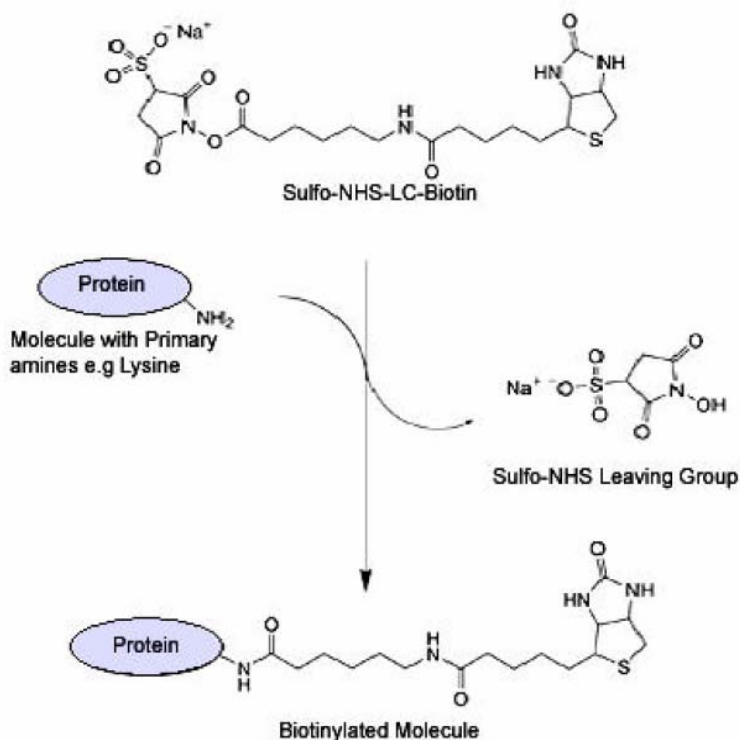


Figure 3. The sulfo-NHS-LC biotin derivative reacts with primary amines forming an amide bond. In proteins and peptides, primary amines and the epsilon amine of lysine which can react with NHS ester on the derivatives (modified from Pierce).

1. 4. Mass spectrometry

Mass spectrometry is a sensitive and accurate analytical method to determine the molecular mass and molecular structure of compounds. In addition, it is an accurate and sensitive technique for the identification and quantitation of different biological molecules such as proteins and nucleotides (Glish and Vachet, 2003). The mass spectrometer consists of three main components: an ionization source, a mass analyser and a detector which measure the mass to charge ratio (m/z) of ions under high vacuum. There are two available ionization sources for mass spectrometer: Electrospray (ESI) (Yamashita and Fenn, 1984) and Matrix-assisted laser desorption ionization (MALDI) (Karas and Hillenkamp, 1988).

MALDI is a soft ionization method that is used to generate gas phase protonated molecules including peptides for mass spectroscopy. The proteolytic peptides are mixed with a matrix compound such as alpha-cyano hydroxycinnamic acid at an approximately 1000 fold molar excess. The mixture is placed on a metallic slide or target and the mixture is allowed to dry. The slide is then inserted into a vacuum chamber and irradiated by nanosecond laser pulses. The small matrix molecules absorb the energy, move away from the target and carry the intact analyte molecules into gas phase (Hillenkamp *et al.*, 1990). As this happens, a proton is transferred from the matrix to the peptides in a process that is not yet fully understood (Karas *et al.*, 2000). All positively charged polypeptides with their different masses get vaporized and are accelerated in an electric field with the help of a high voltage grid to the same kinetic energy and they enter a flight tube of TOF (time of flight) mass analyser where the light ions that have a higher velocity arrived at the detector before the heavy ones. The recorded time of flight is used to calculate the masses of the ions in m/z . For most analytical applications the positive mode is used but negative mode operation is also possible. Negative ionisation that occurs through the generation of deprotonated ions can be used for the analysis of oligonucleotides and oligosaccharides. Several technical developments including reflectron tubes (Cornish and Cotter, 1993) and pulsed extraction (Jensen *et al.*, 1996) have been used to obtain a better and higher mass accuracy. The set of measured masses of generated peptides from protein digest are used to identify the protein by a method which is called peptide mass fingerprints (PMF). The experimental mass profile from spectrum is searched and matched against the theoretical mass from *in silico* digestion of the different protein amino acid sequences in a database.

Different factors are important for the successful protein identification; these include MALDI peak mass accuracy, the relation between assigned and unassigned peaks in spectrum and the size of databases (Perkins *et al.*, 1999). To avoid of possibility of false positive results, the protein identification may be done with peptide fragmentation data by tandem mass spectrometry in the process known as MS/MS. Peptide ions which are selected with a first mass analyser, are fragmented by collision induced association (CID) with argon or helium under low energy conditions and measured with a second analyser. The fragmentation occurs principally at the peptide amide bonds. Two types of

ions are produced by fragmentation: y-ions with intact C-terminus and b-ions with intact N-terminus (Biemann, 1992). The measured mass of fragments are checked against the masses of amino acids and finally matched to amino acid sequences to identify peptides and proteins with the help of different programs including MASCOT (Perkins *et al.*, 1999) or SEQUEST (Sadygov *et al.*, 2004) to search in protein databases like SwissPort and NCBIInr.

In addition to protein identification, mass spectrometry is powerful tool to determine post-translational modifications (PTMs). If the primary amino acid sequence is known in advance, mass spectrometry can be used to detect the differences from the expected protein mass that is produced by modifications of its primary structure. This mass shift is the basis of the detection of PTM by mass spectrometry. In addition, the sites of these modifications can be localized by using either tandem mass spectrometry of the intact proteins, peptide mass fingerprinting following proteolysis, or a combination of the two techniques. Amino acid residues modification by specific tags and crosslinkers in combination with mass spectrometry have been used for probing the tertiary structure of proteins (Bennett *et al.*, 2000; Young *et al.*, 2000; Back *et al.*, 2002; Huang *et al.*, 2004, 2005; Azimzadeh *et al.*, 2007).

1. 5. Study of conformational changes in model protein

In this study, biotinylation using the sulfo-NHS-LC biotin derivative in combination with mass spectrometry analysis has been used to probe conformational changes in the structure of two soluble proteins bovine serum albumin (BSA) and carbonic anhydrase II (CA II) and that of Band III, an integral membrane protein with multiple trans-membrane domains.

1. 5.1. The structure and properties of bovine serum albumin (BSA)

Serum albumin is a highly soluble multidomain protein with mass of 69 kDa which is found in every tissue. It is the most abundant plasma protein with a concentration of 5 mg/100ml and contributes 80% of colloid osmotic blood pressure (Carter and Ho, 1994).

Serum albumin plays an important role in maintaining of blood pH and in the transport of multiple substances within the bloodstream including free fatty acids, phospholipids such as lysophosphatidic acid (LPA), steroid-based hormones, prostaglandins, and heavy metals (Peters, 1985; Carter and Ho, 1994). It is also capable of binding a broad range of metabolites, drugs and organic compounds (Koh *et al.*, 1998; Iglesias *et al.*, 1999).

It was shown that albumin is involved in the sequestering oxygen free radicals and inactivating various toxic lipophilic metabolites such as bilirubin (Emerson, 1989).

Albumin is synthesized initially in the liver as pre-proalbumin in mammals. After removal of the signal peptide, proalbumin undergoes a further processing and it loses six-residues from the new N-terminus (Peters and Anfinsen, 1950). Albumin is released into circulation and has a half-life of 19 days (Carter and Ho, 1994).

The structure and chemistry of albumin has been studied using different methods including hydrodynamics, low-angle X ray scattering, fluorescence energy transfer, electrophoretic methods, NMR, IR, UV, Raman spectroscopies and mass spectrometry (recently reviewed in detail : Carter and Ho, 1994). Amino acid sequences determination, molecular structure and ligand binding properties of the albumin family have been described based on the study of the human serum albumin (HSA) (Carter

and He, 1990; Curry *et al.*, 1998; Sugio *et al.*, 1999). Hydrodynamic experiments (Wright and Thompson, 1975) and low-angle X-ray scattering (Bloomfield, 1966; Bendedouch and Chen, 1983) showed that serum albumin was shaped like an oblate ellipsoid with dimensions of $140 \times 40 \text{ \AA}$. Based on these findings, albumin was suggested to have a cigar shaped three domain model (Carter and Ho, 1994), but electron microscopy (Luft and Lorscheider, 1983) and subsequent studies using resonance energy transfer methods (Hagag *et al.*, 1983) and NMR (Bos *et al.*, 1989) indicated that such a structure was unlikely and suggested that albumin must be folded more having a U shaped molecule with dimension of 80 \AA , which was referred to as heart-shaped structure.

As shown in figure 4, a high percentage similarity has been shown between bovine serum albumin (BSA) and HSA sequences; these proteins share 76% amino acid sequence homology (Peters, 1985). Sequence analysis data indicate that human serum albumin is composed of 585 amino acids (McGilivray *et al.*, 1979; Reed *et al.*, 1980). The amino acid sequence of BSA has been determined by the Edman degradation method (Reed *et al.*, 1980). Automated sequencing and tandem mass spectrometry confirmed the absence of three amino acids in BSA in comparison with HSA (Hirayama *et al.*, 1990). The HSA amino acid composition is characterized by high percentage of charged amino acids, lysine arginine, aspartic and glutamic acid and low percentage of tryptophan and methionine (Carter and Ho, 1994). In addition, albumin has an unusually high content of 35 cysteine residues containing a free sulfhydryl group (Sugio *et al.*, 1999) and having no sites for enzymatic glycosylation (Carter and HO, 1994).

1. Introduction

```

Comparison of:
(A) ./wwwcmp/lalign/.14199.1.seq BSA- 607 aa
(B) ./wwwcmp/lalign/.14199.2.seq HSA- 608 aa

using matrix file: BL50, gap penalties: -14/-4

76.4% identity in 607 aa overlap; score: 3298 E(10,000): 3.7e-286

      10      20      30      40      50      60
BSA  MKWVTFISLLLFSSAYSRCVPRRDTEKSEIAHRPKDLGREHFKGLVLIAPSOYLQCCPF
HSA  MKWVTFISLLLFSSAYSRCVPRRDTEKSEVAHRPKDLGREHFKALVLIAPAQYLQCCPF
      10      20      30      40      50      60
BSA  DEBVKLVNVEITEFAKTCVADESAGCCSKSLBTLFGDLELKVASLRETYGMADCCAKQEP
HSA  DEBVKLVNVEITEFAKTCVADESARNCCSKSLBTLFGDLELKVATLRETYGMADCCAKQEP
      70      80      90     100     110     120
BSA  ERNECFLSBKDDSPDLPLKLPDPHTLCEDEPKCADRCKKFKYLYEIAARRPYPYAPPELLY
HSA  ERNECFLSBKDDSPDLPLKLVPRPVDVNCIAPEDNRETPKLYEIAARRPYPYAPPELLP
      130     140     150     160     170     180
BSA  YANKYNGVFORCCQARDKACLLPKIETMRKVLTSARORLRCASIQKFGERAUKAMAV
HSA  YANKYKAAFTRECCQARDKACLLPKLELRDEGRKASSAKORLRCASIQKFGERAUKAMAV
      190     200     210     220     230     240
BSA  ARLSQKPPKAEFVEVKLVTDLTQVHECCBGDLLECADDRADLAKYICNDTISSKLK
HSA  ARLSQKPPKAEFVEVKLVTDLTQVHECCBGDLLECADDRADLAKYICNDTISSKLK
      250     260     270     280     290     300
BSA  ECCCPLLEKSHCIAEVEIDAIPEHLPLTADPAEDKDKCKNYORAKDIFLGSFLVEYSR
HSA  ECCCPLLEKSHCIAEVEIDAIPEHLPLTADPAEDKDKCKNYORAKDIFLGSFLVEYSR
      310     320     330     340     350     360
BSA  RHPOYSVILLRLAKTYETLEKCCAAADPHCYAKVDFPKPLVEEPQNLIKQNCLEFE
HSA  RHPOYSVILLRLAKTYETLEKCCAAADPHCYAKVDFPKPLVEEPQNLIKQNCLEFE
      370     380     390     400     410     420
BSA  KLGEYKPNALIVRYTRKVPQVSTPTLVEVSRSLGKVGTRCCPKPESEMPCTEDYLSLI
HSA  KLGEYKPNALIVRYTRKVPQVSTPTLVEVSRSLGKVGTRCCPKPESEMPCTEDYLSLV
      430     440     450     460     470     480
BSA  LNRLLCVLHEKTPVSEKVTKCTESLVNRRPCFSALVDETYVPKAFORLPTPHADICTL
HSA  LNRLLCVLHEKTPVSEKVTKCTESLVNRRPCFSALVDETYVPKAFORLPTPHADICTL
      490     500     510     520     530     540
BSA  PDTERQIKKQATALVELLKHKPKATREQLKTVMEKVFVAVKCCADDKRCFAVEGPKLV
HSA  PDTERQIKKQATALVELLKHKPKATREQLKAVMDPAFVAVKCCADDKRCFAVEGPKLV
      550     560     570     580     590     600
BSA  VSTQAL
HSA  AASQAL
600
    
```

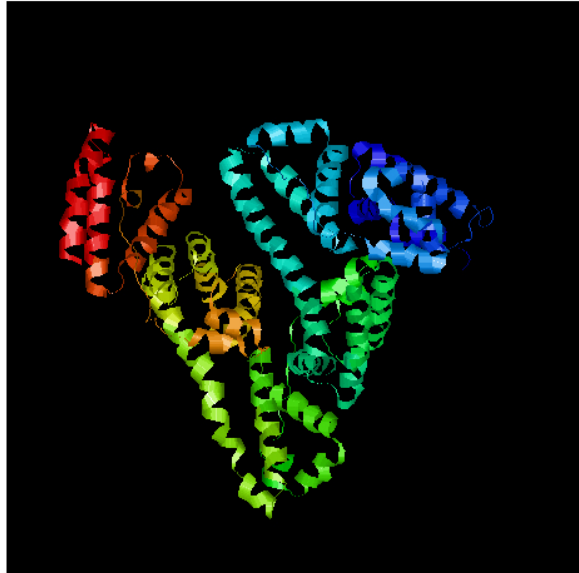


Figure 4. The comparison of primary structure of HAS and BSA. The domain structure of BSA was shown based on the HSA homology. Two proteins share 76% amino acid sequence homology. The 3D structure of BSA was generated by 3d jigsaw software using the HAS sequence.

The primary structure of HSA consists of three homologous domains, domain I (residues 1–195), domain II (196–383) and domain III (384–585) which are topologically identical and very similar in three-dimensional structure (Sugio *et al.*, 1999). Each domain in turn is the product of two subdomains (A and B) (Carter and He, 1990; He and Carter, 1992) which further divides into nine loops (L1-L9) and are cross linked by 17 disulphide bonds (Peters, 1985). The disulphide bonds are located almost between helical segments (Carter and Ho, 1994), they are not accessible to the solvent and protected from reducing agents at neutral pH (Katchalski, 1957). The conformations of the disulphides

bonds are primarily gauche-gauche-gauche and $C\beta_1-S1-S2-C\beta_2$, with torsion angles clustering around $\pm 80^\circ$ (Carter and HO, 1994). The structure and conformation of the disulphide bonds is responsible for the stability of albumin under harsh experimental conditions like high temperature treatment (Carter and HO, 1994; Pico *et al.*, 1997).

The secondary structure of human serum albumin has been well studied using X-ray crystallography (Spector, 1975; He and Carter, 1992; Sugio *et al.*, 1999; Curry *et al.*, 1998), biochemical labelling and NMR spectroscopy (Cistola *et al.*, 1987; Hamilton *et al.*, 1991). Albumin structure is largely (67%) alpha helical, the rest of the protein turns and extended between subdomains with no beta sheets, forming the heart shape molecule. Each of the domains is composed of 10 helices, h1 - 6 for sub-domain A and h7 - 10 for sub-domain B (Peters, 1985). All sub-domains share a common helical motif. The A sub-domains consist of the three helix bundle on the C-terminal side and one smaller disulfide double loop to form a small globin-like structure that is linked by four disulfide bridges. The B sub-domain supplements the helical motif on the N-terminal side with extended polypeptide to form a folding structure of a simple up-down helical bundle. These sub-domains assemble through hydrophobic helix packing interactions involving h2, h3 and h8 (Carter and Ho, 1994). In addition, the sub-domains are joined together by stretches of flexible extended polypeptide (IA-IB, 106-119; IIA-IIB, 292-315; IIA-IIIb, 492-511) (Curry *et al.*, 1998). Domains I and II and domains II and III in turn are connected through helical extensions of h10 (I) - h1 (II) and h10 (II) - h1 (III), creating the two longest helices in albumin (Carter and Ho, 1994).

Structural alterations and conformational flexibility of albumin at thermal denaturation have been previously studied. It was shown that albumin can be heated to 60°C for 10 hours without deleterious effects (Pico *et al.*, 1998). The stability of the albumin depends on the protein concentration and the free-SH groups in the protein structure (Wetzel *et al.*, 1980; Ross and Shrake, 1988). Heating of albumin leads to two stages of structural changes in the protein structure. The first step is heating up to 65°C that leads in reversible changes. The subsequent heating is irreversible but does not necessarily result in a complete destruction of the protein structure (Wetzel *et al.*, 1980). It has been shown that the heating above 65°C causes a partial loss of the alpha helix and induces the beta-sheet in the albumin structures which are amplified on cooling (Wetzel *et al.*,

1980). The comparison of the chemical and thermal denaturations of albumin indicated different structurally unfolded states of the protein. It has been observed that chemical denaturing using guanidine and urea induces a randomly coiled conformation in the unfolded state of albumin structure, while thermal denaturation produces a molten globule state and the aggregation of the protein (Farrugia and Pico, 1999).

Recently, the conformational changes of tertiary structure of BSA (Huang *et al.*, 2006) and HSA (Huang *et al.*, 2005) was probed using different lysine specific cross linking reagents with various spacer arm length before analysis by electrospray tandem mass spectrometry. The obtained distance between lysine residues generate the information about the 3D structure of the albumin proteins. In addition, the changes in the conformation of albumin structure induced by fatty acid binding were detected based on the changes in cross-linked peptides by MS/MS (Huang *et al.*, 2005).

1. 5. 2. The structure and properties of Carbonic anhydrase II (CA II)

The carbonic anhydrase (CA) is a ubiquitous enzyme found in all animals, plants, archaeo and eubacteria, (Supuran and Scozzafava, 2001; Supuran *et al.*, 2003). The structure and function of CA has been extensively investigated (Kannan *et al.*, 1975; Håkansson and Wehnert, 1992; Håkansson and Liljas, 1994; Lindskog, 1997).

CA catalyses different physiological reactions, including the reversible hydration of CO₂ to bicarbonate (Pocker and Stone, 1967; Sly and Hu, 1995), the hydration of certain aldehydes (Pocker and Meany, 1965), and the hydrolysis of certain esters (Tashian *et al.*, 1964). In animals, CA plays an important role in respiration by facilitating transport of carbon dioxide and is involved in the transfer and accumulation of H⁺ and HCO₃⁻ in organs of secretion (Maren, 1967). The CO₂ generated by metabolism in all cells is removed from the body by red blood cells that convert most of it to bicarbonate for transport, then back to carbon dioxide to be exhaled from the lungs.

There are three distinct evolutionary and structurally CA classes, α , β , γ (Hewett-Emmett and Tashian 1996) which have no significant sequence homologies but all of them are zinc containing enzymes (Lindskog, 1997). In contrast to CA β and γ , the mammalian isoenzymes CA α have been well characterized by structural and mechanistic studies

(Christianson and Cox, 1999). Seven genetically α CA have been identified in human (I-VII) which have different tissue distributions and intracellular localizations (Lindskog, 1997). The amino acid sequences of the different human CA have been determined and are quite similar (Andersson *et al.*, 1972; Lin and Deutsch, 1973a and b; Henderson *et al.*, 1976; Lloyd *et al.*, 1986; Okuyama *et al.*, 1992; Nagao *et al.*, 1993; Aldred *et al.*, 1991; Montgomery *et al.*, 1991).

The 29 kDa CA II protein consists of 259 amino acid residues in an one domain polypeptide which contains neither disulfide bonds nor free -SH groups and there is no evidence for formation of polymeric species (Håkansson *et al.*, 1992; Arensson *et al.*, 1995; Lindskog, 1997). The crystal structure of CA II showed that protein has some helical structure and a dominating twisted β -sheet that extends throughout the entire molecule and divides it in two halves (figure 5) (Håkansson *et al.*, 1992; Freskgård *et al.*, 1994; Arensson *et al.*, 1995). Unlike the other larger proteins, which contain several structural domains, CA II appears to be folded in a single unit that includes the entire protein (Lin and Deutsch, 1973). Enzyme activity is due to the zinc atom which is near the bottom of a canonical intermolecular cavity and is coordinated to three histidine residues and water molecule (Lindskog and Nyman, 1964).

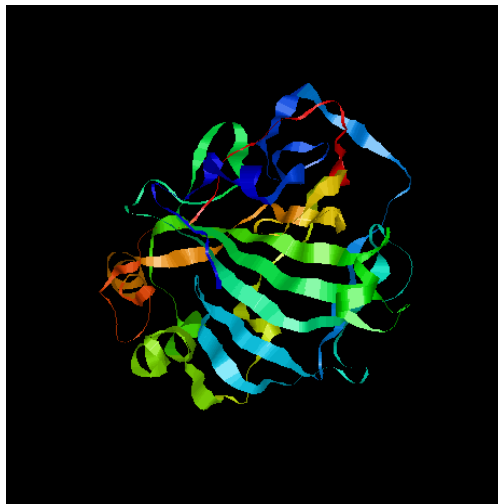


Figure 5. The secondary structure of bovine CA II. CA II is a single domain polypeptide contains some helical structure dominating twisted beta sheets. The 3D structure was generated by 3d jigsaw software.

1. Introduction

The effect of temperature on the structure and activity of CA II has been studied (Lavecchia and Zugaro 1991; Sarraf *et al.*, 2004). The thermal denaturation curve of CA has a classical sigmoid shape with melting temperature of 64.2°C. Only minor structural changes may be expected at this pre-transition temperature (Sarraf *et al.*, 2004). It was shown that the heat treatment of CA II from 25°C to 40°C causes a decrease in the amount of β structures and an increase in the random coil structures. But from 40°C to 52°C, the amount of helix is slightly decreased and there is an increase in the percentage of β structures. The authors suggested that the first decrease may be due to the lower stability of β structures comparing to helices (Sarraf *et al.*, 2004). Chemical denaturation and conformational changes of CA II have been studied using guanidine chloride (Wong and Tanford, 1973; Henkens *et al.*, 1982) and 2,2,2-Trifluoroethanol (TFE) (Wei *et al.*, 2006). It has been shown that the protein is fully unfolded by using 3M guanidine chloride to yield a random coil (Wong and Tanford, 1973) and refolds upon removal of the denaturing conditions to re-form the native structure (Yazgan and Henkens, 1972; Wong and Tanford, 1973). The zinc remains tightly bound to the fully denatured protein (Henkens *et al.*, 1982). It has been reported that CA II undergoes a significant changes in the secondary structure when TFE is used at a concentration above 40 % (v/v) (Wei *et al.*, 2006).

The differences in the physical properties of BSA and CA II make them suitable model proteins to use in comparative analysis studies. These properties are summarized in the table1.

physical properties	BSA	CA II
Number of amino acids	583	259
Molecular weight (Da)	69293.4	28982.5
Theoretical pI	5.82	6.4
Number of Lysine residues	60	18
Number of Cysteine residues	35	0
Number of disulphide bonds	17	0
Sulphydryl group (SH)	1	0

Table 1. The differences in the physical properties of BSA and CA II. The differences in the physical properties of BSA and CA II make them suitable model proteins to use in comparative analysis studies.

1. 6. The structure and properties of Band III protein (Anion Exchanger 1, AE1)

Anion-exchanger (AE) proteins facilitate the electroneutral exchange of Cl^- for HCO_3^- across the plasma membrane of cells and contribute to regulation of intracellular pH, cell volume, bicarbonate metabolism and maintenance of intracellular chloride levels (Casey and Reithmeier, 1991; Jay and Cantely, 1986). The anion exchanger multigene family consists of four members (AE1-4), of which three have been identified and characterized (Kopito and Lodish, 1985; Tanner *et al.*, 1988; Lux *et al.*, 1989; Kopito, 1990; Gehrig *et al.*, 1992; Schofield *et al.*, 1994; Alper *et al.*, 1991). The AE1-3 proteins share significant homology but they are found in different tissues (Alper *et al.*, 1988; Bruce and Tanner, 1999).

The AE1 gene is expressed during erythropoiesis in both avian and mammalian erythroid progenitor cells. The erythroid AE1, also called Band III protein is the most abundant anion transporter in red blood cell (Frazar *et al.*, 2003) with 1.2×10^6 copies per cell (Fairbanks *et al.*, 1971) making up 25% of all red blood cell membrane proteins (Jay und Cantley, 1986). The protein is a homodimer but its tetramer has also been identified (Casey and Reithmeier, 1991, Wang *et al.*, 1993). It was observed that 60% of protein exists as a dimer and 40% as a tetramer in erythrocytes membrane (Yu *et al.*, 1975). The truncated form of AE1 is also found in the kidney; it is expressed in the basolateral

1. Introduction

membrane of alpha-intercalated cells of distal nephron and lacks the 65 amino acids at the N-terminal.

The structure of Band III has been extensively studied using different approaches (Jennings and Anderson, 1987, Jay and Cantely, 1986). The 95 kDa Human Band III protein is a 911 amino acids polypeptide. The complete sequence of human Band III has been deduced from the cDNA sequence (Tanner *et al.*, 1988; Lux *et al.*, 1989). The sequence analysis of Band III protein revealed that the amino acid composition of Band III protein is highly hydrophobic and consisting of approximately 31% charged amino acid residues, 29% apolar amino acid residues; the rest are the residues which have intermediate polarity (Tanner and Boxer, 1972; Ho and Guidotti, 1975; Yu *et al.*, 1975; Benga *et al.*, 1991). It has been shown that polar amino acid residues including lysine, arginine, glutamic acid and histidine are essential in the structure of Band III for transport activity of the protein (Izuhara *et al.*, 1989; Jennings and Anderson, 1987; Zaki, 1981; Garcia and Lodish, 1989; Passow *et al.*, 1986; Okuba *et al.*, 1994; Jin *et al.*, 2003).

Band III consists of two structurally and functionally distinct domains (Yu *et al.*, 1975; Kopito and Lodish, 1985). The 43 kDa N-terminal domain (residues 1-359) is located in the cytosol and associated with peripheral and anchor proteins of the erythrocyte membrane (Rybicki *et al.*, 1986). The 55 kDa C-terminal membrane spanning domain (residues 360-911) traverse the plasma membrane multiple times (Jennings, 1985; Zhang *et al.*, 2000).

The structural features of the cytoplasmic domain of Band III has been studied and analyzed using X-ray crystallography (Chang and Low, 2003), but the topology of the C-terminus is not well established. Current models for the transmembrane (TM) organization of this protein are based on different studies including Cryoelectromicroscopy (Wang *et al.*, 1993), NMR (Gargaro *et al.*, 1994, Askin *et al.*, 1998), hydrophathy analysis (Kopito and Lodish, 1985), proteolysis (Kuma *et al.*, 2002), antibody binding study (Wainwright *et al.*, 1989) and N-glycosylation insertion mutagenesis (Tam *et al.*, 1995; Popov *et al.*, 1997; Popov and Reithmeir, 1999) and cysteine-scanning mutagenesis (Tang *et al.*, 1998; Fujinaga *et al.*, 1999 and Zhu *et al.*, 2003). According to these studies, the membrane domains of Band III might span the membrane 12 to 14 times (Kopito and Lodish, 1985). The three proposed topology

models of Band III are shown in figure 6. There is a general agreement about the topology of first 9 transmembrane domains, but the topologies of the domains TM9 - TM13 have not been conclusively determined. The topology of the 10th region is still not clear (Kanki, *et al.*, 2002). Different experimental approaches indicate that this region is exposed to the extracellular (Fujinaga *et al.*, 1999) or cytoplasmic side of the membrane (Kuma *et al.*, 2002). Different studies have reported that the loops containing residues 430-432, 551-562, 628-658, and 851-854 are exposed on the extracellular surface of erythrocyte (Steck *et al.*, 1976; Popove *et al.*, 1997; Fujinaga *et al.*, 1999; Bruce *et al.*, 1994; Jarolim *et al.*, 1998; Jennings *et al.*, 1985; Cobbe *et al.*, 1990). The region with high flexibility structure is located between amino acids 815-835 but no clear topology for this region was predicted (Zhu *et al.*, 2002; Fujinaga *et al.*, 1999). This region is not predicted to be a transmembrane region by conventional hydropathy analysis (Kopito and Lodish, 1985). It is suggested that this region can be exposed to face outside of cell under some circumstances (Zhu *et al.*, 2002). It has been reported that synthetic monoclonal antibody corresponds to residues 813-824 can bind erythrocytes only after detergent treatment, suggesting that the epitope is not accessible at the extracellular surface normally (Wainwright *et al.*, 1990). In contrast, the 812-827 region exposed as an extracellular antigen, when erythrocytes age (Kay and Lin, 1990). In addition, it has been reported that this region is also differentially recognized in non-infected and in *P. falciparum* infected erythrocytes by a monoclonal antibody (Winograd *et al.*, 2004).

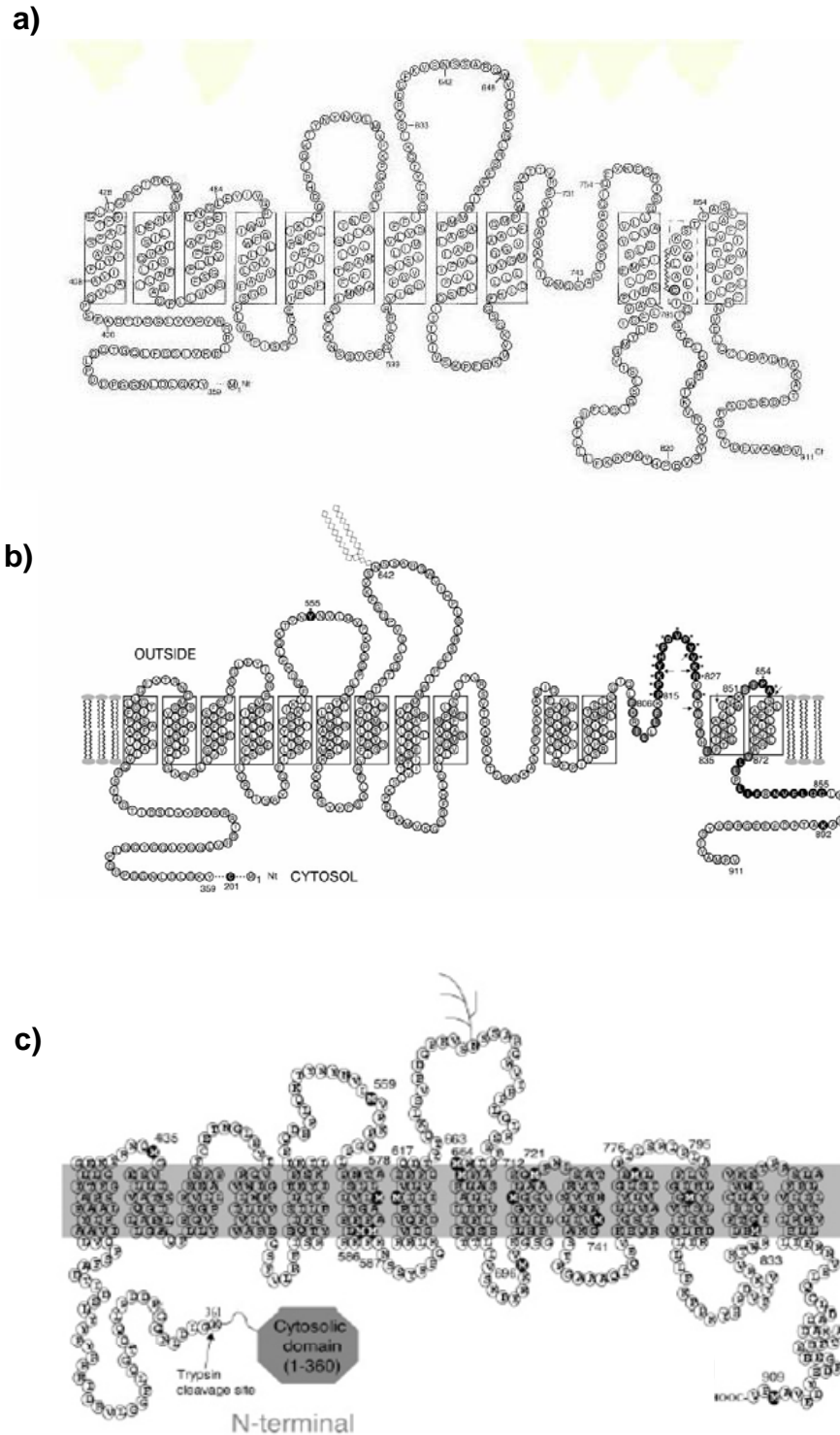


Figure 6. Proposed topology model for Band III protein with 12-14 transmembrane domains. The Band III protein is a transmembrane protein which is predicted to span the lipid bilayer 12 to 14 times. a) 12 span model (Popove *et al.*, 1999); b) 13 span model (Zhu *et al.*, 2002); c) 14 span model (Li *et al.*, 2006).

1. Introduction

Band III protein is known to undergo conformational changes upon malaria infection (Sherman *et al.*, 2004). Confocal microscopy showed the induced reorganization in host membrane proteins and indicated increased aggregation (Giribaldi *et al.*, 2001) and decreased mobility of Band III (Parker *et al.*, 2004).

It has been reported that Band III, together with *PfEMP1* and thrombospondin, is associated with the adhesion of infected erythrocytes to endothelial cells (Crandall *et al.*, 1993; Lucas and Sherman, 1998). The adhesive domain of Band III including residues 534-547 can bind to the anion exchange inhibitor DIDS, this sequence referred to DIDS binding domain (DBR) (Okubo *et al.*, 1994; Winograd *et al.*, 2004).

In addition, the antibodies which were raised against synthetic peptides on putative exofacial loop 3 (amino acids 546-555) (Sherman *et al.*, 2003) and loop 7 (amino acids 821-834) (Crandall *et al.*, 1994) of Band III, inhibit the cytoadherence. These monoclonal antibodies can identify the special epitope on the surface of infected erythrocyte but not in normal red blood cells. The ability of synthetic of Band III peptides to block the cytoadherence is called "*pfalhesin*" (Crandall *et al.*, 1993). It is hypothesized that the *pfalhesin* and DBR sequence are cryptic in non-infected erythrocytes and are exposed during parasite growth (Sherman *et al.*, 2003; Winograd *et al.*, 2005). These sequences have some similarity to the senescent antigen amino acid composition in the Band III (Kay *et al.*, 1990).

It was reported that Band III may be the possible receptor for parasite proteins involved in the invasion of malaria parasite to erythrocytes. Recently, two non-glycosylated exofacial regions of Band III have been identified as a receptor binding the C terminal of merozoite surface protein 1(MSP1) during the invasion of parasites to erythrocytes. Amino acids 720-761 and 807-826 are identified as the core region of the Band III receptor which interacts with MSP1 (Goel *et al.*, 2003). In addition, Band III has been shown to be a possible receptor for the of the parasite acidic-basic repeat antigen (ABRA) which located on the surface of malaria merozoite (Kushwaha *et al.*, 2002).

As it noted previously, there is some similarity between the properties of Band III and NPPs, this has provided reason for investigators to consider native Band III or its

modified form as one of the possible candidate proteins for the NPPs (In: Kirk, 2001; Huber *et al.*, 2002a and b; Thomas and Lew, 2004). It has been reported that Band III behaves as bifunctional protein with both anion exchange (Knauf and Rothstein, 1971; Jennigs, 1985) and swelling-activated osmolyte channel functions (Motais *et al.*, 1997). A broad range of anionic and organic solutes can be transported by Band III (Fievet *et al.*, 1995 and 1998). Furthermore, the anion transport and cell volume regulating activity of Band III can be blocked by specific NPPs inhibitor such as DIDS and H2DIDS (Okubo *et al.*, 1994; Winograd *et al.*, 2004).

It has been observed that the rate of transport of anion substrate depends on the conformational change in the structure of Band III which leads to the transfer of a single substrate across the membrane, and the rates of association and dissociation of the substrate are much faster than the rate of the conformational change that leads to the translocation of the bound anion (Jennigs, 1985; Passow, 1986). It was known that Band III proteins undergoes such modifications upon malaria infection (Giribaldi *et al.*, 2001; Sherman *et al.*, 2003; Winograd and Sherman, 2004; Winograd *et al.*, 2005).

Recently, the effect of protease on the Band III and NPP activity in infected erythrocytes were compared. Because of the different behaviour of Band III and NPP after chymotrypsin treatment, the authors concluded that NPPs activity is not only dependent on Band III (Baumeister *et al.*, 2006). Although Band III itself may not be the actual channel protein mediating the NPP, its conformational change after infection may have an important role for the survival of the parasite within erythrocytes. Therefore, in this study an experimental strategy was applied to more precisely define the position within the Band III molecule where the conformational change could possibly occur.

1. 7. Objectives

The aim of this study is to probe the conformational changes in protein structures using biotinylation patterns. Surface biotinylation of intact cells followed by mass spectrometry is suggested to be a rapid and effective method for identifying putative conformational changes in surface proteins following pathogen infection or under varying physiological conditions. This approach has great potential for the selective chemical modification and analysis of extracellular proteins for the other biological systems.

To initially establish the experimental system and protocols, two soluble model proteins, BSA and CA II were studied to determine if specific, experimentally induced conformational changes, result in a reproducible biotinylation pattern of lysine residues. Additionally, the membrane topology of the erythrocyte Band III protein was studied. It has previously been shown that Band III undergoes a conformational change upon infection of the erythrocyte with *P. falciparum*. To validate our established protocols as a method for analysing conformational changes in membrane proteins, our experimental system was then applied to detect these conformational changes in Band III.

2. Materials and Methods

2.1. Materials

2.1.1. Equipments

Analytical scale 2414	Sartorius, Göttingen
Bench scale 1205 MP	Sartorius, Göttingen
Blotting Apparatus	Phase,Lübeck
Incubator	Heraeus,Hanau
Electrophoresis chamber	Phase
Film Cassettes	Rego
Laborfuge III	Heraeus,Hanau
Lab roller Spiromix	Denley,UK
Magnetic stirrer	Combimag RCH,IKA
Ultraflex mass spectrometer MALDI-TOF	Bruker Daltonik,Bremen
pH-Meter 766	Calimatic,Mering
Power supply 21310	LKB Biochrom, St.Albans, UK
Power supply EPS601	Amersham Pharmacia Biotech,Sweden
Speedvac centrifuge	Eppendorf,Hamburg
Centrifuge	Eppendorf,Hamburg
Thermomixer 5436	Eppendorf,Hamburg
UNO-Thermoblock	Biometra,Göttingen
Vortexer REAX 2000	Sartorius, Göttingen
Waterbath 2219 Multitemp II	LKB,Bromma

2. Materials and Methods

2.1.2. Disposable Materials

Culture flasks	Greiner, Frickenhausen
Eppendorf reaction tubes	Eppendorf, Hamburg
Falcon tubes	Greiner, Frickenhausen
Films	New RX NIF, Fuji, Japan
Glass slides	IDL, Nidderau
Micro concentrator	Millipore Corp, Bedford USA
Nitrocellulose	Schleicher & Schuell, Dassel
Pipettes	Gilson, France
Pipette tips	Greiner, Frickenhausen
Whatman Paper	Schleicher & Schuell, Dassel
Zip Tip gel loading column	Eppendorf, Hamburg

2.1.3. Chemicals and reagents

Acetic acid	Roth, Karlsruhe
Acetone	Roth, Karlsruhe
Acetonitrile	Roth, Karlsruhe
Ammonium hydrogen carbonate	Sigma, Deisenhofen
Ammonium persulfate	Roth, Karlsruhe
BCIP(5-Bromo-4-chloro-3-indolylphosphat)	Biomol, Hamburg
Bovine Serum Albumin Fraction V	Roth, Karlsruhe
Bovine Carbonicanhydrase II	Fluka, NeUlm
Coomassie Brilliant blue R250	Roth, Karlsruhe
Cyano-4-hydroxycinnamic acid	Bruker Daltonik
D-Biotin	Sigma, Deisenhofen
DTT (1,4-diothio-DL-threitol)	Fluka, NeUlm
ECL-Reagent	Amersham Pharmacia Biotech, Sweden
EDTA	Merck, Darmstadt
Ethanol	Roth, Karlsruhe

2. Materials and Methods

Formic acid HPLC grade	Sigma, Deisenhofen
Furosemide	Sigma, Deisenhofen
Gentamycin	Gibco, Eggenstein
Giemsa solution	Merck, Darmstadt
Glycin	Roth, Karlsruhe
Glycerin	Roth, Karlsruhe
HEPES	AppliChem, Darmstadt
Hydrochloric acid	Roth, Karlsruhe
Iodocetamide	Sigma, Deisenhofen
Isopropanol	Roth, Karlsruhe
Magnesium Chloride	Roth, Karlsruhe
Methanol	Roth, Karlsruhe
Milk powder	Roth, Karlsruhe
Nitroblue Tetrazolium Chloride	Biomol, Hamburg
Oligo R3	AppliedBiosystems,USA
Ponceau S pure	Serva, Heidelberg
Poros R2	AppliedBiosystems,USA
Potassium Chloride	Roth, Karlsruhe
RPMI 1640 medium	PAA,Cölbe
Sodium Azide	Roth, Karlsruhe
Sodium Chloride	Roth, Karlsruhe
Sodium dihydrogenphosphate	Roth, Karlsruhe
Sodium hydrogencarbonate	Roth, Karlsruhe
Sodium hydrogenphosphate	Roth, Karlsruhe
Sodium hydroxide	Roth, Karlsruhe
Streptavidin conjugated agarose	Pierce,USA
Sulfo-NHS-LC-Biotin	Pierce,USA
TEMED(N,N,N',N,Tetramethylethylenediamine)	Roth, Karlsruhe
Trifluoroacetic acid (TFA)	Sigma, Deisenhofen
Tris	Roth,Karlsruhe
Trypsin modified sequence grade	Promega,USA

2. Materials and Methods

2.1.4. Solutions and buffers

Acrylamide solution:

30% (w/v) Acrylamide

0.8% (w/v) Bisacrylamide

AP developing buffer:

100 mM Tris-HCL, pH 9.5

100 mM NaCl

5 mM MgCl₂

AP developing solution:

66 µl NBT(nitro blue tetrazolium) stock solution

33 µl BCIP(5-bromo-4-chloro-3-indolyphosphate) stock solution

BCIP stock solution:

5% BCIP in Dimethylformamide

Colloidal Coomassie staining solution:

0, 08% Coomassie Brilliant Blue G250 (CBB G250)

1, 6% ortho-phosphoricacid

8% Ammoniumsulfat

20% Methanol

Electrophoresis buffer:

0.124 M Tris

0.96 M Glycin

0.05 % SDS

Giemsa stain:

1% (v/v) Giemsa solution

9% (v/v) Giemsa buffer

2. Materials and Methods

Giesma buffer 10x ,pH 6.8:

130 mM Na₂HPO₄

100 mM KH₂PO₄

NBT stock solution:

5% NBT in 70% Dimethylformamide

PBS, pH 7.2:

140 mM NaCl

6.5 mM KCl

2.5 mM Na₂HPO₄

1.5 mM KH₂PO₄

Ponceau stain:

0.2% Ponceau S red

3% Trichloroacetic acid

Protease inhibitor cocktail Stock solution:

200 µg/ml of each of the inhibitors antipain,

Chymostatin, Aprotinine, Pepstatin, Trypsin, Leupeptin

Elastinal and Na-EDTA in PBS. Working solution 1:200 dilution

RPS-Medium:

450 ml RPMI 1640 Medium

50 ml heat denatured human plasma

SDS-PAGE concentrating gel pH 6.8:

0.5 M Tris/HCl

0.4% SDS

2. Materials and Methods

SDS sample buffer stock solution:

63 mM Tris/HCl

0.5 M sucrose

0.01 % Bromophenol blue

5 mM EDTA

1 % L-methionine

SDS sample loading buffer:

200 µl 0.5 M DTT

200 µl 20% SDS

600 µl SDS sample buffer stock solution

SDS-PAGE separating gel pH 8.8:

1.5 M Tris/HCl

0.4 % SDS

Washing buffer for strepdavidin beads:

Buffer A: 10 mM Tris-HCl, pH 7.5

0.2% NP-40

2 mM EDTA

150 mM NaCl

Buffer B : 10 mM Tris-HCl, pH 7.5

0.2% NP-40

2 mM EDTA

500 mM NaCl

Buffer C: 10 mM Tris-HCl pH 7.5

Western Blot Buffer:

48 mM Tris/HCl

39 mM Glycine

0.0375% SDS

20% Methanol

2. Materials and Methods

2.1.5. Host cells and parasite isolates

Human erythrocytes, blood group A Rh ⁺	University blood bank, Marburg
<i>Plasmodium falciparum</i> isolate FCBR	Philipps University, Marburg

2.1.6. Antibodies and working concentrations

Mouse anti Band III	Sigma Aldrich, Dilution 1:2000
Rabbit anti Glycophorin	Sigma Aldrich, Dilution 1:2000
Rabbit anti Spectrin	Sigma Aldrich, Dilution 1:2000
Goat anti rabbit, Alkaline Phosphates (AP)	DAKO Glostrup, Dilution 1:2000
Goat anti rabbit, Horse radish peroxidase (HPR)	DAKO Glostrup, Dilution 1:2000
Rabbit anti mouse, Alkaline Phosphatase (AP)	DAKO Glostrup, Dilution 1:2000
Rabbit anti mouse, Horse radish peroxidase (HPR)	DAKO Glostrup, Dilution 1:2000
Horse radish Peroxidase (SAV-HRP) Streptavidin avidin	Pharmingen, USA, Dilution 1:10,000
alkaline Phosphatase (SAV-AP) Streptavidin avidin	Pharmingen, USA, Dilution 1:10,000

2.1.7. Software

Biotoools™	Bruker Daltonic, Bremen
FlexAnalysis™	Bruker Daltonic, Bremen
FlexAcontrol™	Bruker Daltonic, Bremen
SYBYL MOLCAD	MOLCAD GmbH

2.2. Methods

2.2.1. Parasite Cultures

Parasites, *P. falciparum* FCBR were cultured in RPMI 1640 medium supplemented with 10% heat in-activated (56°C, 30 min) human plasma and erythrocytes of blood A+ group (Marburg Blood Bank) using standard procedures (Trager and Jensen, 1976). Trophozoite-infected erythrocytes were enriched to a parasitaemia of > 90% by gel floatation (Pasvol *et al.*, 1978).

2.2.2. Biotin labelling of bovine serum albumin and carbonic anhydrase II

Fatty acid free bovine serum albumin (BSA) was dissolved in phosphate buffered saline (PBS) to a final concentration of 10 mg/ml. For the analysis of the biotinylation pattern of BSA, 1ml of the solution containing 1.449×10^{-4} moles BSA was biotinylated with 1, 20, 40 and 60 molar equivalents of sulfo-LC-biotin for 30 min at 4°C. The reaction was stopped by adding glycine to final concentration of 10 mM. The unreacted biotin derivative was removed from the sample by centrifugation at 3,000 x g using a microconcentrator (Millipore Corp.) with a size exclusion of 5 kDa, this step was repeated twice after dilution with PBS before determining the protein concentration using the BCA system (Pierce). For bovine carbonic anhydrase II (CA II) 1.15×10^{-4} moles were biotinylated using a 40 fold molar excess of biotin derivative and processed as described for BSA.

For the analysis of artificially induced conformational changes, BSA and CA II were prepared as described above and subjected to elevated temperatures of 56°C or 80°C for 30 minutes before cooling and biotinylating with a 1:40 fold molar excess of the biotin derivative. To study BSA protein after thermal and chemical denaturation, BSA was subjected to an elevated temperature of 80°C for 30 min in the presence of 10 mM dithiothreitol (DTT), before cooling and biotinylating with the 40 fold molar excess of the biotin derivative or alternatively BSA was exposed to the temperature above 80°C,

2. Materials and Methods

reduced by 10 mM DTT and alkylated with 50 mM iodoacetamide for 45 min at room temperature in darkness before biotinylation as described.

2.2.3. Biotinylation of erythrocyte membrane protein Band III

Biotinylation was performed on non-infected human erythrocytes and in *Plasmodium falciparum*-infected human erythrocytes. 2×10^8 infected or non-infected erythrocytes were washed with PBS pH 7.6 and incubated in the same buffer containing different concentrations of the biotin derivative (2 mg ml^{-1} , 1 mg ml^{-1} , 0.5 mg ml^{-1}) for 1 h at 4°C in the presence of $100 \mu\text{M}$ furosemide. A negative control was included and the cells in both groups incubated under the same conditions but without biotin. Cells were sedimented by centrifugation at $1,300 \times g$ at 4°C for 5 min. To block and remove unreacted biotin derivative molecules, cells were washed three times in PBS pH 7.6 containing 100 mM glycine and finally in PBS. Soluble proteins were released after resuspending the cells in distilled water supplemented with a protease inhibitor cocktail to inhibit proteolysis and subjected to three cycles of freezing and thawing. A membrane fraction and a soluble fraction were prepared by centrifugation at $18,000 \times g$ for 20 min. The membrane fraction was solubilized using SDS-PAGE sample buffer and separated in a 7.5% SDS-PAGE.

2.2.4. Affinity purification of biotinylated peptides

For each experiment $72 \mu\text{l}$ of streptavidin sepharose beads were washed extensively with a buffer containing 1% NP-40 (v/v) in PBS before mixing with $100 \mu\text{g}$ of BSA or CA II biotinylated with different molar concentrations of biotin and incubating overnight at 4°C . The unbound non-biotinylated protein fraction was obtained as a supernatant after centrifugation at $10,000 \times g$ for 10 min. The pelleted beads containing bound biotinylated protein was washed three times in buffers A, B and finally in buffer C. The bound protein was eluted after boiling in $500 \mu\text{l}$ of denaturing SDS-PAGE sample buffer and separated in a 10% gel.

2.2.5. Gel Electrophoresis (Laemmli, 1970)

For 1D SDS-PAGE protein samples were dissolved in SDS-sample buffer and separated on 7, 5% or 10% gels under reducing conditions. The protein bands were then visualized by Coomassie staining.

2.2.6. Western Blot Analysis (Towbin *et al.*, 1979)

Proteins separated by SDS-PAGE were transferred to nitrocellulose membranes using semi dry-blotting. To detect biotin labeled proteins, the membranes were blocked with 3% BSA in PBS, pH 7.4, for 1 h at room temperature before incubation for 20 min with alkaline phosphatase-conjugated streptavidin (1:10,000/ 3% BSA in PBS, pH 7.4). The membranes were washed with 10 mM Tris-HCl, pH 7.4, 150 mM NaCl for 5 min and then in the same buffer containing 0.05 % Triton-X 100 for another 5 min. The biotin labeled proteins were visualized after staining with NBT and BCIP. The same membranes were then incubated with specific marker proteins at a dilution of 1:500 at 4° C overnight. Specific marker proteins were detected after incubation with horseradish peroxidase-conjugated anti-rabbit IgG (Dako) for 1h at room temperature and development of the filters using the ECL system (Amersham Biosciences) following the suppliers recommendation.

2.2.7. Sample preparation for mass spectrometry

For the analysis of intact protein, the biotinylated and non-biotinylated protein (BSA) in final concentration of 250 µg/ml was dissolved in ammonium bicarbonate 100 mM. The protein solution was purified and concentrated using ZipTips™ columns made from the reverse chromatography resins Poros R2 and Oligo R3 and eluted from the ZipTips™ with 2 µl of 33% (v/v) acetonitrile/ 0.1 % trifluoroacetic acid solution saturated with *sinapinic acid* directly onto a MALDI sample plate and air dried before analysis by the mass spectrometer in linear TOF mode.

2. Materials and Methods

For the analysis of peptides, protein bands were excised from polyacrylamide gels and subjected to in-gel trypsin digestion before mass spectrometric analysis (Helman *et al.*, 1995). Briefly, the excised spots were washed with 50% v/v acetonitrile (ACN) in 200 mM ammonium bicarbonate, the destained protein was in-gel reduced with 10 mM dithiothreitol (DTT) in 100 mM ammonium bicarbonate for 1 h at 56°C and alkylated with 50 mM iodoacetamide in the same buffer for 45 min at room temperature in darkness. The gel pieces were washed with 100 mM ammonium bicarbonate, dehydrated in ACN, and dried. The gels were re-swollen in 15 µl of 40 mM ammonium bicarbonate containing 20 µg ml⁻¹ sequencing grade trypsin (Promega) for 45 min at 4° C. Excess protease containing solution was discarded and the gel pieces were incubated at 37 °C for 18 hours.

To extract the peptides, 15 µl of a diffusion solution (10% ACN, 1% trifluoro-acetic acid (TFA)) were added and the samples sonicated for 45 min at 37 °C. The soluble portion of the sample was evaporated to dryness. For mass spectrometry measurements the samples were redissolved in 15 µl of 0.1% v/v TFA, 5 % v/v ACN in water. The peptides were purified and concentrated using ZipTips™ columns made from the reverse chromatography resins Poros R2 and Oligo R3. The bound peptides were washed with a solution of 0.5% formic acid and eluted from the ZipTips™ with 2 µl of 33% (v/v) acetonitrile/ 0.1 % trifluoroacetic acid solution saturated with *α*-cyano-4-hydroxycinnamic acid directly onto a MALDI sample plate and air dried before analysis in the mass spectrometer.

Alternatively, for the affinity enrichment of biotinylated tryptic peptides, SDS-PAGE separated proteins were transferred to nitrocellulose membrane and visualized by Ponceau staining. The stained membrane was cut into 2 x 2 mm square pieces and thoroughly destained with water, treated with 10 mM dithiothreitol in 100 mM ammonium bicarbonate for 1 h at 56°C and alkylated with 50 mM iodoacetamide in the same buffer for 45 min at room temperature in darkness. The nitrocellulose pieces were washed with 100 mM ammonium bicarbonate and dried. The membranes were incubated in a minimal volume of 40 mM ammonium bicarbonate containing 20 µg ml⁻¹ sequencing grade trypsin (Promega) and incubated at 37°C for 18 hours. The tryptic peptides were extracted from the membrane pieces using 20% ACN in 1% TFA twice, with sonication

at 37°C for 45 min. The eluted peptides were resuspended in 500 µl of 100 mM ammonium bicarbonate and incubated overnight with 72 µl of washed streptavidin sepharose beads to affinity purify the biotinylated peptides. The unbound, non-biotinylated peptide fraction was obtained as a supernatant after centrifugation at 10,000 x g for 10 min. This fraction was evaporated to dryness and resuspended in 0.1% TFA before processing for MS. The sepharose beads containing bound biotinylated peptides were washed three times in 100 mM ammonium bicarbonate, 1% octylglucoside. The bound peptides were eluted with 70% ACN, 5% TFA, and 1 mM D-biotin in 100 mM ammonium bicarbonate at room temperature for 2 h. The solution was evaporated to dryness and resuspended in 0.1% TFA before processing for MS.

2.2.8. Mass spectrometry analysis and protein identification

Mass spectrometry was performed using a Bruker Daltonics Ultraflex™ mass spectrometer equipped with a nitrogen laser (laser 337 nm, 3ns pulse width and 50 Hz repetition rate) and Panoramic mass range focusing (PAN™) technology and High-Precision Calibration (HPC™) for high mass accuracy. For the analysis of intact protein, mass spectra were acquired after an external calibration using reference protein standards; trypsinogen, protein A, Albumin-Bovine, Protein A²⁺ and Albumin-Bovine²⁺ (Protein calibration standard II, Bruker Daltonics). Mass spectra were acquired in the linear positive mode with a pulsed extraction using approximately 100 laser shots and the masses assigned and processed using BiTools™ and FlexAnalysis™ software (Bruker Daltonics). For the tryptic digests peptide mass fingerprint spectra were acquired in the reflectron positive mode with a pulsed extraction using an average of 100 laser shots. The spectra were acquired after an external calibration using reference peptides (Peptide mixture II, Bruker Daltonics). The spectra were further internally calibrated using trypsin autolysis peaks (842.5100, 2211.1046 Da). Monoisotopic masses were assigned and processed using BiTools™ and FlexAnalysis™ software before submission to the Mascot program (www.matrixscience.com) for searches against the non-redundant NCBI database. The following variable modifications were used in the searches; methionine oxidation, lysine sulfo NHS-LC-biotin labelled, Pyro-glu from E at

2. Materials and Methods

the N-terminus, Pyro-glu from Q and a fixed cysteine carbamidomethylation modification. To analyze the effect of missed proteolytic cleavage of peptides on the identification of the proteins and biotinylated lysine residues, the searches were done allowing complete cleavage (0 miscleavage sites) and allowing 1 or 2 miscleavage sites. A mass accuracy of 50 ppm or better was used in all the identifications.

MS-MS analysis was done using the LIFT™ mode to provide i-, a-, b- and y-ions. The masses of the fragmented ions were submitted to the Mascot program for database searching using the following parameters; peptide mass tolerance of 100 ppm, MS-MS tolerance of 0.7 Da and 2 missed cleavage sites. The variable and fixed modifications of amino acid residues were used as described in the peptide mass fingerprint analyses.

3. Results

As noted in the goals section of this thesis, the aim of this study was to use biotinylation patterns in order to probe conformational changes in protein structures. To establish the system, BSA was used as a model protein, as the structure of this protein has been determined using various methods, and it is readily and cheaply available in the laboratory.

3.1. Biotinylation pattern of BSA is saturable.

In order to probe conformational changes in proteins using BSA, it was necessary to establish whether the biotinylation of our model protein BSA is saturable, as this is required to achieve consistent results.

The biotinylation reaction that occurs between the active ester group of sulfo-NHS-LC biotin derivatives and the primary amines of proteins and/or the epsilon amino group of lysine residues with the formation of an amide bond resulting in an increase in mass by 339.1611 Da for each lysine residues in polypeptide (Figure7).

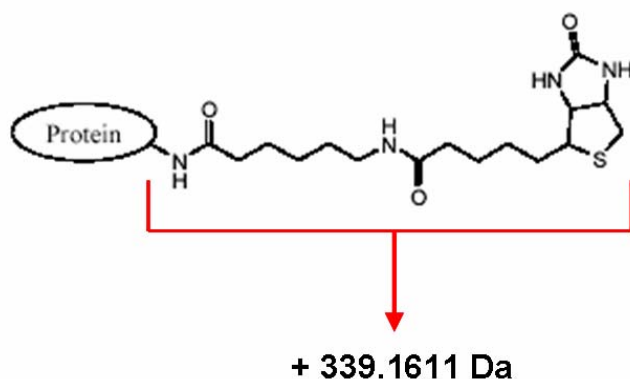


Figure 7. Biotinylation with sulfo-NHS-LC-Biotin increases the mass of peptides by a specific value. Using peptide mass finger printing after mass spectrometry it is possible to identify modified lysine residues in peptides. Modified peptides show a mass shift of 339.1611 Da compared to the non-biotinylated version (modified from Pierce).

3. Results

Since BSA has 60 lysine residues, it is to be expected that under optimal conditions all these residues can be biotinylated. This however assumes that all lysine residues are accessible to the biotin moiety, which is unlikely considering the tertiary protein structure. Nevertheless, if all the 60 lysine residues are biotinylated the calculated mass shift of the protein would be 20.34 kDa. To investigate the effect of biotinylation of BSA on the electrophoretic mobility and mass alteration of protein, the intact protein was biotinylated with an increasing molar ratio concentration of sulfo-NHS-LC-biotin derivatives. After the removal of excess unreacted biotin by size exclusion centrifugation, the biotinylated and non-biotinylated control proteins were subjected to 1D gel electrophoresis and in a parallel experiment the intact protein was directly analyzed by linear TOF by mass spectrometry to determine the number of lysine residues that had been biotinylated. An analysis of biotinylated protein by SDS-PAGE confirmed the increase in molecular mass of Coomassie stainable protein, which was verified by biotin detection with streptavidin (SAV). As shown in figure 8, an increase in the concentration of the biotinylating reagent leads to an increase in the mass of the protein up to a maximum of 40 fold molar excess of biotin (Figure 8, lane 5). Further increase in concentration to 60 fold molar excess does not results in any significant increase in the mass of the protein (Figure 8, Lane 6).

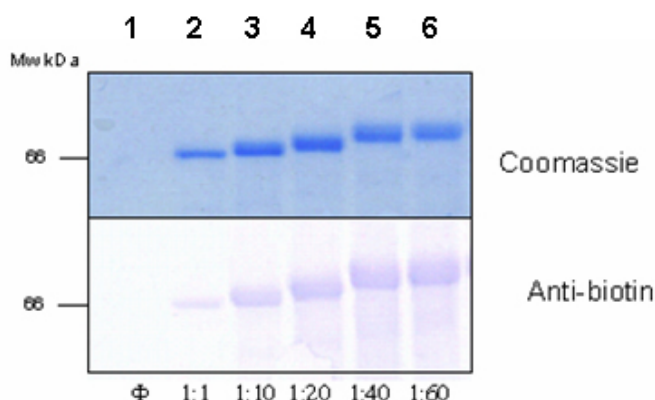


Figure 8. Analysis of the mass of BSA after biotinylation using increasing concentrations of sulfo-NHS-LC-Biotin. BSA was biotinylated with sulfo-NHS-LC biotin at different molar ratios and analyzed by SDS-PAGE and Coomassie staining or by reaction with alkaline phosphatase-conjugated SAV on nitrocellulose filters .

3. Results

The MS-TOF spectrometry in linear mode also showed that the increase in mass of protein is in an almost linear correlation with the molar excess of biotin derivatives up to a 40 fold molar excess of derivative (Figure 9 and Table 2).

Mole ratio Sulfo-NHS-LC-biotin : BSA	Mass of BSA by MS (Da)	Number of incorporated biotinylated residues (Predicted from mass shift)
0	66,525.3	none
1	66,598.0	Not detectable
10	68,269.0	5
20	69,853.9	10
40	72,271.4	17
60	72,599.5	18

Table 2. Effect of the increase in the molar ratio of sulfo-NHS-LC-biotin to BSA on the mass of BSA. BSA was biotinylated with increasing mole ratio concentration of sulfo-NHS-LC-biotin derivatives and the biotinylated protein was subjected to be analyzed by linear mode time of flight mass spectrometry. Each modified lysine residue results in increase in mass of approximately 339 Da.

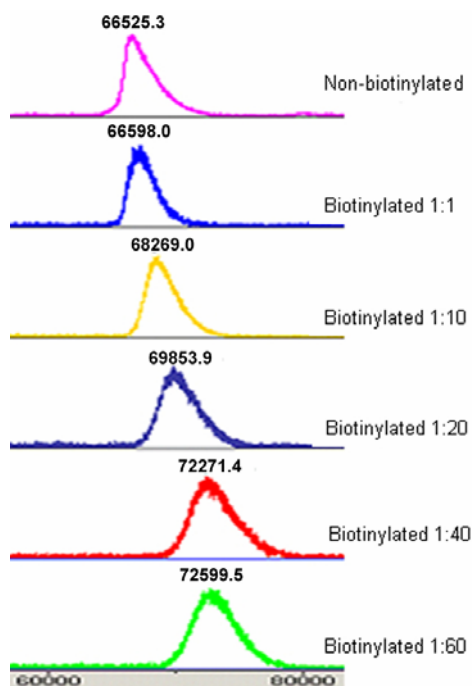


Figure 9. Effect of the increase in the concentration of sulfo-NHS-LC-biotin on the biotinylation and mass of BSA. BSA was biotinylated with increasing mole ratio concentration of sulfo-NHS-LC-biotin derivatives and the biotinylated protein was subjected to be analyzed by linear mode time of flight mass spectrometry.

3.2. Biotinylated lysine residues in BSA are uniformly distributed in the protein

In addition to the analysis of the mass of the intact protein, the biotinylation of BSA was analyzed by peptide mass finger printing (PMF) to investigate whether biotinylation occurred randomly or whether specific lysine residues were preferentially biotinylated. BSA was biotinylated with 1,10,20,40 and 60 fold molar excess of sulfo-NHS-LC-biotin. The biotinylated and non-biotinylated BSA was subjected to 1D gel electrophoresis. The SDS-PAGE separated proteins were digested with trypsin and the eluted peptides subjected to mass spectrometry before identification by peptide mass fingerprinting. As shown in table 3, the number of biotinylated peptides (lysine residues) increased with the increase in the concentration of the biotin derivative. Beyond 40 fold molar excess of the derivative no new biotinylated lysine residues are identified. As in the analysis of the intact protein, there is a correlation between the numbers of the modified lysine residues identified by MS and the predicted numbers after MS of the intact protein in the linear mode. More importantly, when biotin concentrations below the point of maximal incorporation were used, labelling of lysine residues did not occur randomly but at specific sites. Lysine residues which were biotinylated at lower concentrations of the biotin derivative were also biotinylated when higher concentrations were used. All lysine residues which were biotinylated were detected in 5 out of 5 analyses. These findings indicate a concentration dependent, preferential accessibility of individual residues. In addition, the biotinylation process was highly specific and reproducible between experiments suggesting that the labelling is dependent on the conformation of the protein. Since biotinylation of BSA is saturated beyond 40 fold molar excess of biotin derivative, in the subsequent experiments, BSA was biotinylated with this molar ratio of biotin derivative.

3. Results

Lysine (K)	Molar ratio Sulfo-NHS-LC-Biotin / BSA					
	ϕ	1	10	20	40	60
K 36				+	+	+
K 100					+	+
K 156				+	+	+
K 160				+	+	+
K 204				+	+	+
K 211			+	+	+	+
K 228					+	+
K 235		+	+	+	+	+
K 245					+	+
K 266					+	+
K 374					+	+
K 401			+	+	+	+
K 412					+	+
K 420					+	+
K 455		+	+	+	+	+
K 463					+	+
K 498					+	+
K 559					+	+
Total	0	2	4	8	18	18

Table 3. Biotinylation of individual lysine residues follows a concentration dependent specific order. BSA was biotinylated with 1, 10, 20, 40 and 60 fold molar excess of sulfo-NHS-LC-biotin. Tryptic peptides were analyzed by tandem mass spectrometry to identify biotinylated lysine residues. All lysine residues listed as biotinylated were detected in 5 out of 5 analyses.

3.3. Not all lysine residues of BSA can be detected by mass spectrometry

As shown in the previous section, addition of a biotin derivative leads to a circa. 339 Da shift in lysine-containing peptides derived from the BSA protein. In this study one portion of BSA was subjected to be biotinylated using 40 fold higher molar ratio of biotin derivative at room temperature. The other portion of BSA was not biotinylated. After separation by gel electrophoresis, the Coomassie stained protein bands were cut, digested with trypsin and subjected to mass spectrometry in the reflectron mode. The obtained mass list was used to search against database. Protein was identified from peptide mass fingerprints using the Mascot search program with the MSDB database. Mass tolerance of 50 or 100 ppm and one missed cleavage site were used. Oxidation of

3. Results

methionine and carbamidomethylation of a cysteine residue were considered for modifications. Both protein samples were identified as BSA with more than 56% sequence coverage. The sequence coverage was calculated by using all amino acids in the detected peptides which could be identified in the primary sequence of the protein. The obtained sequence coverage of BSA is shown in figure 10. Note that although the sequence coverage is similar, this coverage is composed of peptides that differ between biotinylated and non-biotinylated samples.

Nonbiotinylated	1 MKWVTFISLL LLFSSAYSRG VFRRDTHKSE IAHRFKDLGE EHFKGLVIA
Biotinylated	1 MKWVTFISLL LLFSSAYSRG VFRRDTHKSE IAHRFKDLGE EHFKGLVIA
	51 FSQYLQQCPF DEHVKLVNELTEFAKTCVAD ESHAGCEKSLHTLFGDELCK
	51 FSQYLQQCPF DEHVKLVNELTEFAKTCVAD ESHAGCEKSLHTLFGDELCK
	101 VASLRETYGDMADCCCKQEPERNEC FLSHKDDSPDLPKLPDPNTLCDEF
	101 VASLRETYGDMADCCCKQEPERNEC FLSHKDDSPDLPKLPDPNTLCDEF
	151 KADEKKFWGKYLEIARRHPYFYAPEL LYYANKYNGVFQECQAEDKGAC
	151 KADEKKFWGKYLEIARRHPYFYAPEL LYYANKYNGVFQECQAEDKGAC
	201 LLPKIETMREKVLTSARQRL RCASIQKFGERALKAWSVARLSQKFPKAE
	201 LLPKIETMREKVLTSARQRL RCASIQKFGERALKAWSVARLSQKFPKAE
	251 FVEVTKLVTDLTKVHKEC CHGDLLCADDR ADLAKYICDN QDTISSKLE
	251 FVEVTKLVTDLTKVHKEC CHGDLLCADDR ADLAKYICDN QDTISSKLE
	301 CCDKPLLEKSHCIAEVEKDA IPENLPPLT ADFAEDKDVCK NYQEAKDAFL
	301 CCDKPLLEKSHCIAEVEKDA IPENLPPLT ADFAEDKDVCK NYQEAKDAFL
	351 GSFLYEYSRR HPEYAVSVLLRLAKEYEATLEECCAADDPH ACYSTVFDKL
	351 GSFLYEYSRR HPEYAVSVLLRLAKEYEATLEECCAADDPH ACYSTVFDKL
	401 KHLVDEPQNLIKQNCDFEKLGEY GFQNALIVRYTRKVPQ VSTPTLVEVS
	401 KHLVDEPQNLIKQNCDFEKLGEY GFQNALIVRYTRKVPQ VSTPTLVEVS
	451 RSLGKVGTRC CTKPESERMPCTEDYLSLILNRLCVLHEKTPVSEKVTCC
	451 RSLGKVGTRC CTKPESERMPCTEDYLSLILNRLCVLHEKTPVSEKVTCC
	501 TESLVNRRPC FSALTPDETY VPKAFDEKLF TFHADICTLP DTEKQIKKQT
	501 TESLVNRRPC FSALTPDETY VPKAFDEKLF TFHADICTLP DTEKQIKKQT
	551 ALVELLKHHPKATEEQLKTMENFVAFVDKCCAADDKEACFAVEGPKLVV
	551 ALVELLKHHPKATEEQLKTMENFVAFVDKCCAADDKEACFAVEGPKLVV
	601 STQTALA
	601 STQTALA

Figure 10. Comparison of the detected sequence coverage in biotinylated and non-biotinylated BSA. The identified amino acids are labelled in red. Both proteins were identified with >56% sequence coverage.

3. Results

MS analysis of the non-biotinylated BSA detected 27 different peptides, ranging in mass from 689.41 to 2458.21 Da. Out of the total 60 lysine residues in the BSA amino acid sequence, 26 lysine residues were identified. The mass spectra of peptides from biotinylated BSA shows more peaks than from non-biotinylated BSA. In the modified BSA, 36 different peptides were identified with masses ranging from 599.33 to 2868.51 Da. Among the identified peptides, 34 lysine residues were found of which 18 lysines were biotinylated (Table 4).

Lysine	Non-biotinylated BSA	Biotinylated BSA	Lysine	Non-biotinylated BSA	Biotinylated BSA
K 2	-	-	K 309	+	+
K 28	-	-	K 318	-	--
K 36	+	+	K 336	+	+
K 44	+	-	K 340	+	+
K 65	-	-	K 346	-	-
K 75	+	+	K 374	-	+
K 88	-	-	K 386	-	+
K 100	+	+	K 399	+	-
K 117	-	+	K 401	-	+
K 130	+	-	K 402	+	+
K 138	+	+	K 412	+	+
K 140	+	-	K 420	-	+
K 151	+	-	K 437	+	+
K 155	-	-	K 455	-	+
K 156	-	+	K 463	-	+
K 160	-	+	K 489	-	-
K 183	+	+	K 495	-	-
K 197	+	-	K 498	-	+
K 204	-	+	K 523	+	+
K 211	-	+	K 528	-	-
K 228	-	+	K 544	+	+
K 235	-	+	K 547	-	-
K 245	+	+	K 548	-	-
K 248	-	+	K 557	-	-
K 256	-	-	K 559	-	+
K 263	-	-	K 561	-	-
K 266	-	+	K 568	-	-
K 285	+	-	K 580	+	+
K 297	+	-	K 587	+	-
K 299	-	+	K 597	+	-
K 304	+	+	total	26	34

Table 4. List of detected lysine residues in biotinylated and non-biotinylated BSA. One portion of BSA was biotinylated using 40 fold molar excess of sulfo-NHS-LC-biotin. The other portion of BSA was not biotinylated. Biotinylated and non-biotinylated samples were separated by SDS-PAGE and processed for MS analysis. The bold residues indicate the biotinylated lysine.

3. Results

As shown in Table 4, 16 lysine residues were found in both biotinylated and non-biotinylated samples. Ten Lysine residues were only detected in non-biotinylated BSA where 18 lysine residues were only identified through the modified peptides after biotinylation of BSA with 40 fold molar biotin derivatives. 14 lysine residues were detected neither in biotinylated nor in non-biotinylated BSA. Furthermore four lysine residues were detected in both modified and non-modified versions in biotinylated BSA. To predict the tryptic BSA peptides and to determine the distribution of lysine residues in BSA amino acid sequences, a theoretical digestion of BSA protein was done by ExPASy (Expert Protein Analysis System) proteomic server (www.expasy.org) using trypsin as a protease and setting the input parameters to include oxidation of methionine, carbamidomethylation of cysteine and maximum one missed cleavage site. The *in silico* trypsin digestion of BSA generated 180 theoretical peptides with their corresponding masses between 500.246 to 3579.85 Da. More than half of these peptides contain one or two lysine residues. 11 peptides among the theoretical digested peptides in BSA sequences have a mass of less than 600 Da. These low molecular weight peptides could not be detected, probably because their location on the spectra overlapped with the matrix clusters peaks. Two of these lysine-containing peptides (K156 and K559) were later identified from the biotinylated sample as biotinylated peptides, which increased their mass. Detection of long polypeptides with mass larger than 2000 Da in both samples is also limited because of their hydrophobic character. These high molecular weight peptides contain cysteine or methionine residues. Hydrophobic peptides can be lost during sample preparation because of adsorption to plastic surfaces of pipette tips and cups. In addition, in MALDI mass spectra as m/z of peptide increases, resolution and mass accuracy progressively decrease. This causes unmatched masses which are excluded from the mass list for the protein identification.

3.4. The modified lysine residues are identified by MS and MS/MS analysis

Comparison of the MS spectra from biotinylated and non-biotinylated BSA clearly reveals differences and indicates, as expected, some peaks which are only present in the biotinylated sample but absent in the non-biotinylated sample. As shown in figure 11,

3. Results

in comparing of sections from two mass spectra, three new peaks with m/z of 1156.633, 1329.692 and 1340.712 with significant intensities were observed in the biotinylated sample through all experiments. Further analysis of each of these peptides after fragmentation in tandem MS analysis led to the identification of individual biotinylated lysine residues.

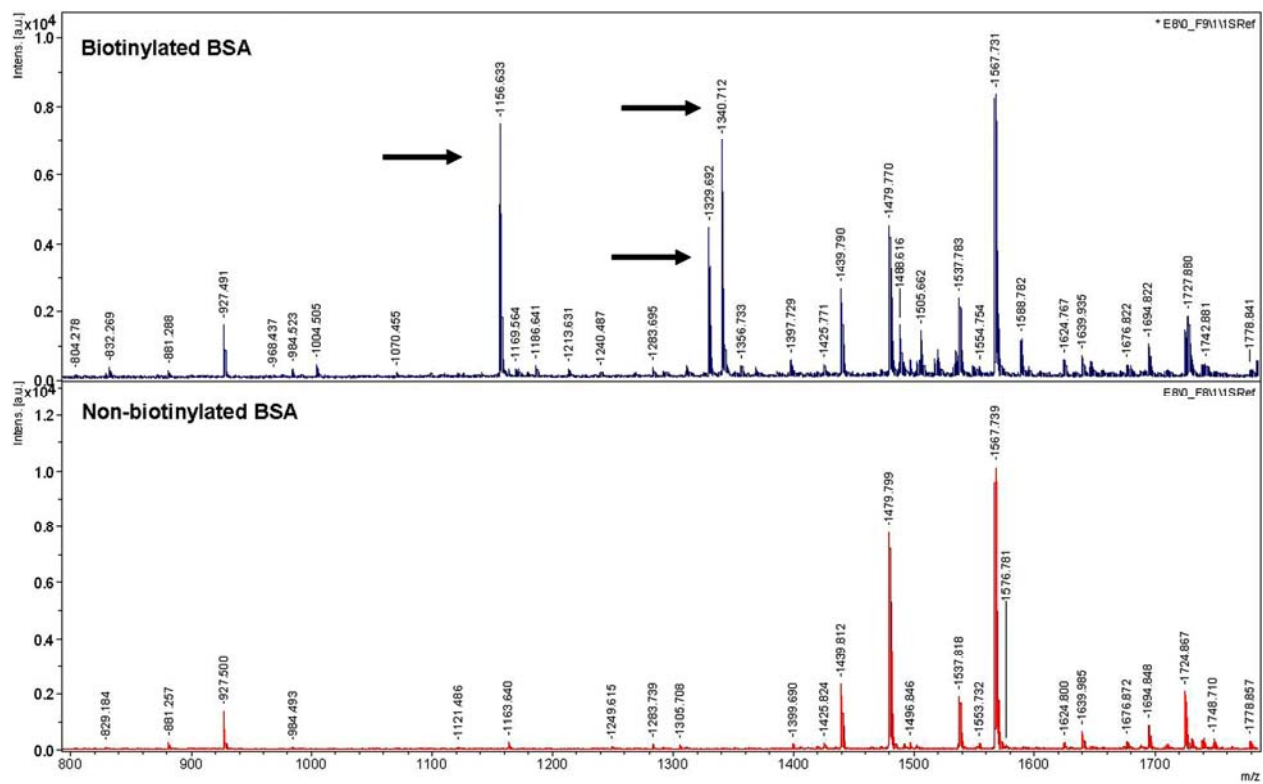
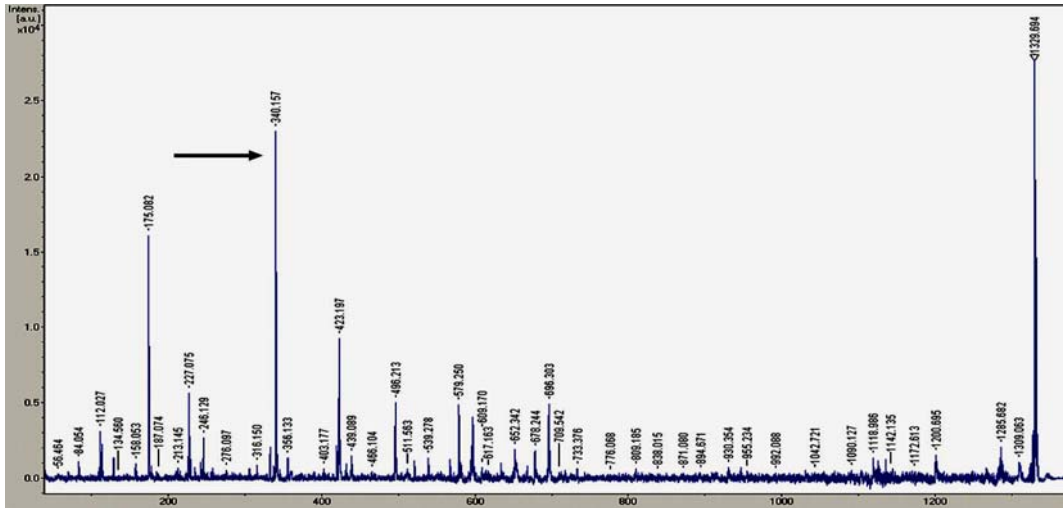


Figure 11. Comparison of biotinylated and non-biotinylated BSA. One fraction of BSA was biotinylated with 40-fold higher mole ratio of biotin derivative. The other fraction was non-biotinylated. The same aliquot of two fractions was separated by 1D gel electrophoresis and later analyzed by mass spectrometry. The upper spectrum is from the biotinylated protein and the other one from non-biotinylated BSA. The marked peaks show the biotinylated peptides.

Analysis of the peptide with m/z 1329.694 by tandem mass spectrometry resulted in the fragmentation of the peptide into its constituent amino acids. MS/MS analysis determined the sequence of the peptide (EKVLTSSAR) (Figure 12). Comparison of the observed mass (1329.694) and theoretical mass (990.5472) of this peptide showed a difference of 339.147 Da, corresponding to the mass of one biotin moiety. As shown in

3. Results

figure 12, the biotin tag is detectable in spectra with a mass of 340.157. In addition the peptide sequence contains one missed cleavage site.



210 - 218 1329.69 R.EKVLTSAR.Q NHS-LC-Biotin (K)

#	b	Seq.	y	#
1	130,05	E	1329,694	9
2	597,31	K	1200,68	8
3	696,37	V	733,42	7
4	809,46	L	634,35	6
5	910,51	T	521,27	5
6	997,54	S	420,22	4
7	1084,57	S	333,19	3
8	1155,61	A	246,16	2
9		R	175,12	1

Figure 12. MS/MS spectra of peptide 1329.694 which was detected in the biotinylated BSA. The sequence of peptide (EKVLTSAR) has one missed cleavage site and the spectrum contains the biotin tag peak in mass 340.157 Da.

3.5. Biotinylated peptides can be effectively affinity purified using streptavidin sepharose beads

In order to isolate only peptides derived from biotinylated BSA molecules, biotinylated intact protein or biotinylated peptides were affinity purified by streptavidin sepharose beads using two different approaches:

3.5.1. Affinity purification of intact biotinylated BSA

In the first experiment, biotinylated BSA was isolated by streptavidin sepharose beads, tryptically in gel digested and the resulting peptides analysed by mass spectrometry (Figure 13, left side).

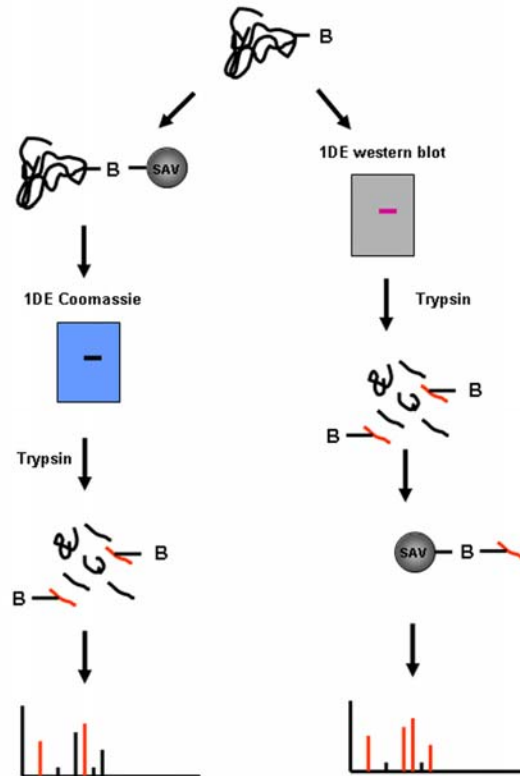


Figure 13. Schematic representation of the experimental methodology for the affinity purification of biotinylated intact BSA or biotinylated BSA peptides using streptavidin beads. BSA was biotinylated with 40-fold higher mole ratio of sulfo-NHS-LC-biotin and purified by streptavidin beads (SAV) either as an intact biotinylated protein or as biotinylated peptides, the purified samples were eluted and analyzed by mass spectrometry.

As shown in figure 14, at a molar ratio of 1:1 most of the BSA is not biotin labelled and it is not bound by Streptavidin beads. At biotin molar ratios 1:20 and 1:40 all the BSA is biotin labelled and it binds to the SAV beads. As expected there is no significant increase in the mass of BSA after labelling with Sulfo NHS-LC- biotin at molar ratios greater than 1:40 (Figure 14, Lane 11 and 12). A substantial amount of biotinylated BSA remains in the unbound fraction at molar ratios 1:60 (Figure 8, lane 6). The

3. Results

densitometric analysis indicated that only boiling of the beads in the denaturing sample buffer yielded a partial recovery of biotinylated protein from streptavidin Sepharose (65% recovery). This could be due to the saturation of the binding sites in SAV beads.

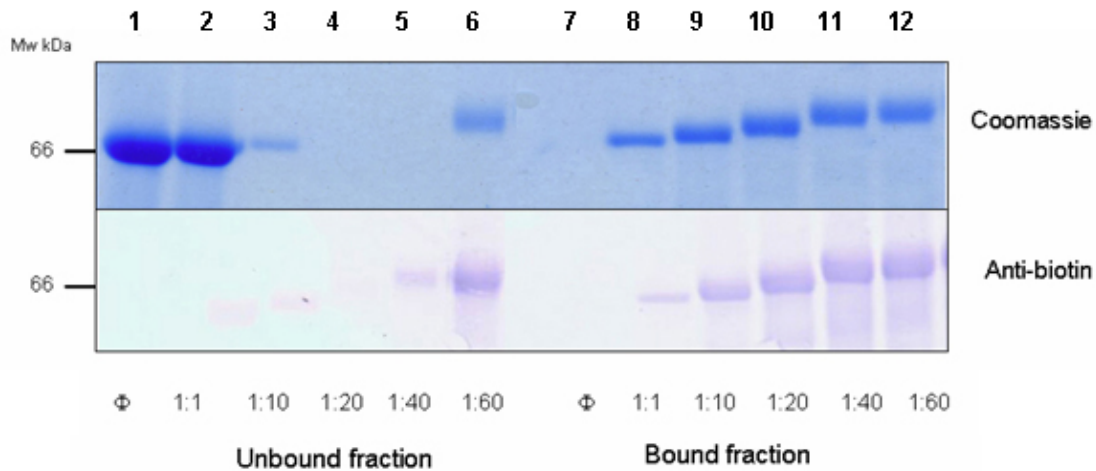


Figure 14. Comparison of bound and unbound fraction of biotinylated BSA. 100 μ g of biotinylated BSA were incubated with 72 μ l of Streptavidin beads, and 10 μ g equivalents of the unbound and bound fractions were analyzed by SDS-PAGE and western blot.

3.5.2. Affinity purification of biotinylated BSA peptides

In a parallel, complementary approach to 3.5.1, biotinylated BSA which was separated by 1D gel electrophoresis and transferred to nitrocellulose membrane, subjected to tryptic digestion and the resulting peptides were then purified by streptavidin sepharose beads as described above (Figure 13, right side). The comparison of the spectra from starting, bound and unbound fractions is shown in figure 15. Data base searching of generated peptides in bound fraction identified the protein as BSA. In the bound fraction, 23 BSA specific peptides were detected by MS. Out of all reported peptides, 95% were biotinylated (Table 4) which indicates the efficient affinity purification of biotinylated peptides from the streptavidin beads. Only 2 peptides containing lysine residues K285 and K386 were observed in the bound fraction which were non-biotinylated and could possibly be binding non-specifically to the streptavidin sepharose beads. These non-biotinylated peptides have very low intensity peaks in the spectra. In contrast to

3. Results

biotinylated peptides the sequences of non-biotinylated peptides [(ADLAK) and (EYEATLEECCA)] have no missed cleavage site. The MS analysis of the unbound fraction identified only four peptides and they all are not biotinylated. Two unmodified lysine residues (K75 and K374) were detected in this fraction.

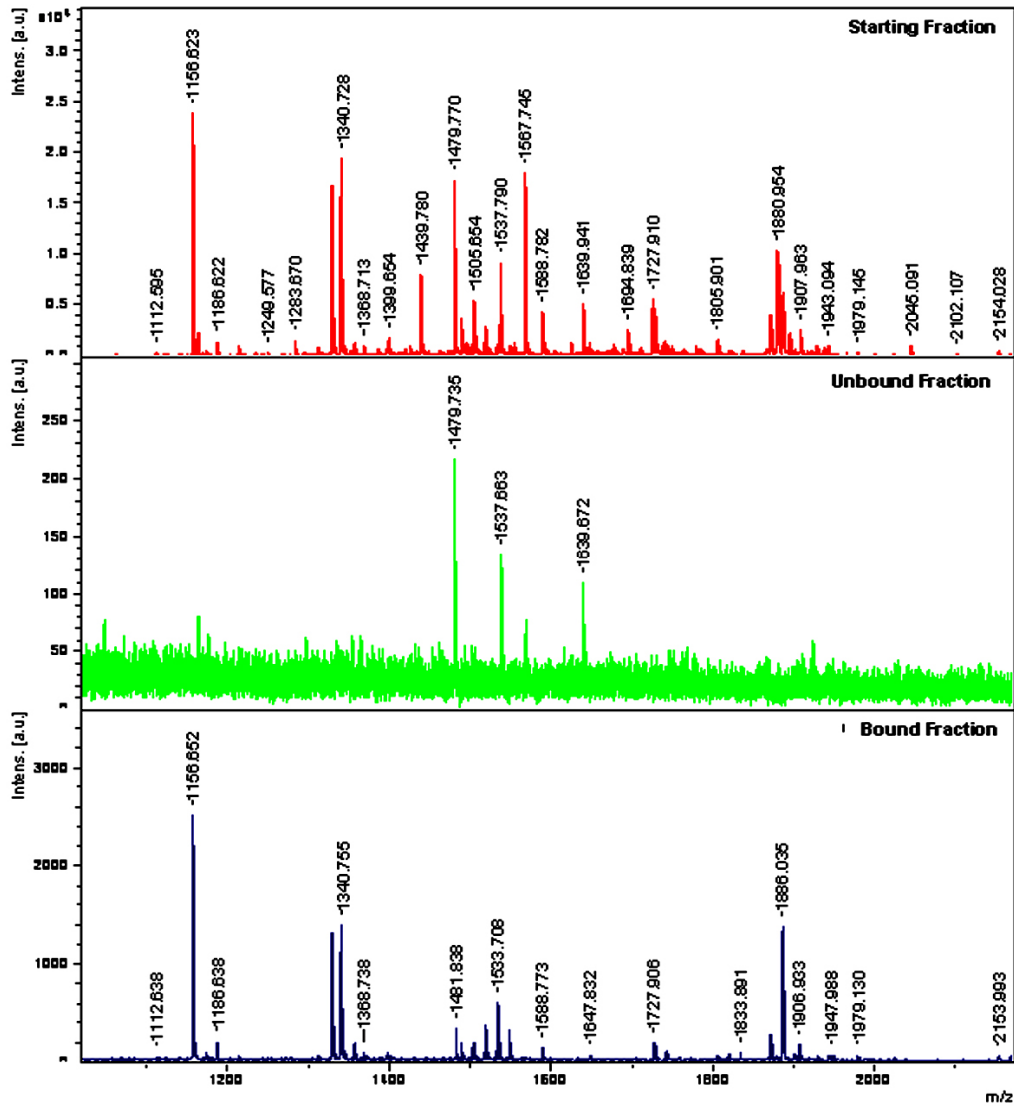


Figure 15. Comparison of generated peptides from starting, bound and unbound fractions of biotinylated BSA. Biotinylated BSA was separated by SDS-PAGE and transferred to nitrocellulose filters. The band was trypsinized and the generated peptides were affinity purified using streptavidin sepharose beads. The starting, bound and unbound fractions were subjected to mass spectrometry using the reflectron mode and the resulting spectra are shown.

3.6. Biotinylated lysine residues are resistant to trypsin cleavage

The identification of proteins by peptide mass fingerprinting (PMF) is dependent on the generation of peptides by protease treatment, determination of their masses by mass spectrometry and comparison of these masses to theoretical masses in databases. Trypsin, the most commonly used protease specifically cleaves peptides at the carboxyl termini of the basic amino acid residues arginine and lysine. This reaction is inhibited by the presence of a proline residue at the C-terminus adjacent to these two amino acids. The inhibition of trypsin cleavage generates partials i.e. peptides with missed cleavage sites. Since biotinylation occurs at the protonated epsilon amino group of the lysine residue, the effect of biotinylation on the recognition and cleavage of lysine residues was analyzed. BSA was biotinylated with 40 molar excess of the biotin derivative and processed as described above. Nitrocellulose bound BSA was subjected to tryptic cleavage in an excess of the protease. The generated peptides were eluted and the biotinylated peptides were affinity purified on streptavidin beads and analyzed by MS before submitting the masses for searching using the MASCOT search machine. In this analysis, setting the missed cleavage site to 0 in the searches did not identify the sample as BSA, clearly indicating that there were several missed cleavage sites after biotinylation. However increasing the missed cleavage sites to 1 in the searches, identified BSA with a high Mascot score and 56% sequence coverage. MS analysis showed that all 21 identified biotinylated BSA peptides, contained a lysine missed cleavage site while the 2 non-biotinylated peptides did not have a missed cleavage site (Table 5). The results showed that the biotinylation of a lysine residue prevents cleavage by trypsin at that site in the lysine-containing peptide. Increasing the number of missed cleavage site to 2 resulted in the identification of only 1 additional biotinylated peptide.

3. Results

amino acids	m/z	Missed cleavage sites	Amino acid sequence
35 - 44	1588.78	1	FK*DLGEEHFK
89 - 105	2285.17	1	SLHTLFGDELCK*VASLR
156 - 160	1004.54	1	K*FWGK
157 - 167	1784.91	1	FWGK*YLYEIAR
198 - 209	1727.90	1	GACLLPK*IETMR
210 - 218	1329.72	1	EK*VLTSSAR
223 - 232	1534.73	1	CASIQK*FGER
233 - 241	1340.76	1	ALK*AWSVAR
242 - 248	1186.67	1	LSQK*FPK
264 - 280	2453.09	1	VHK*ECCHGDLLECADDR
281 - 285	517.39	0	ADLAK
372 - 386	2154.00	1	LAK*EYEATLEECCA
375 - 386	1502.67	0	EYEATLEECCA
400 - 420	3274.72	2	LK*HLVDEPQNLIK*QNCDQFEK
413 - 433	2868.47	1	QNCDQFEK*LGEYGFQNALIVR
452 - 459	1156.66	1	SLGK*VGTR
460 - 468	1505.66	1	CCTK*PESER
496 - 507	1805.89	1	VTK*CCTESLVNR
558 - 568	1647.87	1	HK*PKATEEQLK

Table 5. Biotinylated lysine residues are resistant to trypsin. BSA was biotinylated with 40 molar excess of the biotin derivative and processed as described in materials and methods. The protein was digested and analyzed by MS before submitting the masses for searching using the MASCOT search machine to identify the peptides. K* indicates biotinylated lysine residue, with a missed cleavage site.

3.7. Elevated temperatures expose novel lysine residues in the biotinylation pattern of BSA

Since the biotinylation pattern of BSA is highly reproducible and obviously depends on the accessibility of individual lysine residues in the protein structure, it was examined whether treatments that result in conformational changes of the protein affect biotinylation patterns. BSA molecule has a heart shaped structure made up of three homologous domains which are divided into nine loops by 17 disulphide bonds. Serum albumin when heat-treated, undergoes two different structural stages. The first stage is reversible whilst the second stage is irreversible but does not necessarily result in a complete destruction of the ordered protein structure. Heating up to 65°C can be regarded as the first stage, with subsequent heating above that as the second stage. Therefore heating above 65°C results in thermal denaturation and possibly conformational changes in BSA. The biotinylation pattern of BSA was analyzed after

3. Results

exposing the protein to different temperatures. BSA was biotinylated at room temperature with a 40 fold molar excess of sulfo-NHS-LC-biotin or subjected to elevated temperatures of 56°C and 80°C for 30 min before cooling and biotinylating with the 40 fold molar excess of the biotin derivative as described above. The proteins were separated by SDS-PAGE. As shown in figure 16, heat treatment of BSA to the temperature of 56°C (Lane 3) and 80°C (Lane 4) before biotinylation does not results in the significant difference in the pattern of the protein electrophoresis which suggested that either the biotinylation pattern of BSA after exposure to the different temperature was not changed or only few new lysine were biotinylated after temperature treatment.

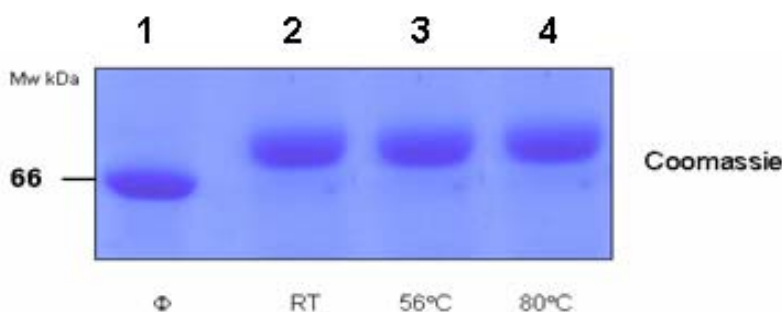


Figure 16. Comparison of the biotinylation pattern of BSA after exposure to different temperatures. BSA was biotinylated with sulfo-NHS-LC biotin at room temperature (RT) or after exposure to 56°C and 80°C before cooling and biotinylation and analyzed by SDS-PAGE and Coomassie staining.

To confirm any changes in the biotinylation pattern of BSA after temperature treatment, the Coomassie stained bands were excised and analyzed as described above by PMF to identify biotinylated peptides. For BSA treated at 56°C, the MS analysis revealed identical biotinylated peptides as detected at room temperature but exposure of BSA to a temperature above 80°C prior to biotinylation results in the biotinylation of two new lysine residues which are not biotinylated at room temperature or after exposure to 56°C (Table 5). The comparison of the spectra of the biotinylated BSA with and without the temperature treatment indicated two extra peaks with m/z 1979.113 (K437) and 2810.104 (K523) in the biotinylated spectra which were detected only in the biotinylated sample after exposure to 80°C (Figures 17 a, b).

3. Results

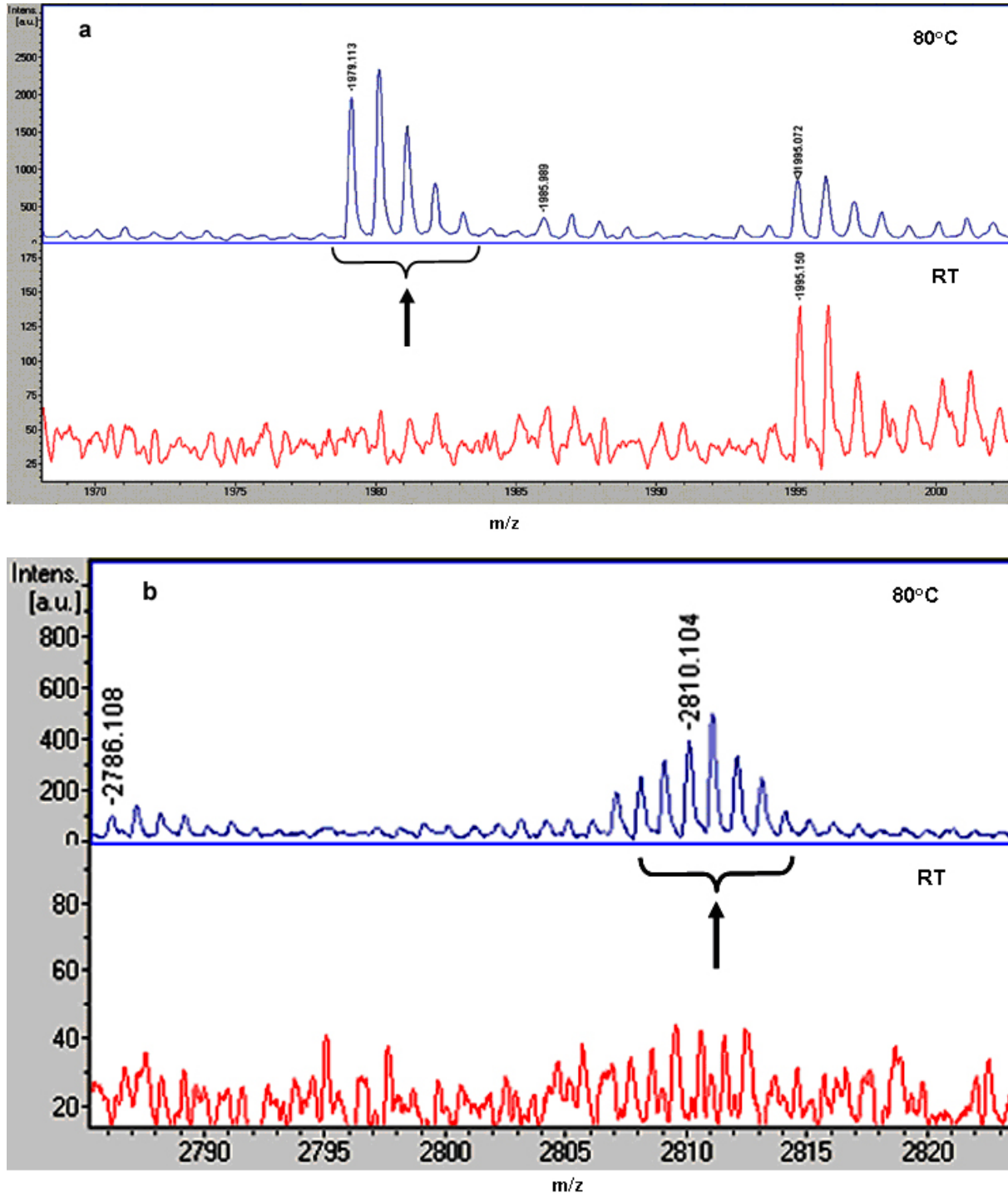
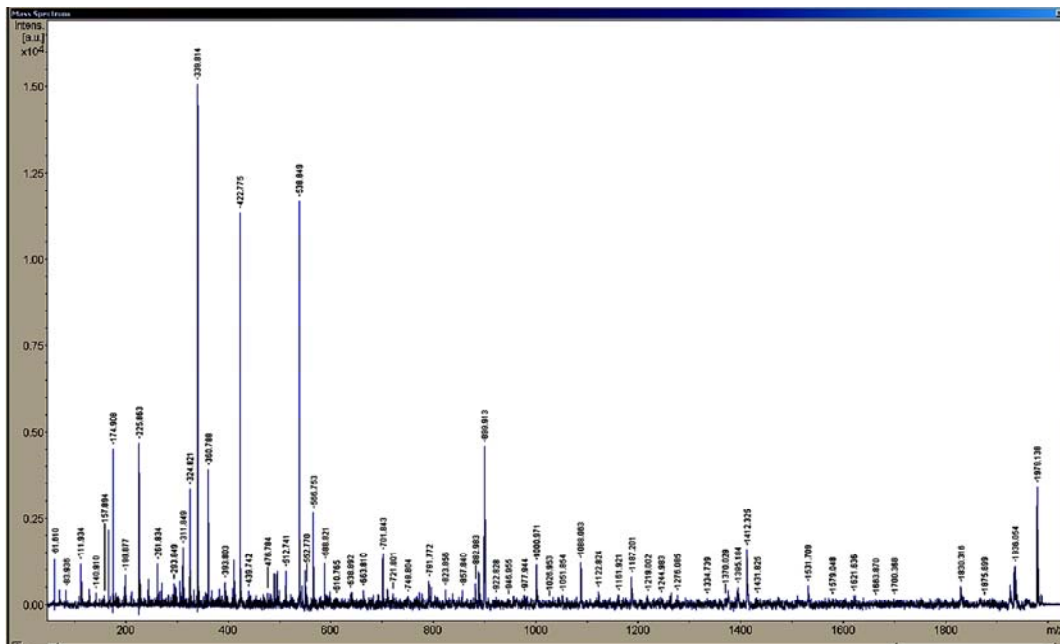


Figure 17. Sections of the MALDI mass spectra for BSA biotinylated at RT and after exposure to an elevated temperature of 80°C. In a, the arrow indicates the peak cluster corresponding to the biotinylated peptide. In a K437 is biotinylated only after BSA is exposed to 80°C. In b, the arrow indicates the peak cluster corresponding to the biotinylated peptide. K523 is biotinylated only after BSA is exposed to 80°C.

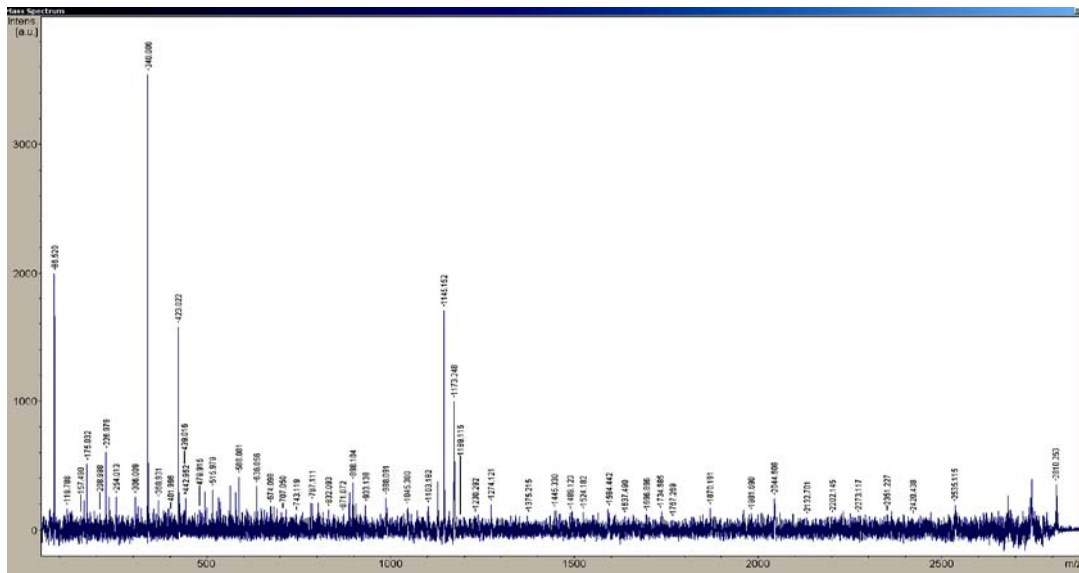
3. Results

These observations were confirmed by MS and tandem mass spectrometry. The peak with m/z 1979.113 corresponds to the peptide 437-451 of BSA with sequence (KVPQVSTPTLVEVSR) in which K437 is biotinylated. The MS/MS spectra and generated fragments ions were shown in figure 18. In contrast to the biotinylated lysine residues which were previously detected, the 1979.113 peptide has no missed cleavage site. This can be explained, as the biotinylated lysine is located at the N-terminus of the peptide and the peptide was generated after cleavage to the C-terminus of the adjacent arginine residue. The peak corresponding to the unmodified form of the peptide with m/z 1639.86 was also detected.



3. Results

Figure 19 shows the MS/MS spectra of the peptide with m/z 2810.100 corresponding to the amino acid sequence 508-528 of BSA. The MS analysis confirmed the sequence (RPCFCSALTPDETYVPKAFDEK) with K523 biotinylated. As described before, biotinylated peptides contained a missed cleaved lysine residue. Unmodified lysine K523 was detected in the shorter peptide with the sequence RPCFCSALTPDETYVPK in both biotinylated and non-biotinylated BSA.



3.8. Reduction has no effect on the biotinylation pattern of BSA

BSA has a total of 35 cysteine residues which form 17 disulphide bonds that join the 9 loops forming the 3 domains of the protein. The primary structure of BSA possesses a single sulfhydryl (Cys-34) group. The disulphide bonds are located almost between helical segments in the BSA sequence as following position:

(1) 77-86; (2) 99-115; (3) 114-125; (4) 147-192; (5) 191-200; (6) 223-269; (7) 268-276; (8) 288-302; (9) 301-312; (10) 339-384; (11) 383-392; (12) 415-461; (13) 460-471; (14) 484-500; (15) 499-510; (16) 537-582; (17) 581-590.

Among the total 60 lysine residues in BSA sequence, 31 lysines residues are located in/around the regions which are involved in forming disulphide bonds. Out of these, 15 lysine residues were biotinylated in the preceding experiments where BSA was biotinylated either at room temperature or after heating to different temperatures.

After showing that an increase in temperature results in the biotinylation of new lysine residues, it was necessary to confirm whether other treatments that result in the unfolding of the protein would lead to the biotinylation of more lysine residues. To achieve this, BSA was subjected to an elevated temperature of 80°C for 30 min in the presence of DTT before cooling and biotinylating with the 40 fold molar excess of the biotin derivative or alternatively BSA was exposed to temperatures above 80°C, reduced by DTT and alkylated with iodoacetamide for 45 min at room temperature in darkness before biotinylation as described. The protein was separated by SDS-PAGE and the protein bands were processed and analyzed as described above by PMF to identify biotinylated peptides. MS analysis showed the identical biotinylated peptides as detected before in the biotinylated BSA after treatment at 80°C. No new lysine residues could be biotinylated after reduction of BSA using DTT (Table 6).

This would imply that the either the new lysine residues are not exposed by this treatment or they simply cannot be biotinylated due to other factors e.g. steric hindrance. These findings are consistent with previous data which indicated that the majority of BSA disulphide bonds are not accessible to the solvent and they are protected from reducing agents at neutral pH. It has been shown that the inaccessibility of the disulfide

3. Results

bridges is involved in the maintenance of the BSA structure (Carter and HO, 1994; Pico *et al.*, 1997; Restani *et al.*, 1988).

Lysine	RT	56°C	80°C	80°C+reduction	80°C+reduction+alkylation
K 36	+	+	+	+	+
K 100	+	+	+	+	+
K 156	+	+	+	+	+
K 160	+	+	+	+	+
K 204	+	+	+	+	+
K 211	+	+	+	+	+
K 228	+	+	+	+	+
K 235	+	+	+	+	+
K 245	+	+	+	+	+
K 266	+	+	+	+	+
K 374	+	+	+	+	+
K 401	+	+	+	+	+
K 412	+	+	+	+	+
K 420	+	+	+	+	+
K437	-	-	+	+	+
K 455	+	+	+	+	+
K 463	+	+	+	+	+
K 498	+	+	+	+	+
K523	-	-	+	+	+
K559	+	+	+	+	+
total	18	18	20	20	20

Table 6. List of biotinylated lysine residues in all five different experiments of labelling BSA under different conditions. BSA was biotinylated with a 40 fold molar excess of sulfo-NHS-LC-biotin after exposure to different temperatures or after reduction with DTT. MS analysis revealed identical biotinylation pattern for BSA after treatment at 80°C and after reduction.

3.9. The biotinylation reaction does not induce structural changes in the biotinylated protein, as detected by circular dichroism.

Recently it has been reported that lysine modification by N-succinimidyl propionate (NSP) lacking the biotin moiety may induce conformational changes in a low molecular mass protein. These alterations are detectable by circular dichroism (CD) measurements (Gao *et al.*, 2006). CD spectroscopy is an analytical method to provide the information about the secondary structure of proteins in solution and determine the

3. Results

conformational changes in the protein structure induced by increasing temperature or chemical denaturant (Greenfield, 2006). CD measures the difference between the absorption of left- and right- handed circularly-polarized light by proteins. The absence of regular structure results in zero CD intensity, while an ordered structure results in a spectrum containing positive and negative signals. It has been shown that the different secondary structures of protein including α -helix, β -sheet, and random coil provide different characteristic CD spectra (Sreerama and Woody, 1994; Brahms and Brahms, 1980).

To investigate the possibility that modification of the lysine residues with sulfo-NHS-LC-biotin may induce structural changes in the BSA molecule, biotinylated and non-biotinylated BSA were analyzed by CD spectroscopy. To analyze the potential alteration in the secondary structure of BSA after biotinylation, BSA was biotinylated with increasing molar ratio of the biotin derivative. Two portions of BSA were modified with a 40 fold molar excess of the sulfo-NHS-LC-biotin after treatment with elevated temperature at 56°C and 80°C. The concentration of biotinylated and non-biotinylated BSA were adjusted to 50 μ M. The samples were transferred to 2 mM HEPES buffer at pH 7.4 by extensive dialysis and subjected to analysis by CD spectroscopy. All analysis was performed using a Jasco-810 spectrometer with the cooperation of Dr. Uwe Linne in the Chemistry/Biochemistry department at Philipps-Universität Marburg. Far-UV (180-300nm) measurements were carried out at room temperature. The observed protein CD spectrum is an average of CD signals from all structures and it reflects the geometric variability in the secondary structure.

As shown in figure 20, the CD spectra of BSA samples are characteristic of macromolecules with high α -helix content which monitored by two well defined negative peaks at 208 and 222 nm, suggesting that the structure of non-biotinylated and biotinylated BSA with the biotin derivative at different molar ratios was not changed. In all cases, the BSA secondary structure is predominantly composed of α -helices and the biotinylation reaction does not induce structural changes that are detectable by CD. As expected, heating of BSA up to 56°C has no effect on the secondary structure of the protein. The only significant change in the conformation structure of BSA was observed

3. Results

after the protein was exposed to 80°C before biotinylation. The structure of BSA showed a shift from α -helix structure to the more open β -sheet conformation after exposure to an elevated temperature of 80° (Figure 20).

The manganese stabilizing protein which has been analysed in the Gao *et al.*, (2006) study is a 33 kDa protein which has a maximum of two disulfide bonds, in contrast, the BSA molecule forms 17 intramolecular disulfide bonds. As described these disulfide bonds stabilize the BSA structure against the structural alteration. The compactness and flexibility of BSA structure is one explanation why this protein does not undergo a conformational change upon biotinylation.

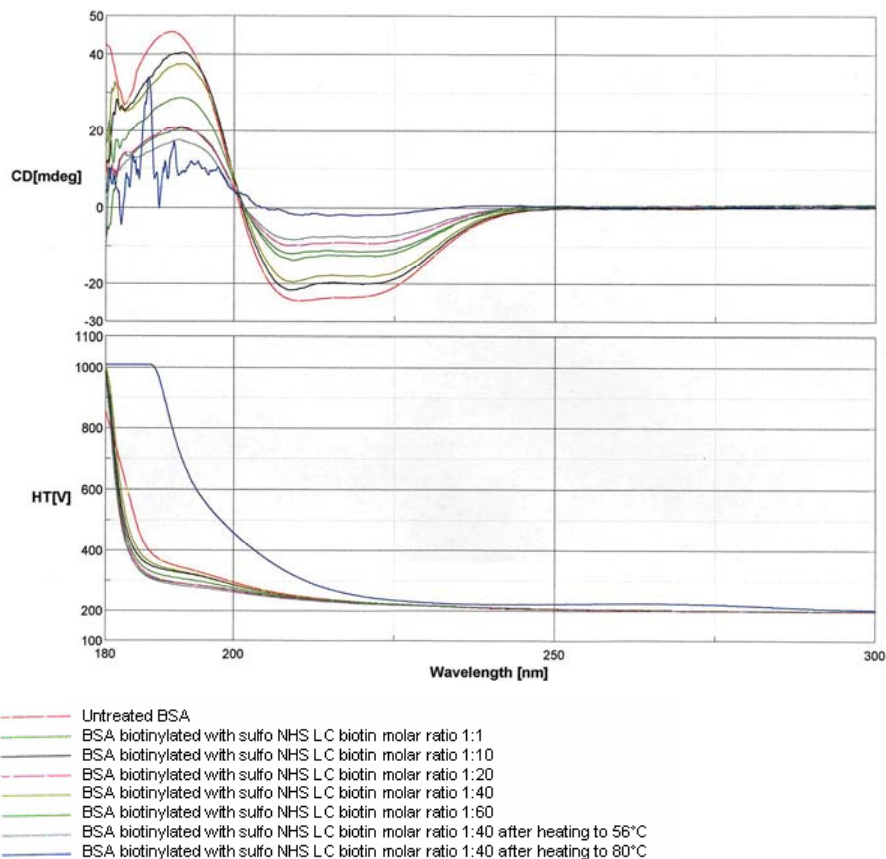


Figure 20. Far-UV CD spectra for different samples of BSA. Biotinylated BSA samples were transferred in 2 mM HEPES pH 7.4. The protein was used at concentration of 50mM at a temperature of 22°C in a path-length of 0.2 cm.

3.10. Involvement of lysine residues in hydrogen bonding may decrease their capacity to be biotinylated.

Since the biotinylation pattern was reproducible and many lysine residues could not be biotinylated, two possible mechanisms can be considered for the accessibility of the lysine residues in BSA structure to the biotin derivative. Either these lysines are involved in the formation hydrogen bonds with the neighbouring residues or they are buried in the structure of protein and the biotin derivative has no access to them because of steric hindrance. The position of all 20 biotinylated lysine residues were studied based on the homology structure between BSA and HSA. The structure of BSA and HSA show high similarity and the two proteins share 76% sequence identity. The heart shaped BSA structure consists of three alpha helices I, II and III. Each of these domains has two sub-domains A and B. As shown in figure 21 and table 7 the biotinylated lysines distributed in the BSA structure in different helices and sub-domains. Five modified lysines (K100, K35, K266, K498 and K559) are located in the hydrophobic cavity.

3. Results

		IA/h1	IA/h2	
BSA 1	MKWVTFISLLLLFSSAYSRGVFRDTHKSEIAHRF K DLGEEHFKGLVLIAFSQYLQCCPF			
HSA	MKWVTFISLLLLFSSAYSRGVFRDAHKSEVAHRFKDLGEEHFKALVLIAFSQYLQCCPF			
	IA/h3	IA/h4	IA/h5	
BSA 61	DEHVKLVNELTEFAKTCVADESHAGCEKSLHTLFGDEL K VASLRETYGDMADCCCKQEP			
HSA	DEHVKLVNELTEFAKTCVADESAENCCKSLHTLFGDKLCTVATLRETYGDMADCCCKQEP			
	IA/h6	IB/h7	IB/h8	
BSA 121	ERNECFLSHKDDSPDLPLK-KPDENTICDEFKADEN KFWGK LYEIAARRHPYFYAPELLY			
HSA	ERNECFLSHKDDNPMLPRLVSRPEVDVICTAEHDNEETFLAKYLYEIAARRHPYFYAPELLY			
	IB/h9	IB/h10 - IIA/h1	IIA/h2	
BSA 180	YANKYNGVFCQCCQAEKDGACLLP K IETMRE K VLTSSARQLRCASIQKFGERALKWSV			
HSA	YAKRYKAFTCCQAAADKAACLLPKLDELRLDEKASSARQLRCASLQKFGERALKAWAV			
	IIA/h3	IIA/h4	IIA	
BSA 240	ARLSQ K FPKAEFVEVTKLVTDLT K VHRECCGGDLECADDRADLAKYICDNQDTISSKLR			
HSA	ARLSQ R FPKAEFAEVSKLVTDLTQVHTECCGGDLECADDRADLAKYICENQDSISSKLR			
	/h5	IIA/h6	IIB/h7	IIB/h8
BSA 300	ECCCKPPLLEKSHCIAEVEKDAIPENLPFLTADFAEDKDVCKNYQAKDAFLGSLYIYYSR			
HSA	ECCCKPPLLEKSHCIAEVENDEMPADLPFLAADFVSEKDVCKNYAEAKDVFLGSLYIYYSR			
	IIB/h9	IIB/h10 - IIIA/h1		
BSA 360	RHPEYAVSVLLRLR K EYEATLECCAKDDPHACYSTVFDK L KHLVDEPQNLIKONCDQFE			
HSA	RHPDYSVLLRLR L AKTYETTLKCCAAADPHCYAKVDFEFLVVEEPQNLIKONCELEF			
	IIIA/h2	IIIA/h3	IIIA/h4	
BSA 420	K LGEYGFONALIVRYTR K IQVSTPTLVEVSRSLG K VGTRCGT K PESEMPCTEDYLSLI			
HSA	QLGEYKFNALIVRYTR K IQVSTPTLVEVSRNLGKVGSKCN-PEARMPCAEDYLSVY			
	IIIA/h5	IIIA/h6	IIIA/h7	
BSA 480	LNRLCVLHEKTPVSEKVT K CCTESLVNRRPCFSALTFDETYVE K AFDEKLFTHADICTL			
HSA	LNRLCVLHEKTPVSEKVT R TRKCTESLVNRRPCFSALTFDETYVPKEFNAETTFHADICTL			
	IIIB/h8	IIIB/h9	IIIB/h10	
BSA 540	EDTEKQIK K OTALVELLKHKPKATSEQLKTVMENFVAFV K CCAADDKEACFAVEGPKLV			
HSA	SEERKQIK K OTALVELLKHKPKATSEQLKAVMDDFAAFVEKCKADDKEACFAVEGPKLV			
BSA 600	VSTQTAL			
HSA	AASQAAL			

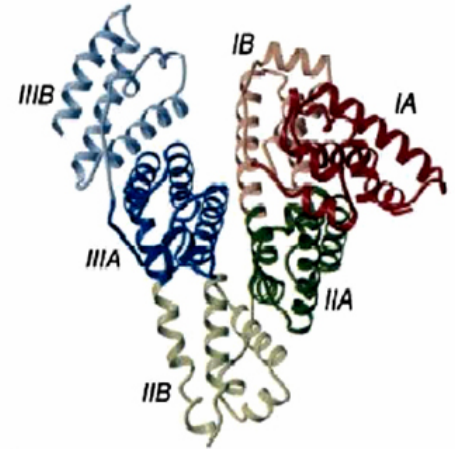


Figure 21. Position of biotinylated lysine residues in the primary structure of BSA. The domain structure of BSA was shown based on the HSA homology. The biotinylated lysine residues in the helices were showed in white bold. Three modified lysines which are located between the helices have been marked in bold red.

3. Results

Lysine	Position
K 36	IA/h1
K 100	IA/h4
K 156	IB/h8
K 160	IB/h8
K 204	Turn between IB and IIA
K 211	Turn between IB and IIA
K 228	Close before h1 and h2 of IIA
K 235	IIA/h2
K 245	Near the interface between H2andH3/IIA
K 266	IIA/h3
K 374	IIIB/h9
K 401	Turn between IIB/IIIA
K 412	Turn between IIB/IIIA
K 420	Turn between IIB/IIIA
K437	IIIA/h2
K 455	IIIA/h3
K 463	Interface between h3 and h4 of IIIA
K 498	IIIA/h5
K523	Between h6 and h7 of IIIA
K559	IIIA/h8

Table 7. Positions of biotinylated lysine residues in the BSA structure. The biotinylated lysines distribute in different helices and sub-domains of BSA structure.

To obtain more information about the accessibility of the lysine residues in the BSA molecule to the biotin derivative, the structure of a homology model of BSA (primary accession number: P02769) was studied based on the crystal structure of human serum albumin (HSA) as a template. All lysine residues of BSA were examined with respect to a possible correlation with the following structural descriptors: the spatial accessibility of lysine residues the solvent accessible surface (ASA), involvement in hydrogen bonding and the local electrostatic potential have been calculated. The latter has been computed and visualized using the MOLCAD module of Sybyl7.1. All analyses have been performed with the cooperation of Dr. Alexander Hillebrecht at the Institute of the Pharmazeutische Chemie at the Philipps-University of Marburg.

As shown in table 8, among the total 60 lysine residues in BSA sequence, 26 are predicted to be involved in a hydrogen bond. Out of 20 lysine residues which reacted with sulfo-NHS-LC-biotin in different experiments, only six lysine residues (K100, K160, K228, K245, K374 and K455) are involved in a hydrogen bond. However, it has to taken into consideration that two lysine residues (K100 and K245) of the six lysines which do

3. Results

not fit the correlation are “mutated” with respect to the crystallographically characterized template used for homology modelling. The data suggests that the involvement of a lysine residue in a hydrogen bond significantly decreases the probability of biotinylation. The analysis did not provide clear evidence for the correlation factors of the solvent accessible surface and the local electrostatic potential.

Lysine	biotinylation	ASA	HB visual	HB energy	Lysine	biotinylation	ASA	HB visual	HB energy
K 28	-	0.32	+	10.53	K 309	-	0.07	+	1.91
K 36	+	0.70	-	0	K 318	-	0.48	-	0
K 44	-	0.20	+	5.57	K 336	-	0.64	+	0
K 65	-	0.63	-	0	K 340	-	0.48	+	10.95
K 75	-	0.33	+	3.96	K 346	-	0.44	+	13.95
K 88	-	0.51	-	0	K 374	+	0.52	+	3.71
K 100*	+	0.62	+	20.84	K 386	-	0.56	-	0
K 117	-	0.41	+	3.06	K 399	-	0.41	-	0
K 130	-	0.06	+	0	K 401	+	0.70	-	0
K 138	-	0.83	-	0	K 412	+	0.44	-	0
K 140	-	0.43	-	0	K 420	+	0.87	-	0
K 151	-	0.67	-	0	K 437	-	0.26	-	0
K 155	-	0.57	+	18.09	K 455	+	0.25	+	4.77
K 156	+	0.46	-	0	K 463	+	0.43	-	0
K 160	+	0.32	+	0	K 489	-	0.95	-	0
K 183	-	0.63	-	0	K 495	-	0.51	-	0
K 197	-	0.35	-	0	K 498	+	0.59	-	1.35
K 204	+	0.33	-	1.09	K 523	-	0.37	+	13.44
K 211	+	0.43	-	0	K 528	-	0.79	-	0
K 228	+	0.63	+	5.03	K 544	-	0.33	-	0
K 235	+	0.29	-	0	K 547	-	0.20	-	0
K 245*	+	0.22	+	5.88	K 548	-	0.21	-	0
K 248	-	0.43	+	7.76	K 557	-	0.08	+	17.53
K 256	-	0.38	+	13.11	K 559	+	0.10	-	0
K 263	-	0.46	+	15.42	K 561	-	0.46	+	4.57
K 266	+	0.43	-	0	K 568	-	0.48	-	6.68
K 285	-	0.63	-	0	K 580	-	0.78	-	0
K 297	-	0.39	+	8.37	K 587	-	0.23	+	7.55
K 299	-	0.63	+	12.29	K 597	-	0.57	-	0
K 304	-	0.27	+	8.58					

Table 8. Analysis of all lysines of BSA for surface accessibility and hydrogen bonding . ASA: accessible surface area (relative units), HB visual: formation of hydrogen bond (+) or not (-) according to visual inspection, HB energy: hydrogen bond energy (arbitrary units). 0 indicates an energy value below 0.5. The asterisk marks two biotinylated residues which are mutated with respect to the template X-ray structure and therefore were excluded from all considerations. Bold residues are biotinylated despite their involvement in hydrogen bonding. All descriptors were deduced from a BSA homology model based on the crystal structure of HSA.

3.11. Analysis of biotinylated and non-biotinylated CA II by MS

As shown in the case of BSA, the biotinylation pattern of a protein is dependent on its conformation. Proteins can be assigned into different classes depending on their quaternary structure and it is plausible that the complexity of the quaternary structure may affect the biotinylation pattern. A similar analysis was carried out on CA II which in contrast to the globular protein (BSA) is a single domain protein. CA II structure is a dominating β -sheet that extends throughout the entire molecule. CA II protein contains 18 lysine residues that are distributed throughout the entire sequence but it has no cysteine residues to form any disulphide bonds. The thermal denaturation curve of CA II has a classical sigmoid shape, with the melting temperature at 64.2°C. Only minor structural changes, if any, are to be expected at this pre-transition temperature.

To investigate the biotinylation pattern of CA II, 1.15×10^{-4} moles of CA II was biotinylated with a 40 fold molar excess of the sulfo-NHS-LC-biotin, either at room temperature or subjected to elevated temperatures of 56°C and 80°C for 30 min before cooling and biotinylating. The biotinylated and non-biotinylated CA II were separated by SDS-PAGE and stained by Coomassie (Figure 22).

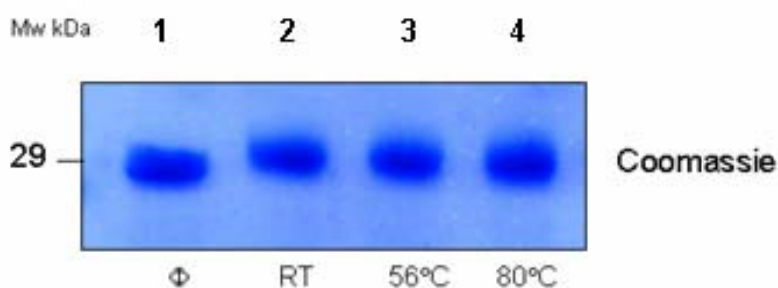


Figure 22. Analysis of the mass of biotinylated CA II after exposure to different temperature. CA II was biotinylated with sulfo-NHS-LC biotin at 40 molar ratios at room temperature (RT) or after exposure to elevated temperature and analyzed by SDS-PAGE and Coomassie staining

As expected, the biotinylated CA II proteins migrate at a higher mass compared to the non-biotinylated sample which indicates the altering mass of protein as a result of biotinylation (Figure 22, Lane 2). As shown in figure 22 exposure of CA II to a

3. Results

temperature of 56°C (Lane 3) and 80°C (Lane 4) before biotinylation does not induce significant differences in the mass of the protein suggesting that the biotinylation patterns of CA II at room temperature and following treatment at different temperatures are similar. To confirm this, the Coomassie stained bands were cut and processed for mass spectrometry as described before. MS analysis of the unlabeled CA II showed 12 different peptides, with masses between 973.57 and 2712.38 Dalton which covered 56% of CA II sequence. The identified peptides contain 9 out of the total 18 lysine residues. In the biotinylated CA II, 20 different peptides were identified ranging in masses from 430.29 to 2868.53 Dalton, accounting for 66% of the protein sequence. Out of total 18 lysine residues, 15 lysine residues were detected by MS, of which 7 residues were biotinylated. Peptides containing lysine residues were also found in a non-biotinylated form in the biotinylated sample. Heating of the protein to 80°C and cooling to room temperature prior to biotinylation had no effect on this pattern, probably due to rapid refolding of the protein (Table 9).

Lysine	nonbiotinylated	RT	56°C	80°C
K9	-	-	-	-
K18	+	+	+	+
K36	-	-	-	-
K45	+	+	+	+
K76	+	+	+	+
K80	-	+	+	+
K112	+	+	+	+
K113	+	+	+	+
K126	+	+	+	+
K148	-	+	+	+
K158	-	-	-	-
K167	+	+	+	+
K169	-	+	+	+
K171	-	+	+	+
K212	-	+	+	+
K224	-	+	+	+
K251	+	+	+	+
K260	-	+	+	+
total	9	15	15	15

Table 9. Effect of temperature on the biotinylation pattern of CA II. Bold residues indicates the biotinylated lysines. The biotinylation pattern in all three experiments was identical.

3. Results

As shown in figure 23, the comparison of modified and unmodified CA II spectra indicates extra peptide peaks which are present in the biotinylated sample but absent in a non-biotinylated version. These new observed peptide peaks with masses of 772.46, 787.35, 1685.96, 1729.93, 1989.00, 2049.01 and 2537.32 indicate the biotinylated peptides. The peptide 787.35 which is not marked in the spectra has a low intensity. All reported biotinylated peptides have a missed cleavage site except the peptide containing K260 which has no missed cleavage site and a modified lysine located at the C-terminus of the peptide sequence.

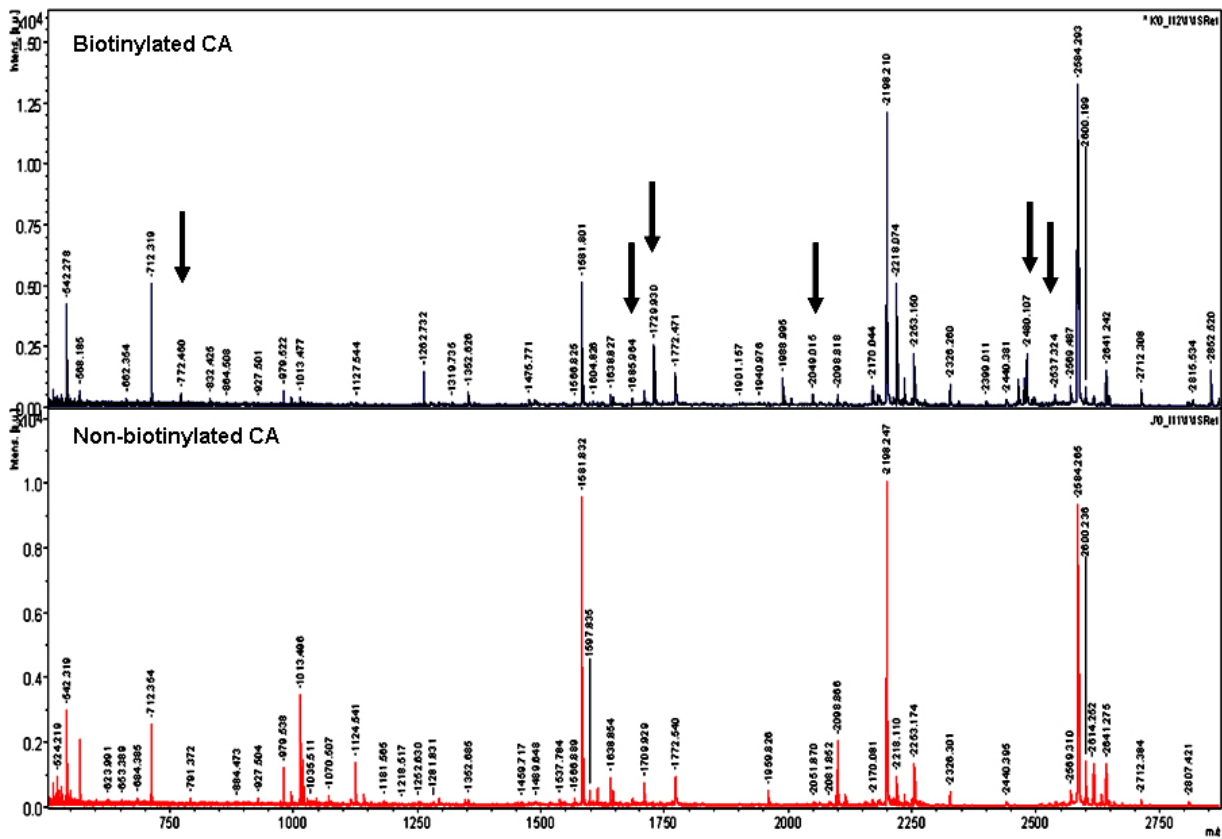


Figure 23. Comparison of biotinylated and non-biotinylated CA II. One fraction of CA II was biotinylated with 40-fold higher mole ratio of biotin derivative. The same amount of CA II was not biotinylated. Two protein samples were separated by 1D gel electrophoresis and subjected to be analyzed by mass spectrometry. The top spectrum is from the biotinylated protein and the other one is non-biotinylated CA II. The marked peaks show the biotinylated peptides.

3. Results

The available crystal structure of bovine CA II was examined for the putative accessibility of the lysine residues. The analysis in this case also suggested a correlation between the involvement of lysine residues in hydrogen bonding and decreased probability of their biotinylation. As shown in table 10, only one lysine residue (K224) of eight biotinylated lysine residues is involved in hydrogen bonding.

Lysine	biotinylated	ASA	HB visual	HB energy
K9	-	0.83	-	0
K18	+	0.64	-	0
K36	-	0.94	-	0
K45	+	0.54	-	0
K76	-	0.25	+	6.63
K80	+	0.40	-	0
K112	-	0.50	-	0
K113	+	0.47	-	0
K126	-	0.61	+	17.00
K148	-	0.49	-	0
K158	-	0.37	+	0
K167	-	0.18	+	6.21
K169	-	0.26	+	7.38
K171	+	0.44	-	0
K212	-	0.20	+	13.08
K224	+	0.25	+	7.08
K251	-	0.41	+	11.76
K260	+	0.74	-	0

Table 10. Analysis of all lysines of CA II for surface accessibility and hydrogen bonding. ASA: accessible surface area (relative units), HB visual: formation of hydrogen bond (+) or not (-) according to visual inspection, HB energy: hydrogen bond energy (arbitrary units). 0 indicates an energy value below 0.5. Lysine residue 224 is biotinylated despite of hydrogen bonding.

3.12. Band III is biotinylated in infected and non-infected erythrocytes.

Band III protein is an abundant membrane protein present on the erythrocyte surface with about 10^6 copies per cell. As described previously, Band III undergoes conformational changes upon infection with *P. falciparum* and these changes may be important for survival of the parasite (Sherman *et al.*, 2003). Based on this observation, it was investigated whether these changes could be detected using the novel method

3. Results

established in this study. Thus, the biotinylation patterns of Band III in infected and non-infected erythrocytes were analysed.

The biotinylation of BSA revealed a linear correlation between the molar ratio of the biotin derivative and biotinylated lysine residues, until all sufficiently reactive residues were saturated. To investigate the optimal concentration of sulfo-NHS-LC-biotin required for labelling the available lysine residues in Band III, 2×10^8 infected and non-infected erythrocytes were biotinylated with an increasing concentration of sulfo-NHS-LC-biotin (0.5 mg ml^{-1} , 1 mg ml^{-1} , 2 mg ml^{-1}). Biotinylation was performed in the presence of furosemide to block NPP activity, and thus minimize internal labelling of infected erythrocytes. Only lysine residues that are exposed at the erythrocyte surface should therefore be biotinylated. The excess unreacted biotin was removed by size exclusion centrifugation. The biotinylated membrane fractions of erythrocytes were separated by SDS-PAGE, stained with Coomassie, or alternatively analyzed by immunoblotting. To allow identification of both Band III and Spectrin on Coomassie stained gels, membranes prepared from SDS-gels run under identical conditions were incubated with anti-Band III and anti-Spectrin antibodies, followed by detection using the ECL system. The monoclonal anti-Band III antibody which was used in this experiment recognizes an epitope in the cytoplasmic domain of the Band III molecule, approximately 20 kDa from the N-terminal end. This antibody recognizes Band III protein (90-100 kDa) and several lower molecular mass peptides migrating in SDS-PAGE gels in the regions of 60, 40 kDa (Figure 24, Lane 1, lower panel). Spectrin could also be detected at the expected mass (Figure 24, Lane 1, upper panel).

3. Results

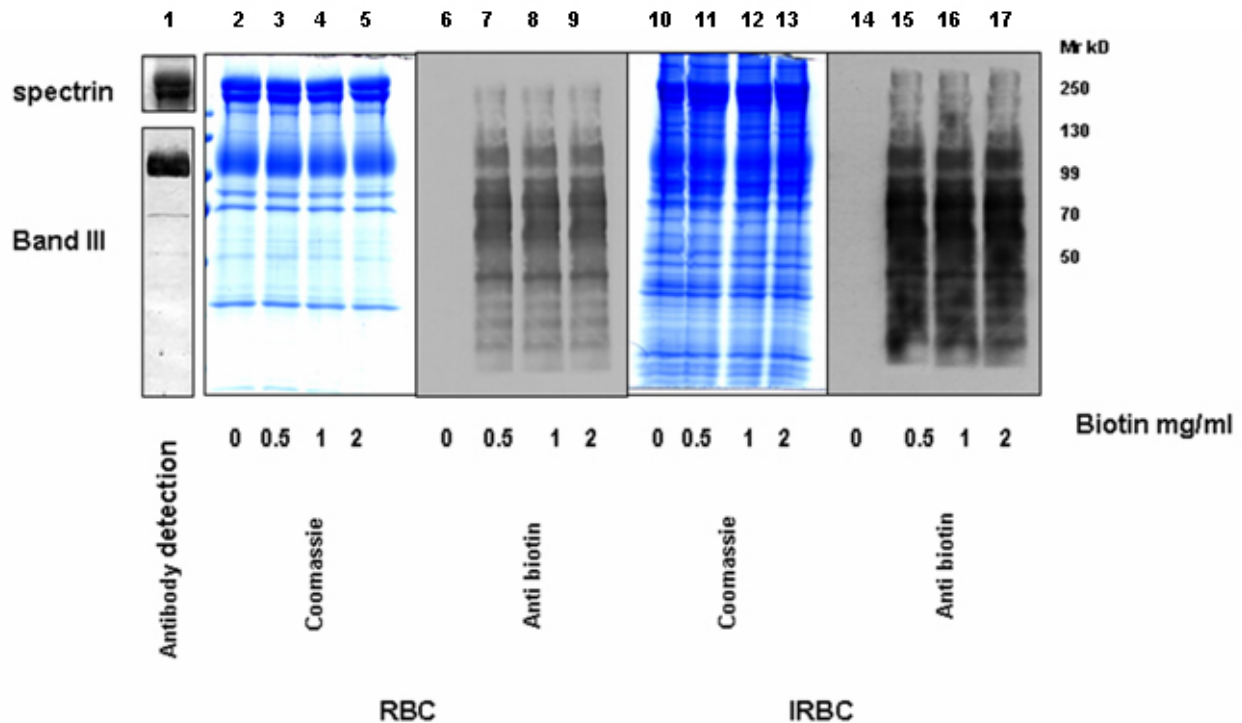


Figure 24. Analysis of biotinylation of membrane protein from infected (IRBC) and non-infected erythrocytes (RBC) with elevated concentration of biotin derivative. 2×10^8 RBC and IRBC were biotinylated in the presence of NPPs inhibitor using different concentrations of sulfo-NHS-LC-biotin and the membrane fraction was solubilized using SDS-PAGE sample buffer and separated in a 7.5% SDS-PAGE and analyzed by Coomassie staining or alternatively analyzed by anti-Band III and anti-Spectrin. The same filter was detected using alkaline phosphatase-conjugated SAV to detect the biotinylated proteins.

As shown in figure 24, although there are large differences in the total protein content and pattern of samples derived from infected or non-infected cells (Lanes 2-5 and Lanes 10-13), no significant differences in the migration behaviour of Band III could be visualised by Coomassie staining. This suggested that either Band III is not biotinylated, or that only few lysine residues are biotinylated. The migration of Band III after labelling with an elevated concentration of biotin derivative (Lanes 3,4,5 and Lanes 11,12,13) does not change significantly compared to the non-treated control (Lane 2 and Lane 10). This indicating that biotinylation of Band III results in only minimal, or non-existent, modification of lysine residues, even when using increasing concentrations of the biotin derivative. Immunoblotting using alkaline phosphatase-conjugated SAV on nitrocellulose membrane reveals that Band III does in fact undergo biotinylation, however a significant

3. Results

change in Band III migration after treatment with increasing biotin concentrations could not be detected by this method, supporting a minimal biotinylation of the Band III protein (Figure 24, Lanes 6-9 and Lanes 14-17). Additionally, the lower molecular mass peptides detected by the anti-Band III antibody can also be detected by anti-biotin (Figure 24).

To confirm that internal membrane proteins were not biotinylated in all experiments, the biotinylation status of spectrin was examined. Spectrin was visualised firstly with anti-spectrin antibody. This antibody reacts specifically with α and β chains of human erythrocyte spectrin which migrate at ~ 280 kDa in the gel. As expected, a strong signal at ~ 280 kDa was detected using anti-Spectrin antibodies, verifying that the transfer of this protein to the nitrocellulose membrane was efficient (Figure 24, Lane 1, upper panel). The same membrane was then probed with alkaline phosphatase conjugated streptavidin. As shown in figure 24, in comparison to the signal migrating at the height of Band III only a weak signal can be visualised at the molecular weight of spectrin, suggesting only a minimal, if any, biotinylation of this protein (Figure 24, Lanes 6-9 and Lanes 14-17). To confirm this, Coomassie stained bands corresponding to spectrin was cut, digested and analyzed by mass spectrometry. MS data in this case identified Spectrin, but no biotinylated Spectrin-derived peptides were found.

3.13. MS analysis identifies Band III

Band III is a multi-spanning membrane protein with 11-14 transmembrane domains. According to the predicted topology, 5 domains are exposed extracellularly. While three domains are composed of less than 10 amino acid residues, two domains (543-568 and 626-663) are composed of 26 and 38 amino acids respectively. One additional domain (802-835) is predicted to exhibit enhanced flexibility which can vary between an extracellular and intracellular topology. Since only a portion of tryptic peptide of a protein can be detected under experimental conditions by mass spectrometry, *In silico* digestion of Band III was performed using ExPASy proteomic server to generate theoretical peptides. The following parameters were used in the prediction: all cysteines were assumed to be alkylated, oxidation of methionines was allowed, monoisotopic masses

3. Results

were used for all amino acid residues, and the maximum number of missed cleavage sites allowed was one. Theoretical digestion of Band III generates approximately 200 peptides with masses in the range of 505.31 to 8960.86 Da, almost half of which contain at least one lysine residue. To analyze Band III under experimental conditions, a Coomassie stained band corresponding to the highest molecular weight Band III signal was excised from biotinylated and non-biotinylated RBC and analyzed by mass spectrometry. Band III MS spectra from biotinylated and non-biotinylated samples are shown in figure 25. Three peaks with m/z 1028.605, 1612.766 and 2864.188 could be detected only in the biotinylated sample (arrows in figure 25).

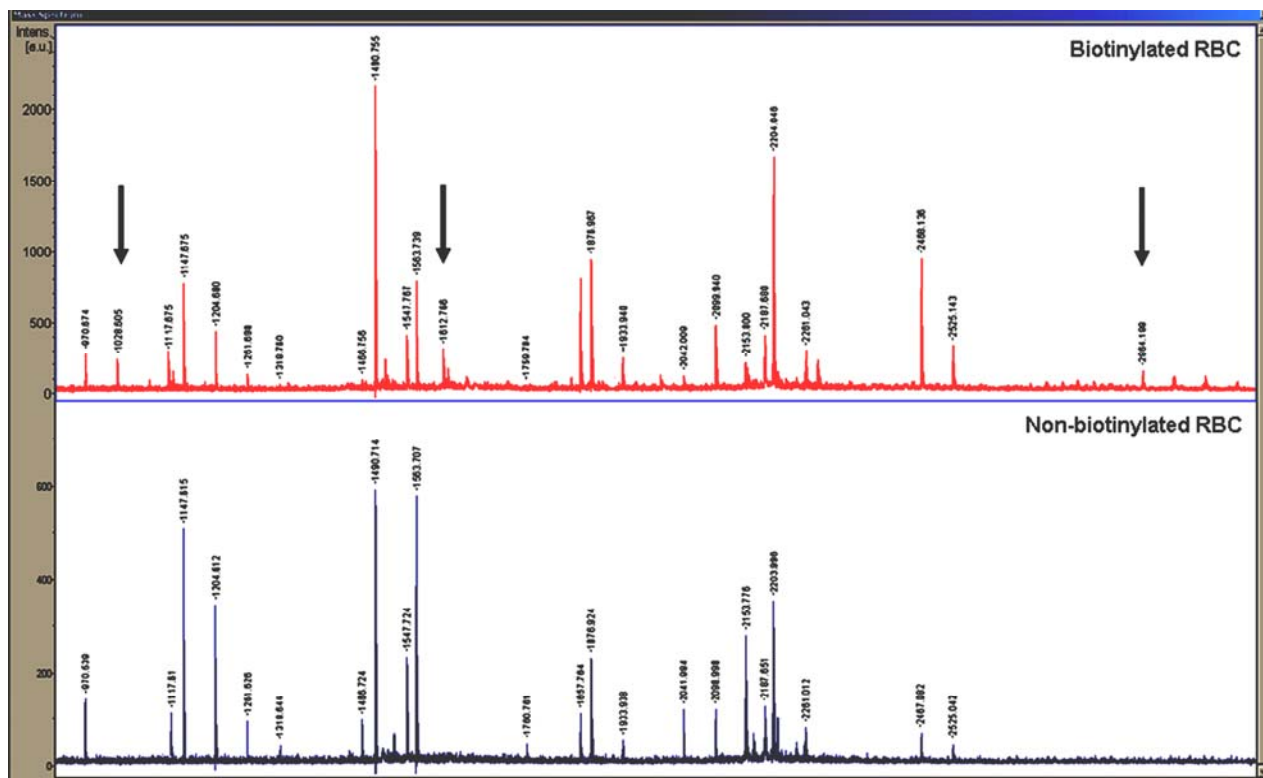


Figure 25. MS analysis of biotinylated and non-biotinylated RBC. 2×10^8 RBC were biotinylated and the membrane fraction was separated by SDS-PAGE. The stained band were cut and analyzed by mass spectrometry in reflectron mode. The arrows marked the extra peaks in biotinylated Band III which indicate the biotinylated peptides.

MS analysis together with a database search verified the two samples as derived from Band III protein with the maximum 30% sequence coverage. The observed sequence is

3. Results

shown in figure 26. 70% of the identified peptides are located at the N-terminus of protein, the remainder derived from the C-terminus. A peptide corresponding to amino acids 647 - 656 (which are in loop 4) and 880 - 901 (located within the cytoplasmic domain of the C-terminus) was identified in both samples. Three extra peaks were observed in the biotinylated Band III sample. Database searches identified these peaks as corresponding to biotinylated peptides covering amino acids 818 - 827 and 828 - 832, residing in the flexible loop of the transmembrane domain of the protein.

3. Results

Biotinylated	1 MEELQDDYED MMEENLEQEE YEDPDIPESQ MEEPAAHDTE ATATDYHTTS
Non-biotinylated	1 MEELQDDYED MMEENLEQEE YEDPDIPESQ MEEPAAHDTE ATATDYHTTS
	51 HPGTHKVVYVELQELVMDEKNQELRWMEARWVQLEENLGENGAWGRPHLS
	51 HPGTHKVVYVELQELVMDEKNQELRWMEARWVQLEENLGENGAWGRPHLS
	101 HLTf WsLL EL RRVfT KGTvL LDl QETsL AG vANQLLD RfI fE DQIRPQDR
	101 HLTf WsLL EL RRVfT KGTvL LDl QETsLAG vANQLLD RfI fED QIRPQDR
	151 EELL RALL LKHS HAGEALGGV KPAV LTR SGD PSQP LLPQHSSLETQLF
	151 EELL RALL LK HSHAGEALGGV KPAV LTR SGDPsQP LLP QHSSLETQLF
	201 CEQGDG GTEG HSps GILEKI PP DSEATLVL VGRA DFLEQpVLGFvRLQEA
	201 CEQGDG GTEG HSps GILEKI PP DSEATLVL VGRA DFLEQpVLGFvRLQEA
	251 AELEA VELPV PIR FLF vLLG PE APHIDYtQ LGR AAATLMS ERvF RiD AYm
	251 AELEA VELPV PIR FLF vLLG PE APHIDYtQ LGR AAATLMS ERvF RiD AYm
	301 AQsRG ELLHS LEGf LDCsLVLPPTD APsEQ ALLsLVp VQR ELLRRRyQSS
	301 AQsRG ELLHS LEGfLDcSLV LPPTD APsEQ ALLsLVp VQR ELLRRRyQSS
	351 PAKP DSSfYK GLDLN GGPDD PLQQT GQLFG GLvRDIRRRY PYYLSDiTDA
	351 PAKP DSSfYK GLDLN GGPDD PLQQT GQLFG GLvR DIRRRY PYYLSDiTDA
	401 FSP QvLAA vI fI YFAA LSPA ITFGG LLGEK TRN QMG vSEL LISTA vQGIL
	401 FSP QvLAA vI fI YFAA LSPA ITFGG LLGEK TRN QMG vSEL LISTA vQGIL
	451 FALL GAQP LLvVGF SGpLLV fEE AFFsF CE TNGLE YIVGR vWIG fWLILL
	451 FALL GAQP LLvVGF SGpLLV fEE AFFsF CE TNGLE YIVGR vWIG fWLILL
	501 vVLvV AF EG s FL vR fIS RyT QEIF sFL ISL IFIY ET fS KL IKIFQ DH PLQ
	501 vVLvV AF EG s FL vR fIS RyT QEIF sFL ISL IFIY ET f SKL IKIFQ DH PLQ
	551 KTYNynvLMV PKPQGpLpNT ALLsLVLMAG TFFfAMMLRk fKNSSYfPGK
	551 KTYNynvLMV PKPQGpLpNT ALLsLVLMAG TFFfAMMLRk fKNSSYfPGK
	601 LRRvIG DFGv PISIL IMvLV DFF IQDT YtQ KLSvP DGfKv SNSS AR GWVI
	601 LRRvIG DFGv PISIL IMvLV DFF IQDT YtQ KLSvP DGfKv SNSS AR GWVI
	651 HPLGLR SEFP IW MMfAS ALP ALLv fILIFL ES QITTLvS KPER KmvKGS
	651 HPLGLR SEFP IW MMfAS ALP ALL vFILIFL ES QITTLvS KPER KmvKGS
	701 GFHLdLLLV GMGGvAALFG MPwLSATTvR svTHANALTYMGKASTPGAA
	701 GFHLdLLLV GMGGvAALFG MPwLSATTvR svTHANALTYMGKASTPGAA
	751 AQI QE vKEQ R ISG LLvA vLV GLsI LM EPIL SRIP LAVLFg IFLYMG vTSL
	751 AQ IQE vKEQ R ISG LLvA vLV GLsI LM EPIL SRIP LAVLFg IFLYMG vTSL
	801 SGIQ LfDRIL LLfK PPKY HP DVPY vKRvKTWR MHLfT GIQ IICLA vLWvV
	801 SGIQ LfDRIL LLf KPPK YHP DVPYv KRvKTWR MHLfT GIQ IICLA vLWvV
	851 KSTP ASLAL P fVL ILTvPLR RvLLPL IFRN vELQCLDADD AKAT fDEEEG
	851 KSTP ASLAL P fVL ILTvPLR RRvLLPLI FRN vELQCLD ADD AKAT fDEEEG
	901 RDEYDEVAMPV
	901 RDEYDEVAMP V

Figure 26. Comparisons of the detected peptides in biotinylated and non-biotinylated Band III. The identified amino acids are labelled in red. Sequence coverage was calculated using the detected amino acids.

3.14. The peaks found in non-biotinylated samples are falsely identified by database searches as corresponding to a biotinylated peptide.

The comparison of spectra of the biotinylated and non-biotinylated Band III revealed some extra peaks only found in biotinylated samples suggesting that these correspond to peptides containing biotinylated lysine residues. However database searches performed with spectra derived from the non-biotinylated sample also predicted the presence of a biotinylated peptide. As (excluding contamination or experimental error) this cannot be the case, the possibility of a false database prediction was investigated. As shown in figure 27, a peak with m/z 1934.012 was seen in spectra derived from both the biotinylated and non-biotinylated Band III samples. This result was reproducible, as this peak was seen in three independent experiments. Database searches including sulfo-NHS-LC-biotin as an optional modification predicted the sequence (VYVELQELVMDEK) corresponding to amino acids 57 – 69 with the K69 being biotinylated. An alternative search with the same parameters but without the biotin modification predicts a different peptide (LQEAAELEAVELPVPIR) corresponding to amino acids 247 - 263. This second peptide does not contain a lysine residue. The theoretical mass of the peptide is 1877.08 and was reported with the carbamidomethylation (N-term) resulting in a 57 Da increase in the predicted mass.

3. Results

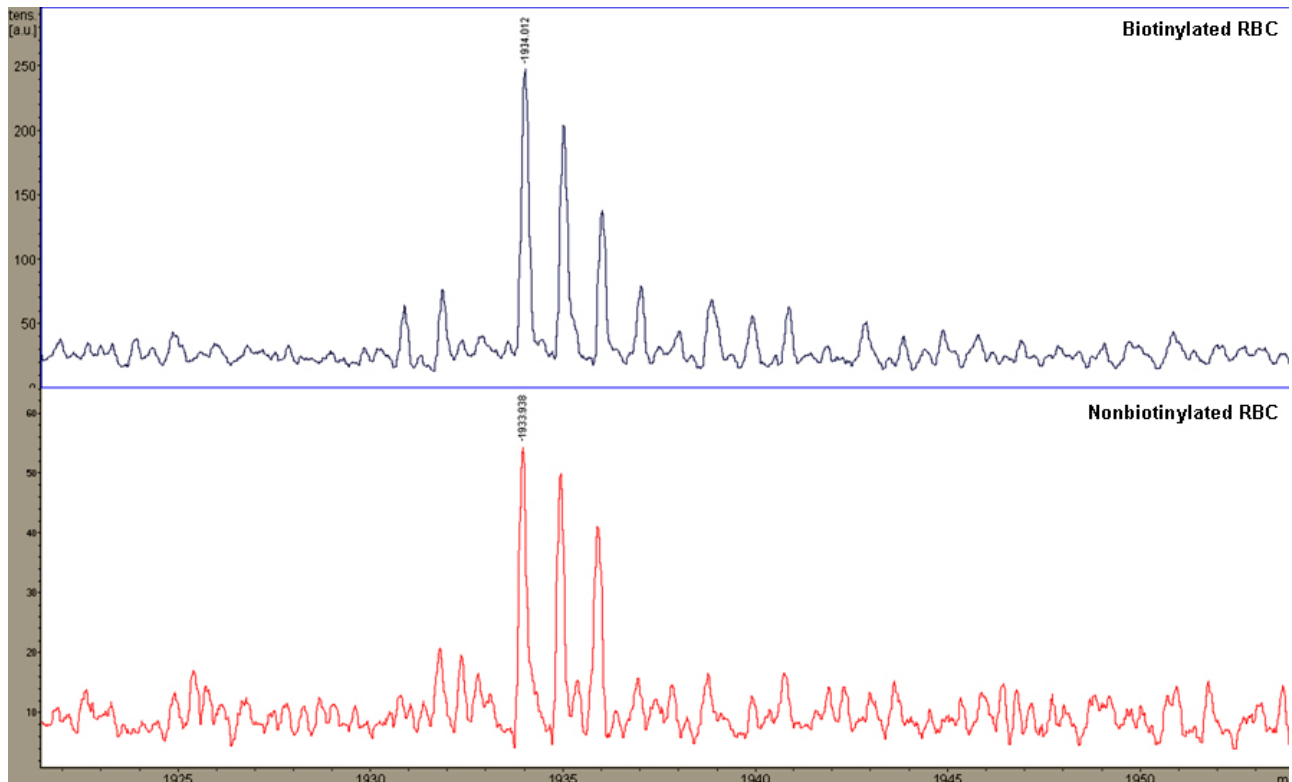
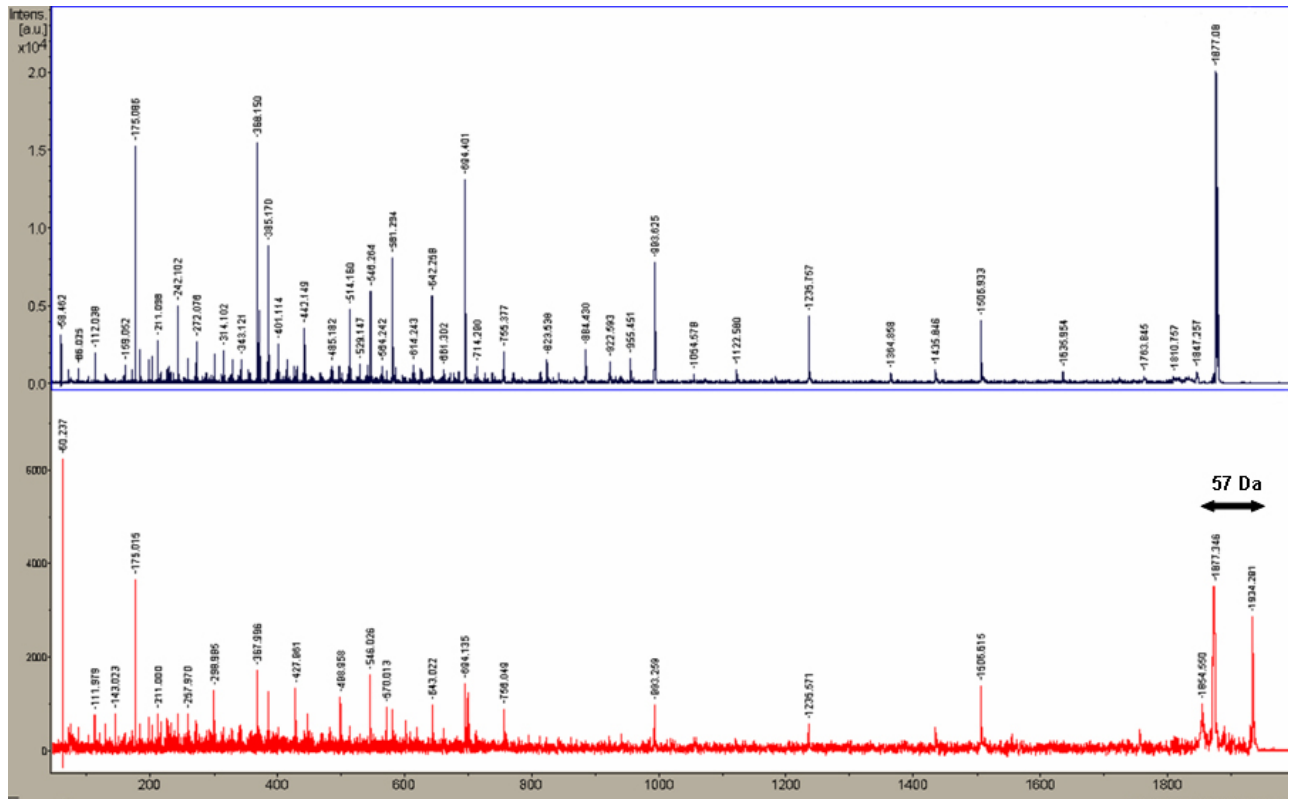


Figure 27. Zoom of section of MS spectra of biotinylated and non-biotinylated RBC including peak with m/z 1934. The peak m/z 1934 was detected in both labelled and unlabeled samples.

To verify which of these predictions is correct; peaks with m/z 1877.346 and 1934.281 from the non-biotinylated Band III sample were analyzed by tandem mass spectrometry (Figure 28). MS/MS analysis confirmed that the peak with m/z 1934.281 corresponded to a non-biotinylated peptide with sequence LQEAAELEAVELPVIPIR. An ion corresponding to the biotin tag (mass 340 Da) was not found. Comparison of the MS/MS spectra verified that the only difference between these two predicted peptides is the carbamidomethylation of the leucine residue (L246) at the N-terminus. This N-terminal carbamidomethylation most likely occurred during sample preparation. A peptide with m/z 1934.281 was also seen in the spectra derived from the biotinylated sample. MS/MS analysis showed that this peak also corresponds to the non-biotinylated peptide. Additional support for this interpretation of the data is that all labelling with non-permeable biotin derivatives was performed in the presence of furosemide to prevent labelling of internal membrane proteins. The K69 resides in the N-terminus cytoplasmic

3. Results

domain of Band III and under the experimental conditions used it is not expected to be biotinylated.



247 - 263 1934.24 R.LQEAAELEAVLPVPIR.F Carbamidomethyl (N-term)

#	b	Seq.	y	#
1	171,11	L	1934,281	17
2	299,17	Q	1763,95	16
3	428,21	E	1635,9	15
4	499,25	A	1506,85	14
5	570,29	A	1435,82	13
6	699,33	E	1364,78	12
7	812,41	L	1235,74	11
8	941,46	E	1122,65	10
9	1012,49	A	993,61	9
10	1111,56	V	922,57	8
11	1240,61	E	823,5	7
12	1353,69	L	694,46	6
13	1450,74	P	581,38	5
14	1549,81	V	484,32	4
15	1646,86	P	385,26	3
16	1759,95	I	288,2	2
17		R	175,12	1

Figure 28. MS/MS analysis of peaks with m/z 1877.34 and 1934.24 from non-biotinylated RBC. Peptides with m/z 1877.34 and 1934.24 were subjected to tandem mass spectrometry and the generated fragments were compared. The comparison of MS/MS analysis and database search indicated the N-terminal modification of a leucine residue in the composition of peptide.

3.15. Biotinylated Band III peptides were rarely detected.

Band III contains a total of 29 lysine residues evenly distributed throughout the primary protein sequence. Several biochemical studies have investigated the position of these residues in relation to the membrane topology of the protein (Kang *et al.*, 1992; Okubo *et al.*, 1994; Kuma *et al.*, 2002; Abe *et al.*, 2004). These data are summarised in figure 29. Eight lysine residues are located within the N-terminal cytoplasmic domain, 7 lysines in the C-terminal cytoplasmic domain and three lysines within the transmembrane domains. 9 lysine residues reside in the extracellular loops, four of which are located in one of two large loops. Four further lysine residues are found in the flexible loop between amino acids 802 -835.

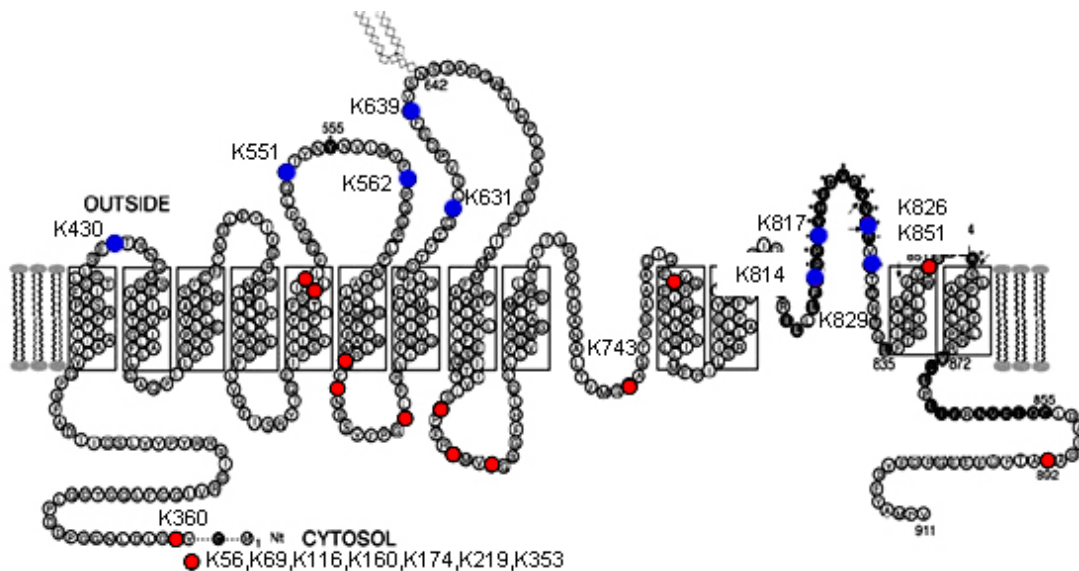


Figure 29. The distribution of lysine residues in the Band III sequence. Band III has a total 29 lysine residues (K), marked by red circles. Lysines which are exposed to the surface of erythrocytes are marked by blue colour (Modified from Zhu *et al.*, 2005).

To investigate the biotinylation pattern of Band III in infected and non-infected erythrocytes, Coomassie stained bands corresponding to the full-length protein were excised and analyzed by mass spectrometry and tandem mass spectrometry. In all three experiments the protein was identified as Band III with a sequence coverage between 15% and 30%. MS and database analysis of biotinylated Band III protein from non-infected erythrocyte predicts 16 peptides ranging in mass from 970.67 to 2864.30 Da. As

3. Results

shown in table 11, 18 lysine residues were predicted in this analysis. In the IRBC sample, 14 peptides were predicted. The peptides were distributed in the same mass range as those from the non-infected sample and contain 15 lysine residues. 7 lysine residues in the RBC and 6 lysines in the IRBC sample are predicted to be found on the extracellular side of the erythrocyte membrane. Of these, four were found non-biotinylated in both the IRBC and RBC samples. The residue K851 was only found in RBC in a non-biotinylated form. Out of the total 29 lysine residues in Band III 9 lysines could not be identified in either the RBC or IRBC samples.

Lysine residue	RBC	IRBC	Position	biotinylated
56	-	-	internal	-
69	+	+	internal	-
116	+	-	internal	-
160	-	-	internal	-
174	+	+	internal	-
219	-	+	internal	-
353	+	+	internal	-
360	+	+	internal	-
430	-	-	external	-
539	-	-	TM	-
542	+	+	TM	-
551	+	+	external	-
562	-	-	external	-
590	-	-	internal	-
592	+	+	internal	-
600	+	+	internal	-
631	-	-	external	-
639	+	-	external	-
691	-	-	internal	-
695	+	-	internal	-
698	+	-	internal	-
743	-	+	external	-
757	-	+	TM	-
814	+	+	external	-
817	+	+	external	-
826	+	+	external	RBC
829	+	+	external	RBC/IRBC
851	+	-	TM	-
892	+	+	internal	RBC/IRBC
total	18	15	29	3

Table 11. Listing of identified lysine residues of Band III in non-infected erythrocytes (RBC) and infected erythrocytes (IRBC) after biotinylation. 2×10^8 erythrocytes were biotinylated with different concentrations of sulfo-NHS-LC-biotin and the membrane protein fraction was separated by 1D gel electrophoresis and analyzed by mass spectrometry.

3. Results

MS spectra analysis showed no variation in the biotinylation pattern between experiments carried out with three different biotin concentrations indicating that an increase in biotin derivative concentration does not result in an increase in the number of biotinylated lysine residues. In the case of infected erythrocytes only two biotinylated lysine residues (K829, K892) could be detected. In non-infected erythrocytes in addition to K829 and K892, K826 is also biotinylated (Figure 30 A, B and C). Peaks corresponding to the peptides containing non-biotinylated lysine residues K826 and K892 were also detected in the MS spectra of the biotinylated sample. The peak of unmodified peptide containing lysine K829 is unfortunately located in the peak cluster from the matrix and could therefore not be detected. The peaks corresponding to the biotinylated peptides in the MS spectra have very low intensities in comparison to the unmodified form. All three biotinylated peptides are predicted to contain one missed cleavage site.

3. Results

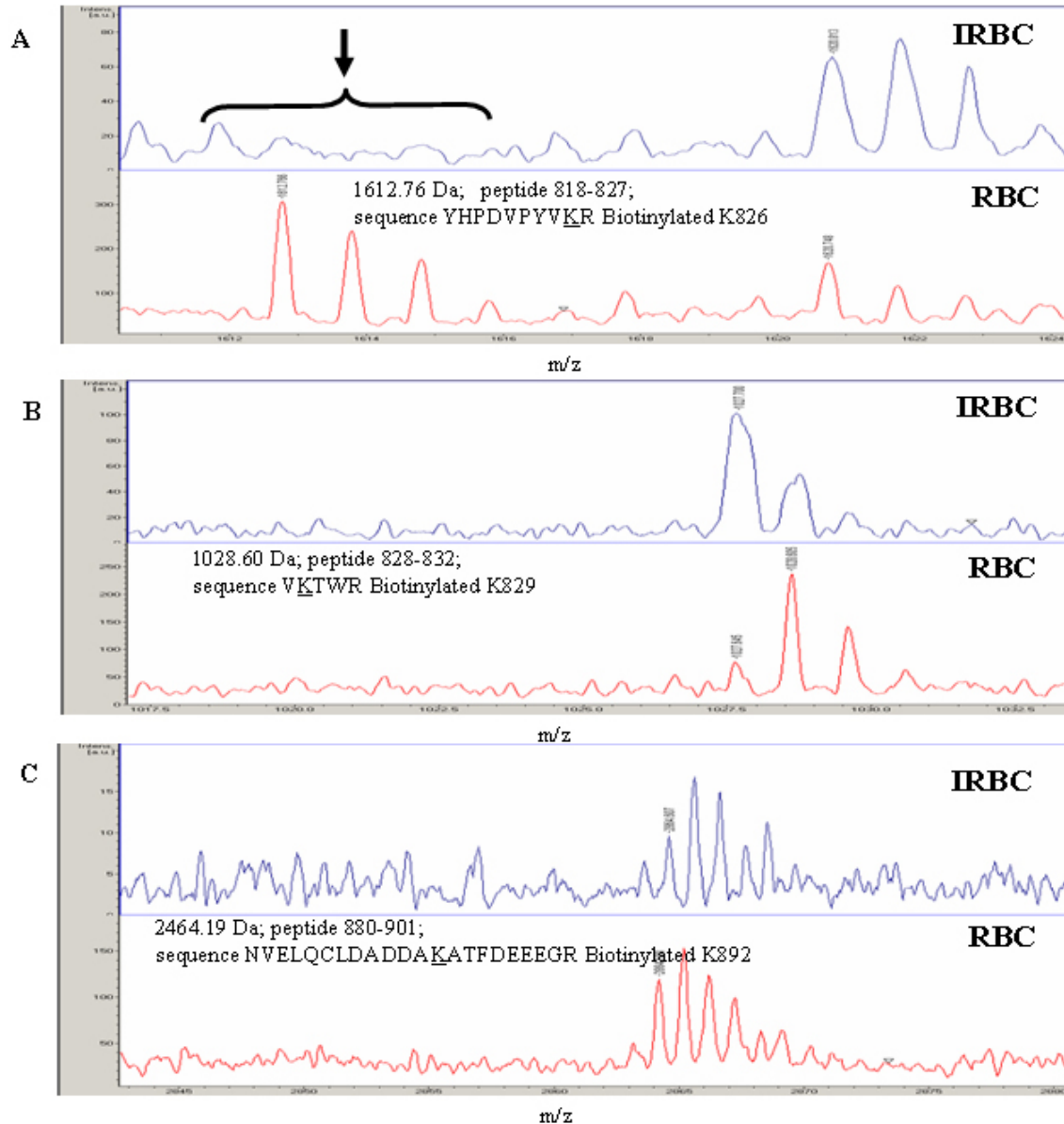
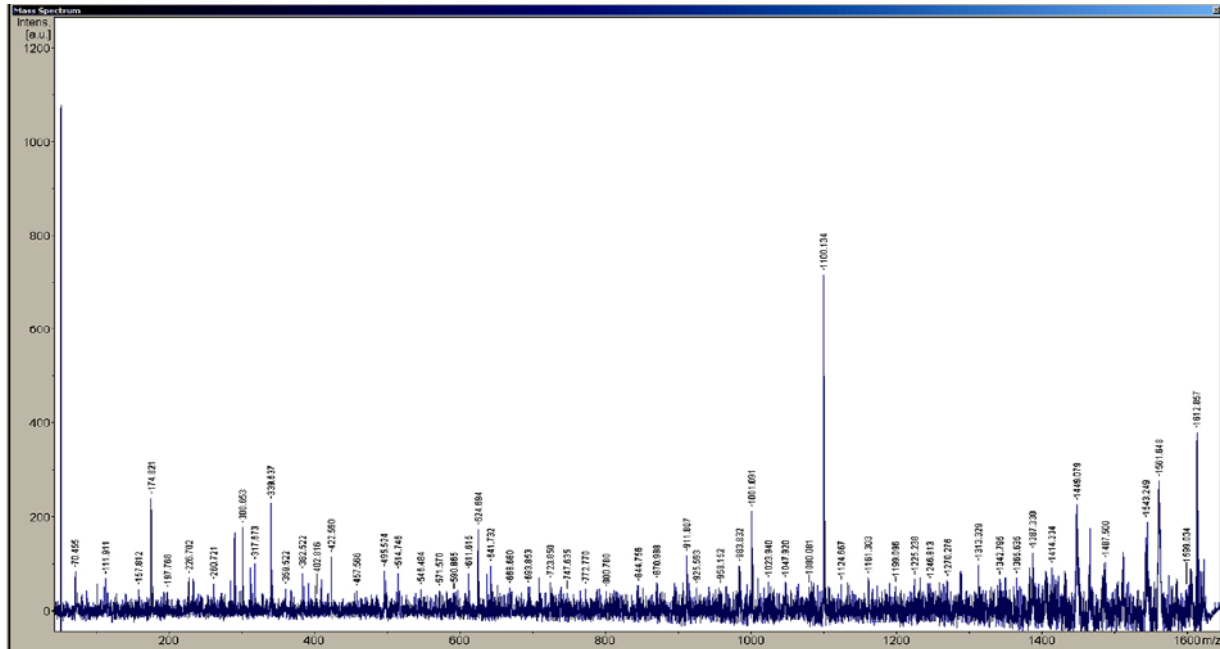


Figure 30. Zoom of sections MS spectra for Band III from infected erythrocytes and non-infected erythrocytes. In non-infected erythrocytes (RBC) lysine residues K826, K829 and K892 corresponding to m/z 1612.76, 1027.700 and 2864.19 respectively are biotinylated. In infected erythrocytes biotinylated K829 and K892 can be detected but not K826. The arrow in Figure A shows the absence of the peak corresponding to the peptide containing biotinylated K826 in infected erythrocytes(IRBC).

Further analysis of the K826 and K829 containing peptides by tandem mass spectrometry identified the individual biotinylated lysine residues. MS/MS Analysis of peptide with m/z 1612.87 confirmed the sequence (YHPDVVPYVKR) and the position of the modified lysine residue (Figure 31). In comparison to the theoretical mass of the peptide (1273.66), the observed mass shows the difference of 339.21 Da, corresponding

3. Results

to the mass of the biotin derivative. The biotin tag is detectable in spectra. In addition, the sequence contains one missed cleavage site.



818 - 827 1612.81 K.YHPDVPYV**K**R.V NHS-LC-Biotin (K)

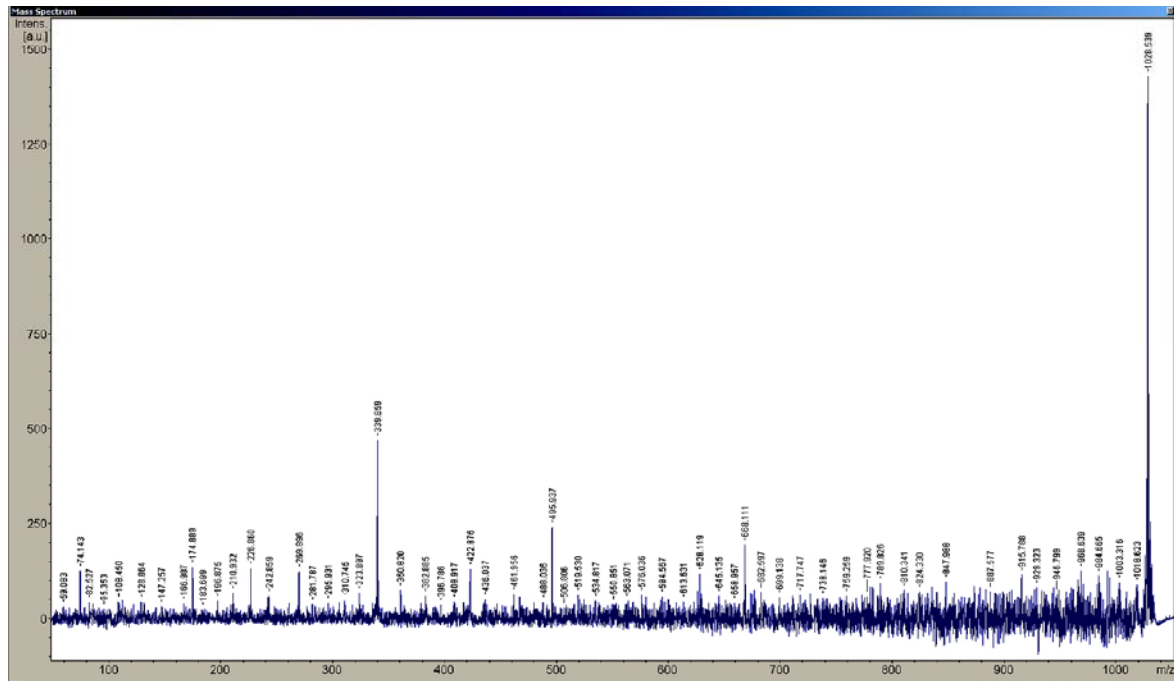
#	b	Seq.	y	#
1	164,07	Y	1612,875	10
2	301,13	H	1449,77	9
3	398,18	P	1312,71	8
4	513,21	D	1215,66	7
5	612,28	V	1100,63	6
6	709,33	P	1001,56	5
7	872,39	Y	904,51	4
8	971,46	V	741,44	3
9	1438,72	K	642,38	2
10		R	175,12	1

Figure 31. MS/MS analysis of peptide 1612.81 that is found only in the biotinylated Band III in RBC. The fragment ions of peptide with m/z 1612.81 confirmed the sequence (YHPDVPYV**K**R) of the peptide and modified lysine residue (K826). The spectrum contains the biotin peak at mass 340 Da and includes one missed cleavage site.

MS/MS analysis of peptide with mass 1028.54 revealed the corresponding sequence of the peptide (VKTWR) containing a biotinylated lysine residue (Figure 32). A 339.14 Da difference between the observed (1028.54) and theoretical mass (689.4093) of the peptide indicate the inclusion of a biotin moiety in the peptide. As shown in figure 26, the

3. Results

biotin tag is detected in spectra. MS/MS analysis confirmed that the sequence contains one missed cleavage site.



828 - 832 1028.53 R.VKTWR.M NHS-LC-Biotin (K)

#	b	Seq.	y	#
1	100,08	V	1028,53	5
2	567,33	K	929,5	4
3	668,38	T	462,25	3
4	854,46	W	361,2	2
5		R	175,12	1

Figure 32. MS/MS analysis of peptide 1028.54 that is found in the biotinylated Band III in RBC and IRBC. The generated fragments revealed the corresponding short sequence of peptide (VKTWR) containing biotinylated K829. The spectrum also reveals a peak corresponding to the mass of the biotin tag.

To confirm the biotinylation of K892 in the peptide with m/z 2864.840, the peptide was also subjected to tandem mass spectrometry. Despite three attempts, the low intensity and amino acid composition of this peptide did not result in good fragmentation ions and subsequently protein identification based on the fragments of peptide was not possible. MS/MS showed only significant fragment ion at m/z 339.414 which could correspond to the biotin tag, suggesting that the lysine residue in this peptide is biotinylated.

3. Results

3.16. Biotinylation does not affect the ionization efficiency of peptides

As described before, in the analysis of the biotinylation a pattern of Band III, the modified peptides were detected with low signal intensity in comparison to peptides containing non-biotinylated lysine residues. To determine if biotinylation has an effect on ionization of peptides during the MALDI process, a synthetic peptide with the sequence corresponding to the Band III peptide YHPDVPYVK (818-826) mass 1116.293 Da was biotinylated. The peptide was biotinylated with an equimolar concentration of sulfo-NHS-LC-biotin and subjected to mass spectrometry. The result shows that biotinylation does not reduce the ionization capacity during the MALDI process (Figure 33).

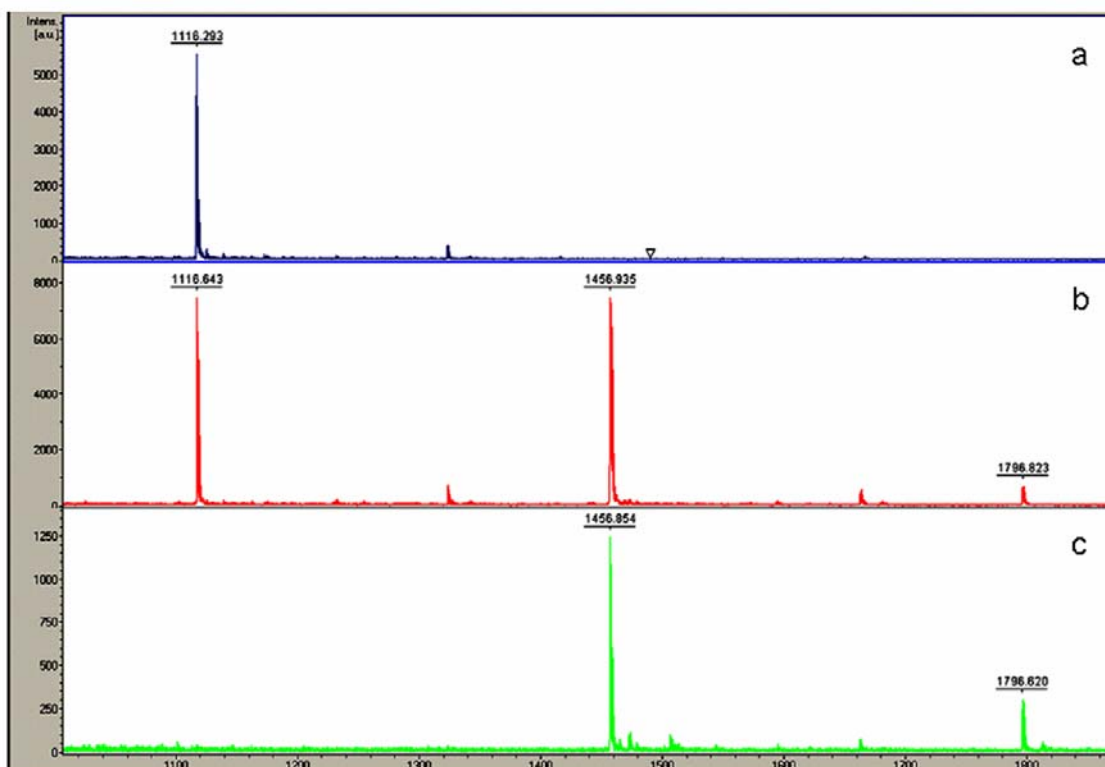


Figure 33. Biotinylation of synthetic Band III peptide using sulfo-NHS-LC-biotin. A synthetic peptide corresponding to the Band III peptide YHPDVPYVK (818-826) with m/z 1116.293 was biotinylated with an equimolar concentration of sulfo-NHS-LC-biotin and subjected to mass spectrometry. a: the non-biotinylated peptide; b: biotinylated peptide using equimolar biotin derivative; c: biotinylated using molar excess biotin derivative.

3. Results

Biotinylation with a molar excess of the biotin derivative leads to complete biotinylation. The non-biotinylated peptide is absent from the spectra and two peaks corresponding to the biotinylated peptides are detected with m/z 1456.955 Da corresponding to the addition of a single biotin molecule and m/z 1796.620 Da corresponding to the addition of 2 biotin molecules (Figure 33c). The biotinylation reaction in this peptide occurs at the epsilon amino group of the lysine residue or at the N-terminus of the peptide.

In spite of these findings, the lack of detection of biotinylated Band III peptides at high intensities in the preceding analysis may be due to other factors e.g. steric hindrance which leads to inefficient biotinylation and detection of the biotinylated peptides. Alternatively it could be due to the hydrophobic nature of the peptides, which has been shown to negatively affect ionization in MALDI due to the low proton affinity.

4. Discussion

Chemical modification of proteins and peptides with the hydrophilic reagent sulfo-NHS-LC-biotin derivative is one of the most commonly used molecule tagging method in biochemical and biomedical research. The ester active group of these derivatives reacts with the primary amines of proteins and/or the epsilon amino group of lysine residues forming an amide bond. The high affinity and specificity of the interaction of biotin to avidin and its bacterial homologue streptavidin, is regarded as the strongest non-covalent, biological interaction known with a dissociation constant, $K_a = 10^{15} \text{ M}^{-1}$. The biotin labelled proteins can be easily visualised with streptavidin derivatives, or they can be captured on streptavidin sepharose beads. The biotin labelled peptides can be purified, although due to the high stability of the biotin-streptavidin interaction, care must be taken to find effective elution conditions that have no effect on downstream analysis, especially mass spectrometry.

In this current study, I investigated whether biotinylation followed by mass spectrometry can be used as a general method to study both protein structure, and alterations in protein structure in response to external influences. To this end ,biotinylation patterns of three model proteins (bovine serum albumin (BSA), bovine carbonic anhydrase II (CA II) and erythrocyte plasma membrane protein Band III) were systematically analysed by mass spectrometry. To investigate whether conformation changes in the protein structure are reflected by changes in biotinylation patterns, these experiments were also carried out under different conditions to determine if specific, experimentally induced conformational changes result in a reproducible biotinylation pattern of lysine residues. We find that biotinylation patterns are highly reproducible under controlled experimental conditions.

4.1. Biotinylated lysine residues can be detected by MS and MS/MS analysis

Analysis of the biotinylated peptides by mass spectrometry showed that biotinylation of lysine residues does not affect the efficiency of ionization of peptides in MALDI-TOF mass spectrometry and that the modified peptides were detectable by MS analysis.

Furthermore, tandem mass spectrometry of the modified peptides together with a database search for the amino acid sequences confirms the sequence of the peptides. As shown in this study, MS/MS analysis of modified peptides reveals a characteristic mass peak at 339.16 Da corresponding to the mass of the biotin tag after breakage of the amide bond between the lysine residue and the biotin derivative, thus providing evidence for biotinylation. The quality of the MS/MS spectra and the intensity of the biotinylated peptides play an important role in such analyses.

4.2 .The biotinylation of protein is reproducible but incomplete

The mass spectrometry of the biotinylated BSA showed that biotin labelling of the protein is highly reproducible. The biotinylation pattern of a protein contains a number of lysine residues which are preferentially labelled and uniformly distributed in the protein. Exactly which lysine residues which can be labelled depends on the concentration of the biotin derivative and the protein structure. In the case of BSA the results showed that out of 60 lysine residues in the primary structure of BSA, only 18 lysine residues can be modified after biotinylation at room temperature. Furthermore, the mass spectrometry results in linear-TOF and reflectron mode indicated that the biotinylation of protein is not complete even when a high molar excess concentration of the biotin derivative is used in the biotinylation reaction. The incomplete biotin labelling could be attributed to the conformation of the protein, where some of the lysine residues are inaccessible to the biotinylating agent.

Recently, Huang *et al.*, (2004) used hydrophilic and hydrophobic cross-linkers and subsequent mass spectrometry to probe the tertiary structure of BSA. These included Bis (Sulfosuccinimidyl) suberate (BS³), a cross linker which has a reaction mechanism

4. Discussion

similar to that of sulfo-NHS- LC-biotin. The structure of the reagent is shown in figure 34. BS³ is a water-soluble, non-cleavable and membrane impermeable cross-linker that contains an amine-reactive *N*-hydroxysulfosuccinimide (NHS) ester. NHS esters react with primary amines in the side chain of lysine residues or the N-terminus of each polypeptide and form stable amide bonds at pH 7-9. BS³ has a spacer arm in with 11.4 Angstroms in length. Huang *et al.*, (2004) used BS³ to crosslink the lysines in the hydrophilic or surface regions in the BSA structure. The unmodified and BS³ modified BSA samples were digested by trypsin and analyzed using ESI MS and MS/MS.

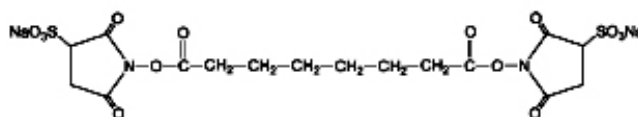


Figure 34. Structure of cross-linkers was Bis (sulfosuccinimidyl) substrate. The NHS ester groups at each end joined with an 8 carbon spacer arm with length of 11.4 Angstrom (modified from Pierce).

A comparison of the data from Huang *et al.*, (2004) experiment and this study revealed some differences (Table12). Huang *et al.*, (2004) identified a total of 20 modified lysine residues using BS³ cross-linker 13 of which were also labelled with sulfo-NHS-LC-biotin. Three of the modified residues (K138, K140 and K495) identified in that study were detected only in a non-biotinylated form in all of the experiments using sulfo-NHS-LC-biotin. One lysine residue (K88) was not detected in this current study using sulfo-NHS-LC-biotin labelling, and one residue (K399) was detected only once, in its biotinylated form. Two residues (K437 and K523) were also labelled with sulfo-NHS-LC-biotin however only after exposure of BSA to high temperature. Five further lysine residues were identified in a biotinylated form in this study which were not detected by Huang *et al.*, (2004). 7 lysine residues (K204, K211, K228, K245, K412, K420 and K463) which were modified by sulfo-NHS-LC- biotin, are (based on the Huang *et al* study) predicted to be exposed to the surface of BSA.

4. Discussion

Lysine	current study		Huang <i>et al.</i> ,2004
	LC-biotinylation at RT	LC-biotinylation at 80°C	BS ³ -cross linking
K 36	+	+	
K 88			+
K100	+	+	
K138			+
K140			+
K 156	+	+	+
K 160	+	+	+
K 204	+	+	+
K 211	+	+	+
K 228	+	+	+
K 235	+	+	+
K 245	+	+	+
K 266	+	+	
K 374	+	+	+
K 399			+
K 401	+	+	+
K 412	+	+	+
K 420	+	+	+
K 437		+	+
K 455	+	+	+
K 463	+	+	+
K 489			+
K 495			+
K 498	+	+	
K 523		+	
K 559	+	+	
Total	18	20	20

Table 12. The comparison of identified labelled lysine residues in current study and Huang *et al.*, (2004) study. The majority of the modified lysine residues were identical in both studies, underscoring the reproducibility of the biotinylation reaction. RT: room temperature; BS: Bis (Sulfosuccinimidyl) suberate cross linker.

Differences in the experimental procedure between Huang *et al.*, (2004) and this current study make direct comparison of the labelling status in these two experiments difficult. Nevertheless, although two different ionization conditions (ESI vs. MALDI) and different labelling reagents (BS³ or sulfo NHS-LC-biotin) were used, both the approach of Huang *et al.*, and our own approach identified almost identical peptides. Additionally, the modification status of the lysine residues in these peptides were almost identical in both studies, consistent with the reproducibility of the biotinylation reaction as described above.

4.3 .The conformational changes are reflected in the biotinylation pattern

Since the biotinylation pattern of the protein is dependent on protein conformation; any alteration in the protein structure is predicted to lead to an alternative biotinylation pattern. To study this possibility, BSA was subjected to higher temperatures and treatment with reducing agents, conditions which induce both reversible and irreversible conformational changes of the protein structures.

As described before, the heat denaturing of BSA molecule happens in two significant stages: up to 65°C the conformational change of BSA is reversible and the protein will return to the native state after cooling. Beyond 65°C, the irreversible alteration is induced in the structure but does not necessarily result in a complete destruction of the protein structure (Lin *et al.*, 1976; Wetzel *et al.*, 1980). During the heating above 65°C, the alpha helix can be partially unfolded and converts to the beta-sheet. This situation can be amplified by cooling (Wetzel *et al.*, 1980). Based on these concepts, the biotinylation patterns of BSA at room temperature and after heating at 56°C before biotinylation were identical. In contrast, exposure of BSA to the temperature of up to 80°C before biotinylation results in the detection of two additional biotinylated lysines. These results show that two new lysine residues were labelled after artificially inducing conformational changes, and that these changes are detectable with mass spectrometry.

Since the reduction of disulphide bonds in the structure of protein can induce the unfolding form, in this study the effect of reducing agents on the biotinylation pattern of BSA has been examined. MS analysis showed that no new lysine residues are biotinylated after reduction of BSA. The result confirms a previous study that suggested that most of the disulphide bonds in BSA are located almost between helical segments in the protein structure, where they are protected from reducing agents at neutral pH (Carter and Ho, 1994).

4.4. The biotinylated lysine residues are resistant to trypsin cleavage

Since biotinylation occurs at the protonated epsilon amino group of the lysine residue, in this study, the effect of biotinylation on the recognition and trypsin cleavage of lysine residues was analyzed. Using an effective and compatible elution protocol, quantitative recovery of biotinylated peptides from streptavidin sepharose were performed and the modified peptides were analyzed by mass spectrometry and tandem mass spectrometry. Data showed that approximately all of the biotinylated peptides which were identified in this study contained a missed cleavage, suggesting that trypsin cleavage at the C-termini of lysine residues is inhibited upon biotinylation.

4.5. Involvement of lysine residues in hydrogen bonding may prevent the biotinylation

Since only a certain number of lysine residues could be modified by biotinylation after different treatments in this study, it was suggested that the other lysines were not accessible to the modifying reagent. These non-biotinylated lysine residues are suggested to form hydrogen bonds with other residues or they are superficially buried in hydrophobic regions of the protein where they are shielded from the biotin derivative reagent through steric effects. Data in this study confirmed that the involvement of a lysine residue in a hydrogen bond significantly decreases the probability of biotinylation. The accessibility of the lysine residues in BSA structure to biotin derivative was also analyzed, the results showed no correlation between predicted accessibility of lysine residues to the surface and biotinylation. However, Huang *et al.*, (2004), based on cross linking experiments that lysine residues which reside at the interface between helices or turns between domains are exposed on the surface of the BSA molecule. Based on this prediction, seven biotinylated lysine residues (K204, K211, K228, K245, K412, K420 and K463) in the current study were exposed and available for biotin derivative.

4.6. Only few biotinylated lysine residues in Band III structure are detected

After showing that alteration in biotinylation pattern can be detected by mass spectrometry, the biotinylation of Band III from infected and non-infected erythrocytes was compared. Various proteomics studies have previously indicated that the identification of hydrophobic membrane proteins by mass spectrometry is problematic. Low sequence coverage of membrane proteins is a recognised phenomenon in such proteomics approaches (Santoni *et al.*, 2000; Low *et al.*, 2002; Abe *et al.*, 2004).

The Band III protein is divided into three regions: a hydrophilic, cytoplasmic domain (residues 1- 403) which interacts with a variety of membrane and cytoplasmic proteins; a hydrophobic, transmembrane domain (residues 404-882) which facilitates the anion transport and an acidic, C-terminal domain (residues 883-911) which interacts with carbonic anhydrase. The majority of the peptides which are located in the highly hydrophobic transmembrane domain of Band III could not be detected in this study. The identification of Band III with low sequence coverage could be attributed to the high hydrophobicity and low solubility of the protein, resulting in decreased trypsin accessibility to the cleavage sites. In addition, it has been shown that the hydrophobic nature of the peptides negatively affect the ionization in MALDI due to the low proton affinity (Olumee *et al.*, 1995). The low sequence coverage after peptide mass fingerprinting may also be due to the limited number of trypsin cleavage sites (lysine and arginine residues) within the protein sequence, resulting in the generation of only a small number of tryptic peptides.

Peptide mapping of the Band III protein using different chemical modification showed that the labelling of exposed lysine residues in the structure of Band III is not complete and only few lysine residues can be labelled with modifying reagents because of either function or structure of lysine residue in the protein structure (Kang *et al.*, 1992; Okubo *et al.*, 1994; Kuma *et al.*, 2002; Abe *et al.*, 2004).

4. Discussion

Analysis of biotinylation pattern of Band III in normal and South-east Asian ovalocytosis (SAO, containing abnormal Band III) erythrocytes after modification using sulfo-NHS-SS-biotin produced identical results (Kuma *et al.*, 2002). The authors labelled the available lysine residues in the transmembrane domains of Band III with a biotin derivative in a final concentration of 0.1-1 mg/ml. The transmembrane domains were obtained after removing the cytosolic N-terminus domain of the protein by trypsin treatment and separation from peripheral membrane proteins by alkali treatment. The membrane domains of protein were digested with trypsin and analyzed by MALDI-TOF mass spectrometry. The results showed that only two lysine residues (K892 and K814 / K817) were modified in normal Band III where the biotinylation of K814 and K817 could not be distinguished because they were identified in the same peptide. The Band III protein in the SAO membrane contains three extra modified lysines (K851, K691 and K757). In comparison to the Kuma *et al.*, (2002) analysis, our study also detected K814 and K817, but only in a non-biotinylated form. K851 was only found in RBC and K757 was detectable only in the IRBC sample, both in a non-biotinylated form. Lysine residue K691 was not detected at all.

These findings are also consistent with the cross-linking experiments data. It has been shown that the stilbene compounds DIDS and H₂DIDS which covalently react with a lysine residue, have distinct binding site in Band III. H₂DIDS reacts with K539 and K851 in Band III, and induces an intra-molecular cross-linkage between them (Okuba *et al.*, 1994). DIDS also reacts with K539, but no cross-link with K851 is formed except under partial denaturing conditions (Kang *et al.*, 1992). In another study, Abe *et al.* (2002) used further stilbene compounds 4-Acetamido-4'-isothiocyanatostilbene-2,2-disulfonic acid (SITS) and 2,4-Dinitrofluorobenzene (DNFB) to modify Band III. The authors showed that SITS modified only K539 and DNFB labelled K590 and K539.

The lack of detection of biotinylated Band III peptides at high intensities in our analyses may be due to other factors like steric hindrance, leading to only a sub-set of lysine residues being biotinylated. In fact, out of a possible 29 lysine residues (9 of which are predicted to be exposed at the erythrocyte surface) within the Band III protein sequence, only 3 could be detected in a biotinylated form. In addition the chemical modification and

4. Discussion

Lysine K826 is located in the extracellular flexible loop (Kuma *et al.*, 2002; Zhu *et al.*, 2003) whose lysine and histidine residues have been shown to be required for anion transport of Band III (Muller *et al.*, 1995). Peptides containing K826 and K829 are thus found in a region of Band III which appears to be important for protein function. This region is known to mediate the removal of aged erythrocytes by exposure of the senescent antigen (Kay *et al.*, 1990). K826 is also positioned in a region that is differentially recognized in non-infected and in infected erythrocytes by a monoclonal antibody (Winograd and Sherman, 2004). It was shown that synthetic peptides with residues 821-834 were able to inhibit the adhesion of *P. falciparum* infected erythrocytes in vitro and to affect sequestration (Crandallm and Sherman, 1994). The amino acids 807-826 are also identified as the core region of the Band III receptor for parasite MSP1 (Goel *et al.*, 2003).

At this point there is no explanation for the biotinylation of K892, which is predicted to be intracellular. It has been suggested that processing of the C-terminus or its association with other host proteins like carbonic anhydrase (Mori *et al.*, 1995; Vince and Reithmeier, 1998, 2000) possibly results in its surface exposure. This observation should be further investigated given that the C-terminus of the protein has been implicated in the physiological process other than anion transportation.

As shown in this study, analysis of the altered biotinylation pattern for the Band III molecule in non-infected and infected erythrocytes suggests a conformational change in the protein structure, consistent with previous results obtained using other methods.

4.8. Future directions and implications of this study

This study has established the protocols for the analysis of conformational changes in protein structure. The method of choice was labelling with biotin derivatives, followed by mass spectroscopy. Applying these methods show that changes in conformation can be detected using this method, and used further, the established protocol was used to verify changes in the structure of the Band III protein upon infection of the human erythrocyte with *P. falciparum*. Although in this particular case, the method used to study the influence of a pathogen on its host cell, it is envisaged that this method may also be applied to study changes in protein conformation in other cells and systems. Thus, the potential exists that this method can be applied more generally for the analysis of protein structure.

5. Literature

Abe Y, Chaen T, Jin, XR, Hamasaki, T, Hamasaki N. (2004). Massspectrometric analyses of transmembrane proteins in human erythrocyte membrane. *J Biochem.* 136(1):97-106.

Aikawa M. (1971) Parasitological review. Plasmodium: the fine structure of malarial parasites. *Experimental Parasitology.* 30, 284-320.

Aikawa, M., Kamanura, K., Shizashi, S., Matsumoto, Y., Arwati, H., Torii, M., Ito, Y., Takeuchi, T. Tandler, B. (1996). Membrane Knobs of Unfixed *Plasmodium falciparum* Infected Erythrocytes: New Findings as Revealed by Atomic Force Microscopy and Surface Potential Spectroscopy. *Experimental Parasitology.* 84, 339–343.

Aldred P, Fu P, Barrett G, Penschow JD, Wright RD, Coghlan JP, Fernley RT. (1991). Human secreted carbonic anhydrase: cDNA cloning, nucleotide sequence, and hybridization histochemistry. *Biochemistry.* 30(2):569-75.

Alkhalil A, Cohn JV, Wagner MA, Cabrera JS, Rajapandi T, Desai SA (2004) Plasmodium falciparum likely encodes the principal anion channel on infected human erythrocytes. *Blood.* 104, 4279-86.

Alper SL. (1991). The band 3-related anion exchanger (AE) gene family. *Annu Rev Physiol.* 53:549-64.

Alper SL, Kopito RR, Libresco SM, Lodish HF. (1988). Cloning and characterization of a murine band 3-related cDNA from kidney and from a lymphoid cell line. *J Biol Chem.* 263(32):17092-9.

Andersson B, Nyman PO, Strid L. (1972) Amino acid sequence of human erythrocyte carbonic anhydrase B. *Biochem Biophys Res Commun.* 7;48(3):670-7.

Anderson RA, and Lovrien RE. (1984). Glycophorin is linked by band 4.1 protein to the human erythrocyte membrane skeleton *Nature.* 307(5952): 655-8.

Anderson RA, and Marchesi VT. (1985). Regulation of the association of membrane skeletal protein 4.1 with glycophorin by a polyphosphoinositide. *Nature.* 318(6043):295-8.

Aronsson G, Mårtensson LG, Carlsson U, Jonsson BH. (1995). Folding and stability of the N-terminus of human carbonic anhydrase II. *Biochemistry.* 34(7):2153-62.

Askin D, Bloomberg GB, Chambers EJ, Tanner MJ. (1998). NMR solution structure of a cytoplasmic surface loop of the human red cell anion transporter, band 3. *Biochemistry.* 37(33):11670-8.

Atamna, H., and Ginsburg, H. (1993). Origin of reactive oxygen species in erythrocytes infected with *Plasmodium falciparum*. *Mol Biochem Parasitol* 61 (2), 231-241.

Atamna, H. and Ginsburg, H. (1997). The malaria parasite supplies glutathione to its host cell—investigation of glutathione metabolism in human erythrocytes infected with *Plasmodium falciparum*. *Eur J Biochem.* 250, 670–679.

Azimzadeh O, Hillebrecht A, Linne U, Marahiel MA, Klebe G, Lingelbach K, Nyalwidhe J. (2007). Use of biotin derivatives to probe conformational changes in proteins. *J Biol Chem.* 282(30):21609-17.

Back JW, Notenboom V, de Koning LJ, Muijsers AO, Sixma TK, de Koster CG, de Jong L. (2002). Identification of cross-linked peptides for protein interaction studies using mass spectrometry and ¹⁸O labeling. *Anal Chem.* 74(17):4417-22.

Bannister, L., Mitchell, G. (2003). The ins, outs and roundabouts of malaria. *Trends Parasitol* 19, 209-213.

Barnwell, J. (1990) Cytoadherence and sequestration in falciparum malaria. *Experimental Parasitology* 67, 407-412.

Baruch, D. I., Pasloske, B. L., Singh, H. B., Bi, X., Ma, X. C., Feldman, M., Taraschi, T. F., and Howard, R. J. (1995). Cloning the *P. falciparum* gene encoding PfEMP1, a malarial

5. Literature

variant antigen and adherence receptor on the surface of parasitized human erythrocytes. *Cell*. 82, 77-87.

Baumeister, S., Endermann, T., Charpian, S., Nyalwidhe, J., Duranton, C., Huber, S., Kirk, K., Kang, F., Lingelbach, K. (2003). A biotin derivative blocks parasite induced novel permeation pathways in *Plasmodium falciparum*-infected erythrocytes. *Mol Biochem Parasitol*. 132, 35–45.

Baumeister, S., Winterberg, M., Duranton, C., Huber, S., Lang, F., Kirk, K., Lingelbach, K. (2006). Evidence for the involvement of *Plasmodium falciparum* proteins in the formation of new permeability pathways in the erythrocyte membrane. *Molecular Microbiology* . (2), 493–504.

Benga G, Pop VI, Popescu O, Benga I, Ferdinand W. (1991). Amino acid composition of band 3 protein from red blood cells of normal and epileptic children. *Biosci Rep*. 11(1):53-7.

Bennett KL, Kussmann M, Björk P, Godzwon M, Mikkelsen M, Sørensen P, Roepstorff P. (2000). Chemical cross-linking with thiol-cleavable reagents combined with differential mass spectrometric peptide mapping--a novel approach to assess intermolecular protein contacts. *Protein Sci*. (8):1503-18.

Berendt, A. R., Simmons, D. L., Tansey, J., Newbold, C. I., Marsh, K. (1989). Intercellular adhesion molecule-1 is an endothelial cell adhesion receptor for *Plasmodium falciparum*. *Nature*. 341, 57-59.

Biemann K. (1992). Mass spectrometry of peptides and proteins. *Annu Rev Biochem*. 61:977-1010.

Bloomfield, V. (1966). The structure of bovine serum albumin at low pH. *Biochemistry*. 5(2):684-9.

Blythe JE, Suretheran T, Preiser PR. (2004). STEVOR--a multifunctional protein? *Mol Biochem Parasitol*. 134(1):11-5.

Bos OJ, Labro JF, Fischer MJ, Wilting J, Janssen LH. (1989). The molecular mechanism of the neutral-to-base transition of human serum albumin. Acid/base titration and proton nuclear

magnetic resonance studies on a large peptic and a large tryptic fragment of albumin. *J Biol Chem*. 15;264(2):953-9.

Bouyer G, Egée S, Thomas SL. (2006). Three types of spontaneously active anionic channels in malaria-infected human red blood cells. *Blood Cells Mol Dis*. 36(2):248-54.

Brahms S, Brahms J. (1980). Determination of protein secondary structure in solution by vacuum ultraviolet circular dichroism. *J Mol Biol*. 138(2):149-78.

Branton D, Cohen CM, Tyler J. (1981). Interaction of cytoskeletal proteins on the human erythrocyte membrane. *Cell*. (1):24-32.

Braschi S, Wilson RA. (2006). Proteins exposed at the adult schistosome surface revealed by biotinylation. *Mol Cell Proteomics*. 5(2):347-56.

Breuer, W. V., Kutner, S., Sylphen, J., Ginsburg, H. and Cabantchik, Z.I. (1987).

Covalent modification of the permeability pathways induced in the human erythrocyte membrane by the malarial parasite *Plasmodium falciparum*. *J Cell Physiol* 133, 55-63.

Bruce LJ, Anstee DJ, Spring FA, Tanner MJ. (1994). Band 3 Memphis variant II. Altered stilbene disulfonate binding and the Diego (Dia) blood group antigen are associated with the human erythrocyte band 3 mutation Pro854-->Leu. *J Biol Chem*. 269(23):16155-8.

Bruce LJ, Tanner MJ. (1999). Erythroid band 3 variants and disease. *Baillieres Best Pract Res Clin Haematol*. 12(4):637-54.

Cappellaro C, Mrsa V, Tanner W. (1998) New potential cell wall glucanases of *Saccharomyces cerevisiae* and their involvement in mating. *J Bacteriol*. 1998 Oct;180(19):5030-7.

Carter Richard and Mendis Kamini N. (2002). Evolutionary and Historical Aspects of the Burden of Malaria. *CMR*. 15.4.564–594.

Carter DC, He XM, Munson SH, Twigg PD, Gernert KM, Broom MB, Miller TY. (1989). Three-dimensional structure of human serum albumin. *Science*. 244 (4909): 1195-8.

5. Literature

- Carter, DC., He, XM. (1990) Structure of human serum albumin. *Science*. 20; 249 (4966):302-3.
- Carter, DC and Ho, JX (1994). Structure of serum albumin. *Adv Protein Chem*. 45:153-203
- Casanova M, Lopez-Ribot JL, Martinez JP, and Sentandreu R. (1992). Characterization of cell wall proteins from yeast and mycelial cells of *Candida albicans* by labelling with biotin: comparison with other techniques. *Infection and Immunity* 60, 4898-4906.
- Casey, J.R. and Reithmeier, R.A.F. (1991). Analysis of the oligomeric state of band 3, the anion transport protein of the human erythrocyte membrane, by size exclusion high performance liquid chromatography. Oligomeric stability and origin of heterogeneity. *J Biol Chem* 266 (24), 15726-15737.
- Chang SH, Low PS. (2003). Identification of a critical ankyrin-binding loop on the cytoplasmic domain of erythrocyte membrane band 3 by crystal structure analysis and site-directed mutagenesis. *J Biol Chem*. 278(9):6879-84.
- Chasis JA, Mohandas N, Shohet SB. (1985). Erythrocyte membrane rigidity induced by glycophorin A-ligand interaction. Evidence for a ligand-induced association between glycophorin A and skeletal proteins. *J Clin Invest*. 75(6):1919-26.
- Cheng Q, Cloonan N, Fischer K, Thompson J, Waine G, Lanzer M, Saul A. (1998). *stevor* and *rif* are *Plasmodium falciparum* multicopy gene families which potentially encode variant antigens. *Mol Biochem Parasitol*. 97(1-2):161-76.
- Christianson DW, Cox JD. (1997) Catalysis by metal-activated hydroxide in zinc and manganese metalloenzymes. *Annu Rev Biochem*. 68:33-57.
- Cistola DP, Small DM, Hamilton JA. (1987). Carbon 13 NMR studies of saturated fatty acids bound to bovine serum albumin. I. The filling of individual fatty acid binding sites. *J Biol Chem*. 262(23):10971-9.
- Cobb CE, Beth AH. (1990). Identification of the eosinyl-5-maleimide reaction site on the human erythrocyte anion-exchange protein: overlap with the reaction sites of other chemical probes. *Biochemistry*. 29(36):8283-90.
- Cohen AM, Liu SC, Lawler J, Derick L, Palek J. (1988). Identification of the protein 4.1 binding site to phosphatidylserine vesicles. *Biochemistry*. 27(2):614-9.
- Cornish TJ, Cotter RJ. (1993). A curved-field reflectron for improved energy focusing of product ions in time-of-flight mass spectrometry. *Rapid Commun Mass Spectrom*. 7(11):1037-40.
- Crandall I. and Sherman IW. (1991). *Plasmodium falciparum* (human malaria)-induced modifications in human erythrocyte band 3 protein. *Parasitology*. 3:335-40.
- Crandall I, Collins WE, Gysin J, Sherman IW. (1993). Synthetic peptides based on motifs present in human band 3 protein inhibit cytoadherence/sequestration of the malaria parasite *Plasmodium falciparum*. *Proc Natl Acad Sci U S A*. 90(10):4703-7.
- Crandall I. And Sherman IW. (1994). Antibodies to synthetic peptides based on band 3 motifs react specifically with *Plasmodium falciparum* (human malaria)-infected erythrocytes and block cytoadherence. *Parasitology* 108, 389-396.
- Cranmer SL, Conant AR, Gutteridge WE, Halestrap AP. (1995). Characterization of the enhanced transport of L- and D-lactate into human red blood cells infected with *Plasmodium falciparum* suggests the presence of a novel saturable lactate proton cotransporter. *J Biol Chem*. (25):15045-52
- Craig, A., Scherf, A. (2001). Molecules on the surface of the *Plasmodium falciparum* infected erythrocyte and their role in malaria pathogenesis and immune evasion. *Mol Biochem Parasitol*. 115 (2), 129-143.
- Curry S, Mandelkow H, Brick P, Franks N. (1998). Crystal structure of human serum albumin complexed with fatty acid reveals an asymmetric distribution of binding sites. *Nat Struct Biol*. 5(9):827-35.
- Daniels G. (2007). Functions of red cell surface proteins. *Vox Sang*. 93(4):331-40.

5. Literature

- Davis LH, Bennett V. (1990). Mapping the binding sites of human erythrocyte ankyrin for the anion exchanger and spectrin. *J Biol Chem.* 265(18):10589-96.
- Decherf G, Egee S, Staines HM, Ellory JC, Thomas SL (2004) Anionic channels in malaria-infected human red blood cells. *Blood Cells Mol Dis* 32, 366-71.
- Deitsch, K., Wellems, W. (1996). Membrane modifications in erythrocytes parasitized by *Plasmodium falciparum*. *Mol Biochem Parasitol.* 76, 1-10.
- De Rosa MC, Carelli Alinovi C, Galtieri A, Scatena R, Giardina B. (2007). The plasma membrane of erythrocytes plays a fundamental role in the transport of oxygen, carbon dioxide and nitric oxide and in the maintenance of the reduced state of the heme iron. *Gene.* 398(1-2):162-71.
- Desai, S.A., Bezrukov, S.M., Zimmerberg, J. (2000). A voltage-dependent channel involved in nutrient uptake by red blood cells infected with the malaria parasite. *Nature* 406, 1001–1005.
- Deuticke B, Beyer E, Forst B. (1982). Discrimination of three parallel pathways of lactate transport in the human erythrocyte membrane by inhibitors and kinetic properties. *Biochim Biophys Acta.* 684(1):96-110.
- Deuticke B. (2003). Membrane lipids and proteins as a basis of red blood cell shape and its alterations. In: Red Cell Membrane Transport in Health and Disease. Edited by Bernhardt, Vj., Ellory, J. *Springer.* 2, 27-60.
- Dumaswala UJ, Zhuo L, Jacobsen DW, Jain SK, Sukalski KA. (1999). Protein and lipid oxidation of banked human erythrocytes: role of glutathione. *Free Radic Biol Med.* 27(9-10):1041-9.
- Durantón C, Huber SM, Lang F (2002). Oxidation induces a Cl(-)-dependent cation conductance in human red blood cells. *J Physiol* 539, 847-55.
- Durantón, C., Huber, S.M., Tanneur, V., Lang, K.S., Brand, V., Sandu, C.D., Lang, F. (2003). Electrophysiological properties of the *Plasmodium falciparum*-induced cation conductance of human erythrocytes. *Cell Physiol Biochem.* 13, 289-298.
- Durantón C, Huber SM, Tanneur V, Brand VB, Akkaya C, Shumilina EV, Sandu CD, Lang F (2004). Organic Osmolyte Permeabilities of the Malaria-induced Anion Conductances in Human Erythrocytes. *J Gen Physiol* 123, 417-26.
- Egée, S., Lapaix, F., Decherf, G., Staines, H.M., Ellory, J.C., Doerig, C., Thomas, S.L. (2002). A stretch-activated anion channel is up-regulated by the malaria parasite *Plasmodium falciparum*. *J Physiol* 542, 795–801.
- Emerson, TE, Jr. (1989). Unique features of albumin: a brief review. *Crit Care Med.* 17(7):690-4.
- Elford, B. C., Haynes, J. D., Chulay, J. D. and Wilson, J.R. (1985). Selective stagespecific changes in the permeability to small hydrophilic solutes of human erythrocytes infected with *Plasmodium falciparum*. *Mol Biochem Parasitol* 16, 43-60.
- Fairbanks, G., Steck, T. and Wallach, D. (1971). Electrophoretic analysis of the major polypeptides of the human erythrocyte membrane. *Biochemistry*, 10, 2606-2617.
- Farruggia B, Picó GA. 1999 Thermodynamic features of the chemical and thermal denaturations of human serum albumin. *Int J Biol Macromol.* 26(5):317-23
- Fievet, B., Gabillat, N., Borgese, F., Motais, R. (1995). Expression of band 3 anion exchanger induces chloride current and taurine transport: structure-function analysis. *The EMBO Journal*, 14:21,5158-5169.
- Fievet, B., Perset, F., Gabillat, N., Guizouran, H., Borgese, F., Ripoche, P., Motais, R. (1998). Transport of uncharged organic solutes in *Xenopus* oocytes expressing red cell anion exchangers (AE1s). *Proc. Natl. Acad. Sci. USA*, 95, 10996–11001.
- Fernandez V, Hommel M, Chen Q, Hagblom P, Wahlgren M. (1999). Small, clonally variant antigens expressed on the surface of the *Plasmodium falciparum*-infected erythrocyte are encoded by the rif gene family and are the target

5. Literature

of human immune responses. *J Exp Med*. 190(10):1393-404.

Florens L, Liu X, Wang Y, Yang S, Schwartz O, Peglar M, Carucci DJ, Yates JR 3rd, Wub Y. (2004). Proteomics approach reveals novel proteins on the surface of malaria-infected erythrocytes. *Mol Biochem Parasitol*. 135. (1):1-11.

Foster AJ, Bird RA, Smith SN. (2007). Biotinylation and characterization of *Cryptococcus neoformans* cell surface proteins. *J Appl Microbiol*. 103(2):390-9.

Frazar TF, Weisbein JL, Anderson SM, Cline AP, Garrett LJ, Felsenfeld G, Gallagher PG, Bodine DM. (2003). Variegated expression from the murine band 3 (AE1) promoter in transgenic mice is associated with mRNA transcript initiation at upstream start sites and can be suppressed by the addition of the chicken beta-globin 5' HS4 insulator element. *Mol Cell Biol*. 23(14):4753-63.

Freskgård PO, Mårtensson LG, Jonasson P, Jonsson BH, Carlsson U. (1994). Assignment of the contribution of the tryptophan residues to the circular dichroism spectrum of human carbonic anhydrase II. *Biochemistry*. 33(47):14281-8.

Fujinaga J, Tang XB, Casey JR. (1999). Topology of the membrane domain of human erythrocyte anion exchange protein, AE1. *J Biol Chem*. 274(10):6626-33.

Gao JP, Zhang F, Zhang L, Guo YL, Ruan KC, Jiang DA, Xu CH. (2006). Six specific lysine residues are crucial in maintaining the structure and function of soluble manganese stabilizing protein. *Acta Biochim Biophys Sin (Shanghai)*. 38(9):611-9.

Garcia AM, Lodish HF. (1989). Lysine 539 of human band 3 is not essential for ion transport or inhibition by stilbene disulfonates. *J Biol Chem*. 264(33):19607-13.

Gargaro AR, Bloomberg GB, Dempsey CE, Murray M, Tanner MJ. (1994). The solution structures of the first and second transmembrane-spanning segments of band 3. *Eur J Biochem*. 221(1):445-54.

Gehrig, H, Müller, W, Appelhans, H. (1992). Complete nucleotide sequence of band 3 related anion transport protein AE2 from human kidney. *Biochim Biophys Acta*. 1130(3):326-8.

Ginsburg H, Krugliak M, Eidelman O, Cabantchik ZI. (1983). New permeability pathways induced in membranes of *Plasmodium falciparum* infected erythrocytes. *Mol Biochem Parasitol*. (2):177-90.

Ginsburg, H., Kutner, S., Krugliak, M. and Cabantchik, Z.I. (1985). Characterization of permeation pathways appearing in the host membrane of *Plasmodium falciparum* infected red blood cells. *Mol Biochem Parasitol* 14, 313-322.

Ginsburg, H., Kirk, K. (1998). Membrane transport in the malaria-infected erythrocyte. *Malaria parasite biology, pathogenesis and protection*. ASM press. 219-232.

Giribaldi, G., Ulliers, D., Mannu, F., Arese, P. and Turrini, F. (2001). Growth of *Plasmodium falciparum* induces stage-dependent haemichrome formation, oxidative aggregation of band 3, membrane deposition of complement antibodies, and phagocytosis of parasitized erythrocytes. *Br J Haematol* 113, 492-499.

Greenfield NJ. (2006). Using circular dichroism spectra to estimate protein secondary structure. *Nat Protoc*. 1(6):2876-90.

Glish GL and Vachet RW. (2003). The basics of mass spectrometry in the twenty-first century. *Nat Rev Drug Discov*. 2(2):140-50.

Goel VK, Li X, Chen H, Liu SC, Chishti AH, Oh SS. (2003). Band 3 is a host receptor binding merozoite surface protein 1 during the *Plasmodium falciparum* invasion of erythrocytes. *Proc Natl Acad Sci U S A*. 100(9):5164-9.

Hamilton JA, Era S, Bhamidipati SP, Reed RG. (1991). Locations of the three primary binding sites for long-chain fatty acids on bovine serum albumin. *Proc Natl Acad Sci U S A*. 88(6):2051-4.

Håkansson K, Wehnert A. (1992). Structure of cobalt carbonic anhydrase complexed with bicarbonate. *J Mol Biol*. 228(4):1212-8.

5. Literature

- Håkansson K, Carlsson M, Svensson LA, Liljas A. (1992). Structure of native and apo carbonic anhydrase II and structure of some of its anion-ligand complexes. *J Mol Biol.* 227(4):1192-204.
- Håkansson K, and Liljas A. (1994). The structure of a complex between carbonic anhydrase II and a new inhibitor, trifluoromethane sulphonamide. *FEBS Lett.* 350(2-3):319-22.
- Hagag N, Birnbaum ER, Darnall DW. (1983). Resonance energy transfer between cysteine-34, tryptophan-214, and tyrosine-411 of human serum albumin. *Biochemistry.* 10;22(10):2420-7.
- He, XM and Carter, DC. (1992). Atomic structure and chemistry of human serum albumin. *Nature.* 16; 358(6383): 209-15.
- Henkens RW, Kitchell BB, Lottich SC, Stein PJ, Williams TJ. (1982). Detection and characterization using circular dichroism and fluorescence spectroscopy of a stable intermediate conformation formed in the denaturation of bovine carbonic anhydrase with guanidinium chloride. *Biochemistry.* 21(23):5918-23.
- Henderson LE, Henriksson D, Nyman PO. (1976). Primary structure of human carbonic anhydrase C. *J Biol Chem.* 251(18):5457-63.
- Hellman U, Wernstedt C, Góñez J, Heldin CH. (1995). Improvement of an "In-Gel" digestion procedure for the micropreparation of internal protein fragments for amino acid sequencing. *Anal Biochem.* 224(1):451-5.
- Helmsby H, Cavalier L, Pettersson U, Wahlgren M. (1993). Rosetting Plasmodium falciparum-infected erythrocytes express unique strain-specific antigens on their surface. *Infect Immun.* 61(1):284-8.
- Hewett-Emmett D, Tashian RE. (1996). Functional diversity, conservation, and convergence in the evolution of the alpha-, beta-, and gamma-carbonic anhydrase gene families. *Mol Phylogenet Evol.* 5 (1): 50-77.
- Hillenkamp, F. and Karas, M. (1990). Mass spectrometry of peptides and proteins by matrix-assisted ultraviolet laser desorption/ionization. *Methods Enzymol* 193, 280-295.
- Hillenkamp F, Karas M, Beavis RC, Chait BT. (1991). Matrix-assisted laser desorption/ionization mass spectrometry of biopolymers. *Anal Chem.* 63(24):1193A-1203A.
- Ho, MK, Guidotti, G. (1975). A membrane protein from human erythrocytes involved in anion exchange. *J Biol Chem.* 250(2):675-83.
- Hornig R, Lutz HU. (2000). Band 3 protein clustering on human erythrocytes promotes binding of naturally occurring anti-band 3 and anti-spectrin antibodies. *Exp Gerontol.* 35(8):1025-44.
- Huang BX, Kim HY, Dass C. (2004). Probing three-dimensional structure of bovine serum albumin by chemical cross-linking and mass spectrometry. *J Am Soc Mass Spectrom.*(8):1237-47
- Huang BX, Dass C, Kim HY. (2005). Probing conformational changes of human serum albumin due to unsaturated fatty acid binding by chemical cross-linking and mass spectrometry. *Biochem J.* 387(Pt 3):695-702.
- Huber, S. M., Uhlemann, A.C., Gamper, N.L., Durantón, C., Kremsner, P.G., Lang, F. (2002a). Plasmodium falciparum activates endogenous Cl⁻ channels of human erythrocytes by membrane oxidation. *EMBO J.* 21, 22–30.
- Huber, S.M., Durantón, C., Uhlemann, A.C., Kremsner, P., Lang, F. (2002b). Anion and organic osmolyte channels of human erythrocytes infected with Plasmodium falciparum. *Pflügers. Arch.* 443 (Suppl.), S164.
- Hirayama K, Akashi S, Furuya M, Fukuhara K (1990). Rapid confirmation and revision of the primary structure of bovine serum albumin by ESIMS and Frit-FAB LC/MS. *Biochem Biophys Res Commun.* 14; 173(2):639-46.
- Iglesias, J., Abernethy, V.E., Wang, Z., Lieberthal, W., Koh, J.S., Levine, J.S. (1999). Albumin is a major serum survival factor for renal tubular cells and macrophages through scavenging of ROS. *Am J Physiol Renal Physiol*, 277:711-722.
- Ingrosso D, D'angelo S, di Carlo E, Perna AF, Zappia V, Galletti P. (2000). Increased methyl esterification of altered aspartyl residues in erythrocyte membrane proteins in response to

5. Literature

- oxidative stress. *Eur J Biochem.* 267(14):4397-405.
- Izuhara K, Okubo K, Hamasaki N. (1989). Conformational change of band 3 protein induced by diethyl pyrocarbonate modification in human erythrocyte ghosts. *Biochemistry.* 28(11):4725-8.
- Jarolim P, Rubin HL, Zakova D, Storry J, Reid ME. (1998). Characterization of seven low incidence blood group antigens carried by erythrocyte band 3 protein. *Blood.* 92(12):4836-43.
- Jay D, Cantley L. (1986). Structural aspects of the red cell anion exchange protein. *Annu Rev Biochem.* 55:511-38.
- Jennings, M., Monaghan, R., Douglas, S., Nicknisch, S. (1985). Functions of Extracellular Lysine Residues in the Human Erythrocyte Anion Transport Protein. *J. GEN. PHYSIOL*, 86, 653-669.
- Jennings ML, Anderson MP. (1987). Chemical modification and labeling of glutamate residues at the stilbenedisulfonate site of human red blood cell band 3 protein. *J Biol Chem.* 262(4):1691-7.
- Jensen ON, Podtelejnikov A, Mann M. (1996). Delayed extraction improves specificity in database searches by matrix-assisted laser desorption/ionization peptide maps. *Rapid Commun Mass Spectrom.* 10(11):1371-8.
- Jin XR, Abe Y, Li CY, Hamasaki N. (2003). Histidine-834 of human erythrocyte band 3 has an essential role in the conformational changes that occur during the band 3-mediated anion exchange. *Biochemistry.* 42(44):12927-32.
- Kannan KK, Notstrand B, Fridborg K, Lövgren S, Ohlsson A, Petef M. (1975). Crystal structure of human erythrocyte carbonic anhydrase B. Three-dimensional structure at a nominal 2.2-Å resolution. *Proc Natl Acad Sci U S A.* 72(1):51-5.
- Kang D, Okubo K, Hamasaki N, Kuroda N, Shiraki H. (1994). A structural study of the membrane domain of band 3 by tryptic digestion. Conformational change of band 3 in situ induced by alkali treatment. *J Biol Chem.* 267(27):19211-7.
- Karas M and Hillenkamp F. (1988). Laser desorption ionization of proteins with molecular masses exceeding 10,000 daltons. *Anal Chem.* 60(20):2299-301.
- Kanki, T., Sakaguchi, M., Kitamura, A., Sato, T., Milhara, K. and Hamasaki N. (2002). The tenth membrane region of band 3 is initially exposed to the luminal side of the endoplasmic reticulum and then integrated into a partially folded band 3 intermediate. *Biochemistry* 41 (47), 13973-13981.
- Karas M, Glückmann M, Schäfer J. (2000). Ionization in matrix-assisted laser desorption/ionization: singly charged molecular ions are the lucky survivors. *J Mass Spectrom.* 35(1):1-12.
- Katchalski, E., Benjamin, G., Ross, R. (1957). The Availability of the Disulfide Bonds of Human and Bovine Serum Albumin and of Bovine γ -Globulin to Reduction by Thioglycolic Acid. 97: 4096-4099.
- Kaviratne M, Khan SM, Jarra W, Preiser PR. (2002). Small variant STEVOR antigen is uniquely located within Maurer's clefts in Plasmodium falciparum-infected red blood cells. *Eukaryot Cell.* 1(6):926-35.
- Kay, MM and Lin, FB. (1990). Molecular mapping of the active site of an aging antigen: senescent cell antigen requires lysine(s) for antigenicity and is located on an anion-binding segment of band 3 membrane transport protein. *Gerontology.* 36(5-6):293-305.
- Kirk K, Wong HY, Elford BC, Newbold CI, Ellory JC. (1991). Enhanced choline and Rb⁺ transport in human erythrocytes infected with the malaria parasite Plasmodium falciparum. *Biochem J.* 278 (Pt 2):521-5.
- Kirk, K., Horner, H.A., Spillett, D.J., Elford, B.C. (1993). Glibenclamide and meglitinide block the transport of low molecular weight solutes into malaria-infected erythrocytes. *FEBS Lett.* 323, 123-128.
- Kirk, K., Horner, H.A., Elford, B.C., Ellory, J.C. and Newbold, C.I. (1994). Transport of Diverse Substrates into Malaria-infected Erythrocytes via a Pathway Showing Functional Characteristics of

5. Literature

a Chloride Channel. *J Biol Chem* 269, 3339-3347.

Kirk, K., Horner, H.A. (1995a). In search of a selective inhibitor of the induced transport of small solutes in *Plasmodium falciparum*-infected erythrocytes: effects of arylaminobenzoates. *Biochem J.* 311 (3), 761-768.

Kirk, K., Horner, H.A. (1995b). Novel anion dependence of induced cation transport in malaria-infected erythrocytes. *J Biol Chem* 270, 24270–24275.

Kirk, K., Horner, H. A. and Kirk, J. (1996). Glucose uptake in *Plasmodium falciparum*-infected erythrocytes is an equilibrative not an active process. *Mol Biochem Parasitol* 82, 195-205.

Kirk K, Tilley L, Ginsburg H. (1999). Transport and trafficking in the malaria-infected erythrocyte. *Parasitol Today*.15(9):355-7.

Kirk, K. (2001). Membrane transport in the malaria-infected erythrocyte. *Physiol Rev* 81, 495–537.

Kirk, K. (2004). Channels and transporters as drug targets in the Plasmodium-infected erythrocyte. *Acta Trop.* 89(3):285-98.

Knauf, P.A. and Rothstein, A. (1971). Chemical modification of membranes. I. Effects of sulfhydryl and amino reactive reagents on anion and cation permeability of the human red blood cell. *J Gen Physiol* 58 (2), 190-210.

Knuepfer, E., Rug, M., Klonis, N., Tilley, L., Cowman, A.F. (2005). Trafficking of the major virulence factor to the surface of transfected *P falciparum*-infected erythrocytes. *Blood* ,105, 4078-4087.

Kriek N, Tilley L, Horrocks P, Pinches R, Elford BC, Ferguson DJ, Lingelbach K, Newbold CI. (2003). Characterization of the pathway for transport of the cytoadherence-mediating protein, PfEMP1, to the host cell surface in malaria parasite-infected erythrocytes. *Mol Microbiol.* 50(4):1215-27.

Koh, J.S., Lieberthal, W., Heydrick, S., Levine, J.S. (1998). Lysophosphatidic Acid Is a Major Serum Noncytokine Survival Factor for Murine

Macrophages Which Acts via the Phosphatidylinositol 3-Kinase Signaling Pathway. *J. Clin. Invest.* 102, 4, 716–727

Kopito, R.R. (1990). Molecular biology of the anion exchanger gene family. *Int Rev Cytol* 123, 177-199.

Kopito RR, Lodish HF. (1985). Structure of the murine anion exchange protein. *J Cell Biochem.* 29(1):1-17.

Kriek N, Tilley L, Horrocks P, Pinches R, Elford BC, Ferguson DJ, Lingelbach K, Newbold CI. (2003). Characterization of the pathway for transport of the cytoadherence-mediating protein, PfEMP1, to the host cell surface in malaria parasite-infected erythrocytes. *Mol Microbiol.*; 50(4):1215-27.

Kuma, H., Shinde, A.A., Howren, T.R., and Jennings, M.L. (2002). Topology of the anion exchange protein AE1: the controversial sidedness of lysine 743. *Biochemistry* 41, 3380-3388.

Kutner S, Ginsburg H, Cabantchik ZI, (1983). Permselectivity Changes in Malaria (*Plasmodium falciparum*) Infected Human Red Blood Cell Membranes. *J Cellular Physiology.* 114:245-251.

Kutner S, Breuer WV, Ginsburg H, Aley SB, Cabantchik ZI. (1985). Characterization of permeation pathways in the plasma membrane of human erythrocytes infected with early stages of *Plasmodium falciparum*: association with parasite development. *J Cell Physiol.* 125, 521-7.

Kushwaha, A., Perween, A., Mukund, S., Majumdar, S., Bhardwaj, D., N., Chowdhury, Chauhan, V. (2002). Amino terminus of *Plasmodium falciparum* acidic basic repeat antigen interacts with the erythrocyte membrane through band 3 protein. *Molecular & Biochemical Parasitology*, 122, 45-54.

Kyes S, Horrocks P, Newbold C. (2001). Antigenic variation at the infected red cell surface in malaria. *Annu Rev Microbiol.* 55:673-707.

Kyes SA, Rowe JA, Kriek N, Newbold CI. (1999). Rifins: a second family of clonally variant proteins expressed on

5. Literature

- the surface of red cells infected with *Plasmodium falciparum*. *Proc Natl Acad Sci U S A*. 96(16):9333-8.
- Laemmli, U. K. (1970). Cleavage of structural proteins during the assembly of the head of bacteriophage T4. *Nature* 227, 680-685.
- Lavecchia R, Zugaro M. (1991). Thermal denaturation of erythrocyte carbonic anhydrase. *FEBS Lett*. 292(1-2):162-4.
- Li C, Takazaki S, Jin X, Kang D, Abe Y, Hamasaki N. (2006). Identification of oxidized methionine sites in erythrocyte membrane protein by liquid chromatography/electrospray ionization mass spectrometry peptide mapping. *Biochemistry*. 45(39):12117-24.
- Lin KT, Deutsch HF. (1973a). Human carbonic anhydrases. X. Preparation of large peptide fragments of carbonic anhydrase B used for sequence studies. *J Biol Chem*. 248(6):1881-4.
- Lin KT, Deutsch HF. (1973b) Human carbonic anhydrases. XI. The complete primary structure of carbonic anhydrase B. *J Biol Chem*. 248(6):1885-93.
- Lin KD, Deutsch HF. (1973c). Simplified methods for automated ion-exchange separation of peptides and accelerated manual Edman degradations. *Anal Biochem*. 56(1):155-64.
- Lin VJ, Koenig JL. (1976). Raman studies of bovine serum albumin. *Biopolymers*. 15(1):203-18.
- Lindskog S. (1997) Structure and mechanism of carbonic anhydrase. *Pharmacol Ther*. (1):1-20.
- Lindskog, S, Nyman, PO. (1964). Metal-binding properties of human erythrocyte carbonic anhydrase. *Biochim Biophys Acta*. 85:462-74.
- Lloyd J, McMillan S, Hopkinson D, Edwards YH. (1986). Nucleotide sequence and derived amino acid sequence of a cDNA encoding human muscle carbonic anhydrase. *Gene*. 41(2-3):233-9.
- Lucas JZ, and Sherman IW. (1998). *Plasmodium falciparum*: thrombospondin mediates parasitized erythrocyte band 3-related adhesion binding. *Exp Parasitol*. 89(1):78-85.
- Luft BJ, Jiang W, Munoz P, Dattwyler RJ, and Gorevic PD. (1989). Biochemical and immunological characterization of the surface proteins of *Borrelia burgdorferi*. *Infection and Immunity* 57, 3637-3645.
- Luft, AJ, and Lorscheider, FL (1983). Structural analysis of human and bovine alpha-fetoprotein by electron microscopy, image processing, and circular dichroism. *Biochemistry*. 6;22(25):5978-81.
- Lux, SE, John, KM, Kopito, RR, Lodish, HF. (1989). Cloning and characterization of band 3, the human erythrocyte anion-exchange protein (AE1). *Proc Natl Acad Sci U S A*. 86(23):9089-93.
- Mackintosh, C, Beeson, J, Marsh, K. (2004). Clinical features and pathogenesis of severe malaria. *TRENDS in Parasitology* 20(12) 597-603
- Malaney, P, Spielman, A and Sachs, J. (2004). The malaria gap. *Am. J. Trop. Med. Hyg.*, 71(Suppl 2), 141-146.
- Maren TH. (1967) Carbonic anhydrase: chemistry, physiology, and inhibition. *Physiol Rev*. 47(4):595-781.
- Marti M, Baum J, Rug M, Tilley L, Cowman AF. (2005). Signal-mediated export of proteins from the malaria parasite to the host erythrocyte. *J Cell Biol*. 171(4):587-92.
- McGillivray RT, Chung DW, Davie EW. (1979). Biosynthesis of bovine plasma proteins in a cell-free system. Amino-terminal sequence of prealbumin. *Eur J Biochem*. 98(2):477-85.
- Miller, L., Good, M., Milon, G. (1994). Malaria pathogenesis. *Science*, 264, 1878-1883
- Montgomery JC, Venta PJ, Eddy RL, Fukushima YS, Shows TB, Tashian RE. (1991). Characterization of the human gene for a newly discovered carbonic anhydrase, CA VII, and its localization to chromosome 16. *Genomics*. 11(4):835-48.
- Mori A, Okubo K, Kang D, Hamasaki N. (1995). A structural study of the carboxyl terminal region of the human erythrocyte band 3 protein. *J Biochem*. 118(6):1192-8.

5. Literature

- Motais, R., Fievet, B., Borgese, F., Garcia-Romeu, F. (1997). Association of the band 3 protein with a volume-activated, anion and amino acid channel: a molecular approach. *J Exp Biol* 200, 361-367.
- Mueller TJ, Morrison M. (1981). Glycoconnectin (PAS 2), a membrane attachment site for the human erythrocyte cytoskeleton. *Prog Clin Biol Res.* 1981;56:95-116.
- Müller-Berger S, Karbach D, König J, Lepke S, Wood PG, Appelhans H, Passow H. (1995). Inhibition of mouse erythroid band 3-mediated chloride transport by site-directed mutagenesis of histidine residues and its reversal by second site mutation of Lys 558, the locus of covalent H2DIDS binding. *Biochemistry.* 34(29):9315-24.
- Nagao Y, Platero JS, Waheed A, Sly WS. (1993). Human mitochondrial carbonic anhydrase: cDNA cloning, expression, subcellular localization, and mapping to chromosome 16. *Proc Natl Acad Sci U S A.* 90(16):7623-7.
- Newbold CI, Marsh K. Antigens on the Plasmodium falciparum infected erythrocyte surface are parasite derived: a reply. *Parasitol Today.* 6(10):320-2.
- Nyalwidhe, J., Baumeister, S., Hibbs, A.R., Tawill, S., Papakrivov, J., Volker, U., Lingelbach, K. (2002). A non-permeant biotin derivative gains access to the parasitophorous vacuole in Plasmodium falciparum-infected erythrocytes permeabilized with streptolysin O. *J Biol Chem.* 277, 40005–40011.
- Nyalwidhe, J, Lingelbach K. (2006). Proteases and chaperones are the most abundant proteins in the parasitophorous vacuole of Plasmodium falciparum-infected erythrocytes. *Proteomics.* (5):1563-73.
- Ockenhouse, CF, Tegoshi T, Maeno Y, Benjamin C, Ho M, Kan KE, Thway Y, Win K, Aikawa M, Lobb RR. (1992). Human vascular endothelial cell adhesion receptors for Plasmodium falciparum-infected erythrocytes: roles for endothelial leukocyte adhesion molecule 1 and vascular cell adhesion molecule 1. *J Exp Med.* 176(4):1183-9.
- Oh, SS, Voigt S, Fisher D, Yi SJ, LeRoy PJ, Derick LH, Liu S, Chishti AH. (2000). Plasmodium falciparum erythrocyte membrane protein 1 is anchored to the actin-spectrin junction and knob-associated histidine-rich protein in the erythrocyte skeleton. *Mol Biochem Parasitol.* 108(2):237-47.
- Olumee, Z., Sadeghi, M., Tang, X.D. and Vertes, A. (1995). Amino acid composition and wavelength effects in matrix-assisted laser desorption/ionization. *Rapid Commun Mass Spectrom* 9, 744-752.
- Okubo, K., Kang, D., Hamasaki, N., Jennings, M.L. (1994). Red Blood Cell Band3: Lysine 539 and lysine 851 react with the same H2DIDS (4,4'-Diisothiocyanohydrostilbene-2,2'-Disulfonic acid) molecule. *J Biol Chem* 269, 1918-1926.
- Okuyama T, Sato S, Zhu XL, Waheed A, Sly WS. (1992). Human carbonic anhydrase IV: cDNA cloning, sequence comparison, and expression in COS cell membranes. *Proc Natl Acad Sci U S A.* 89(4):1315-9.
- Papakrivov, J., Newbold, C., Lingelbach, K. (2005). A potential novel mechanism for the insertion of a membrane protein revealed by a biochemical analysis of the Plasmodium falciparum cytoadherence molecule PfEMP-1. *Molecular Microbiology.* 55(4), 1272–1284.
- Parker PD, Tilley L, Klonis N. (2004). Plasmodium falciparum induces reorganization of host membrane proteins during intraerythrocytic growth. *Blood.* 103(6):2404-6.
- Pasternack GR, Anderson RA, Leto TL, Marchesi VT. (1985). Interactions between protein 4.1 and band 3. An alternative binding site for an element of the membrane skeleton. *J Biol Chem.* 260(6):3676-83.
- Passow, H. (1986). Molecular aspects of band 3 protein-mediated anion transport across the red blood cell membrane. *Rev Physiol Biochem Pharmac* 103, 62–186.
- Pasvol, G., Wilson, R. J., Smalley, M. E., and Brown, J. (1978). Separation of viable schizont-infected red cells of Plasmodium falciparum from human blood. *Ann Trop Med Parasitol* 72, 87-88.

5. Literature

- Peters, T. (1985) Serum albumin. *Adv Protein Chem.* 37:161-245.
- Peters, T., Anfinsen, C.B. (1950). Net production of serum albumin by liver slices. *J Biol Chem.* 186(2):805-13.
- Perkins DN, Pappin DJ, Creasy DM, Cottrell JS. (1999). Probability-based protein identification by searching sequence databases using mass spectrometry data. *Electrophoresis.* 20(18):3551-67.
- Pico, G. (1997) Thermodynamic features of the thermal unfolding of human serum albumin. *Inte J of Biological Macromolecules.* 20, 63-73.
- Pocker, Y, Meany, J.E. (1965). Photoregeneration of faded alkali metal solutions. The catalytic versatility of carbonic anhydrase from erythrocytes, the enzyme-catalyzed hydration of acetaldehyde. *J Am Chem Soc.* 20;87:1809-11.
- Pocker Y, Stone JT. (1967) The catalytic versatility of erythrocyte carbonic anhydrase. 3. Kinetic studies of the enzyme-catalyzed hydrolysis of p-nitrophenyl acetate. *Biochemistry.* 6(3):668-78.
- Popov, M., Tam, L.Y., Li, J. and Reithmeier, R.A.F. (1997). Mapping the ends of transmembrane segments in a polytopic membrane protein. *J Biol Chem* 272 (29), 18325-18332.
- Popov, M., Li, J. and Reithmeier, R. (1999). Transmembrane folding of the human erythrocyte anion exchanger (AE1, Band 3) determined by scanning and insertional N-glycosylation mutagenesis. *Biochem. J.* 339, 269-279.
- Przyborski JM, Miller SK, Pfahler JM, Henrich PP, Rohrbach P, Crabb BS, Lanzer M. (2005). Trafficking of STEVOR to the Maurer's clefts in *Plasmodium falciparum*-infected erythrocytes. *EMBO J.* 24(13):2306-17.
- Reed RG, Putnam FW, Peters T Jr. (1980). Sequence of residues 400-403 of bovine serum albumin. *Biochem J.* 191(3):867-8.
- Ross PD, and Shrake A. (1988). Decrease in stability of human albumin with increase in protein concentration. *J Biol Chem.* 263(23):11196-202.
- Roberts, D.D., Sherwood, J.A., Spitalnik, S.L., Panton, L.J., Howard, R.J., Dixit, V.M., Frazier, W.A., Miller, L.H. and Ginsburg, H. (1985). Thrombospondin binds *falciparum* malaria parasitized erythrocytes and may mediate cytoadherence. *Nature.* 318 (6041), 64-66.
- Roberts DJ, Craig AG, Berendt AR, Pinches R, Nash G, Marsh K, Newbold CI. (1992) Rapid switching to multiple antigenic and adhesive phenotypes in malaria. *Nature.* 25; 357(6380):689-92.
- Rogerson SJ, Chaiyaroj SC, Ng K, Reeder JC, Brown GV. (1995). Chondroitin sulfate A is a cell surface receptor for *Plasmodium falciparum*-infected erythrocytes. *J Exp Med.* 182(1):15-20.
- Rybicki AC, Schwartz RS, Hustedt EJ, Cobb CE. (1996). Increased rotational mobility and extractability of band 3 from protein 4.2-deficient erythrocyte membranes: evidence of a role for protein 4.2 in strengthening the band 3-cytoskeleton linkage. *Blood.* 88(7):2745-53.
- Sabarth N, Lamer S, Zimny-Arndt U, Jungblut PR, Meyer TF, and Bumann D. (2002). Identification of surface proteins of *Helicobacter pylori* by selective biotinylation, affinity purification, and two-dimensional gel electrophoresis. *J Biol Chem.* 277, 27896-27902.
- Sachs J, Malaney P. (2002). The economic and social burden of malaria. *Nature.* 415(6872):680-5.
- Sadygov RG, Cociorva D. (2004). Large-scale database searching using tandem mass spectra: looking up the answer in the back of the book. *Nat Methods.* 1(3):195-202.
- Santoni V, Kieffer S, Desclaux D, Masson F, Rabilloud T. (2000). Membrane proteomics: use of additive main effects with multiplicative interaction model to classify plasma membrane proteins according to their solubility and electrophoretic properties. *Electrophoresis.* 21(16):3329-44.
- Saliba, K.J., Kirk, K. (1998). Uptake of an antiplasmodial protease inhibitor into *Plasmodium falciparum*-infected human

5. Literature

erythrocytes via a parasite-induced pathway. *Mol Biochem Parasitol* 94, 297–301.

Saliba, K. J. and Kirk, K. (2001). H⁺-coupled Pantothenate Transport in the intracellular malaria parasite. *J Biol Chem.* 276 (21), 18115–18121.

Sarraf NS, Saboury AA, Ranjbar B, Moosavi-Movahedi AA. (2004). Structural and functional changes of bovine carbonic anhydrase as a consequence of temperature. *Acta Biochim Pol.* 51(3):665-71.

Sharling L, Sowa KM, Thompson J, Kyriacou HM, Arnot DE. (2007). Rapid and specific biotin labelling of the erythrocyte surface antigens of both cultured and ex-vivo Plasmodium parasites. *Malar J.* 6:66

Scheurer SB, Roesli C, Neri D, Elia G. (2005). A comparison of different biotinylation reagents, tryptic digestion procedures, and mass spectrometric techniques for 2-D peptide mapping of membrane proteins. *Proteomics.* 2005 Aug;5(12):3035-9.

Scheurer SB, Rybak JN, Roesli C, Brunisholz RA, Potthast F, Schlappbach R, Neri D, Elia G. (2005). Identification and relative quantification of membrane proteins by surface biotinylation and two-dimensional peptide mapping. *Proteomics.* 5(11):2718-28.

Schofield AE, Martin PG, Spillett D, Tanner MJ. (1994). The structure of the human red blood cell anion exchanger (EPB3, AE1, band 3) gene. *Blood.* 84(6):2000-12.

Sherman IW, and Winograd E. (1990). Antigens on the Plasmodium falciparum infected erythrocyte surface are not parasite derived. *Parasitol Today.* 1990 Oct;6(10):317-20.

Sherman, I.W., Eda. S., Winograd, E. (2003). Cytoadherence and sequestration in Plasmodium falciparum: defining the ties that bind. *Microbes and Infection.* 5, 897–909.

Sherman, I. W., Eda, S. and Winograd, E. (2004). Erythrocyte Aging and Malaria. *Cell Mol Biol.* 50 (2), 159-169.

Smith JD, Chitnis CE, Craig AG, Roberts DJ, Hudson-Taylor DE, Peterson DS, Pinches R, Newbold CI, Miller LH. (1995). Switches in

expression of Plasmodium falciparum var genes correlate with changes in antigenic and cytoadherent phenotypes of infected erythrocytes. *Cell.* 82(1):101-10.

Snow, R., Guerra, C., Noor, A., Myint, H., Hay, S. (2005). The global distribution of clinical episodes of Plasmodium falciparum malaria. *Nature.* 434, 214-217

Sly WS, Hu PY. (1995). Human carbonic anhydrases and carbonic anhydrase deficiencies. *Annu Rev Biochem.* 64:375-401.

Spector AA. (1975) Fatty acid binding to plasma albumin. *J Lipid Res.* 16(3):165-79

Squire PG, Moser P, O'Konski CT. (1968). The hydrodynamic properties of bovine serum albumin monomer and dimer. *Biochemistry.* 7(12):4261-72.

Sreerama N, Woody RW. (1994). Protein secondary structure from circular dichroism spectroscopy. Combining variable selection principle and cluster analysis with neural network, ridge regression and self-consistent methods. *J Mol Biol.* 242(4):497-507.

Staines HM, Kirk K. (1998). Increased choline transport in erythrocytes from mice infected with the malaria parasite Plasmodium vinckei vinckei. *Biochem J.* 1998 Sep 15;334 (Pt 3):525-30.

Staines, H.M., Rae, C., Kirk, K. (2000). Increased permeability of the malaria-infected erythrocyte to organic cations. *Biochim et Biophys acta* 1463, 88–98.

Staines, H.M., Powell, T., Ellory, J.C., Egée, S., Lapaix, F., Decherf, G., Thomas, S.L.Y., Duranton, C., Lang, F., Huber, S.M. (2003). Modulation of whole-cell currents in Plasmodium falciparum-infected human red blood cells by holding potential and serum. *J Physiol.* 552, 177-183.

Staines, H.M., Powell, T., Thomas, S.L.Y. and Ellory, J.C. (2004). Plasmodium falciparum-induced channels. *Int J Parasitol.* 34, 665-673.

Staines HM, Alkhalil A, Allen RJ, De Jonge HR, Derbyshire E, Egée S, Ginsburg H, Hill DA, Huber SM, Kirk K, Lang F, Lisk G, Oteng E, Pillai AD, Rayavara K, Rouhani S, Saliba KJ, Shen C, Solomon T, Thomas SL, Verloo P, Desai SA.

5. Literature

- (2007). Electrophysiological studies of malaria parasite-infected erythrocytes: current status. *Int J Parasitol.* 37(5):475-82.
- Steck TL, Ramos B, Strapazon E. (1976). Proteolytic dissection of band 3, the predominant transmembrane polypeptide of the human erythrocyte membrane. *Biochemistry.* 15(5):1153-61.
- Su, X.Z., Heatwole, V.M., Wertheimer, S.P., Guinet, F., Herrfeldt, J.A., Peterson, D.S., Ravetch, J.A. and Wellem, T.E. (1995). The large diverse gene family *var* encodes proteins involved in cytoadherence and antigenic variation of *Plasmodium falciparum*-infected erythrocytes. *Cell.* 82, 89-100.
- Sugio S, Kashima A, Mochizuki S, Noda M, Kobayashi K. (1999). Crystal structure of human serum albumin at 2.5 Å resolution. *Protein Eng.* 12(6):439-46.
- Supuran CT, Briganti F, Tilli S, Chegwidan WR, Scozzafava A. (2001). Carbonic anhydrase inhibitors: sulfonamides as antitumor agents? *Bioorg Med Chem.* (3):703-14.
- Supuran CT, Scozzafava A, Casini A. (2003). Carbonic anhydrase inhibitors. *Med Res Rev.* (2):146-89.
- Tam LY, Loo TW, Clarke DM, Reithmeier RA. (1994). Identification of an internal topogenic signal sequence in human Band 3, the erythrocyte anion exchanger. *J Biol Chem.* 269(51):32542-50.
- Tanner M.J., Martin P.G. and High S. (1988). The complete amino acid sequence of the human erythrocyte membrane anion-transport protein deduced from the cDNA sequence. *Biochem J.* 256, 703-712.
- Tang XB, Fujinaga J, Kopito R, Casey JR. (1998). Topology of the region surrounding Glu681 of human AE1 protein, the erythrocyte anion exchanger. *J Biol Chem.* 273(35):22545-53.
- Tanner MJ, Boxer DH. (1972). Separation and some properties of the major proteins of the human erythrocyte membrane. *Biochem J.* 129(2):333-47.
- Tashian RE, Douglas DP, Yu YS. (1964). Esterase and hydrolase activity of carbonic anhydrase. I. From primate erythrocytes. *Biochem Biophys Res Commun.* 14:256-61.
- Trager W, and Jensen JB. (1976). Human malaria parasites in continuous culture. *Science.* 193, 673-675.
- Trager, W. (1994). Cultivation of malaria parasites. *Methods Cell Biol.* 45, 7-26.
- Treutiger, C.J., Heddini, A., Fernandez, V., Muller, W.A., Wahlgren, MPE. (1997). Cam-1/CD31, an endothelial receptor for binding *Plasmodium falciparum*-infected erythrocytes. *Nat Med.* 3; 1405-1408.
- Thomas, S. L.Y. and Lew, V.L. (2004). *Plasmodium falciparum* and the permeation pathway of the host red blood cell. *TRENDS in Parasitology*, 20, 3, 122-125
- Towbin, H., Staehelin, T. and Gordon, J. (1979). Electrophoretic transfer of proteins from polyacrylamide gels to nitrocellulose sheets: procedure and some applications. *PNAS.* 76, 4350-4354.
- Turner GD, Ly VC, Nguyen TH, Tran TH, Nguyen HP, Bethell D, Wyllie S, Louwrier K, Fox SB, Gatter KC, Day NP, Tran TH, White NJ, Berendt AR. (1998). Systemic endothelial activation occurs in both mild and severe malaria. Correlating dermal microvascular endothelial cell phenotype and soluble cell adhesion molecules with disease severity. *Am J Pathol.* 152(6):1477-87.
- Tse WT, Lux SE. (1999). Red blood cell membrane disorders. *Br J Haematol.* 104(1):2-13.
- Upston, J.M., and Gero, A.M. (1995). Parasite-induced permeation of nucleosides in *Plasmodium falciparum* malaria. *Biochim et Biophys Acta.* 1236, 249-258.
- Van Dort HM, Knowles DW, Chasis JA, Lee G, Mohandas N, Low PS. (2001). Analysis of integral membrane protein contributions to the deformability and stability of the human erythrocyte membrane. *J Biol Chem.* 276(50):46968-74.

5. Literature

- Verloo P, Kocken CH, Van der Wel A, Tilly BC, Hogema BM, Sinaasappel M, Thomas AW, De Jonge HR. (2004). Plasmodium falciparum-activated chloride channels are defective in erythrocytes from cystic fibrosis patients. *J Biol Chem.* 279(11):10316-22.
- Vince JW and Reithmeier RA. (1998). Carbonic anhydrase II binds to the carboxyl terminus of human band 3, the erythrocyte C1-/HCO₃-exchanger. *J Biol Chem.* 273(43):28430-7.
- Vince J.W. and Reithmeier R.A.F. (2000). Identification of the carbonic anhydrase II binding site in CL-/HCO₃ - the anion exchanger AE1. *Biochemistry* 39, 5527-5533.
- Viitala J, Järnefelt J. (1985). The red cell surface revisited. *Trends Biochem Sci* 14: 392-395.
- Voigt S, Hanspal M, LeRoy PJ, Zhao PS, Oh SS, Chishti AH, Liu SC. (2000). The cytoadherence ligand Plasmodium falciparum erythrocyte membrane protein 1 (PfEMP1) binds to the P. falciparum knob-associated histidine-rich protein (KAHRP) by electrostatic interactions *Mol Biochem Parasitol.* 110(2):423-8.
- Wainwright SD, Tanner MJ, Martin GE, Yendle JE, Holmes C. (1989). Monoclonal antibodies to the membrane domain of the human erythrocyte anion transport protein. Localization of the C-terminus of the protein to the cytoplasmic side of the red cell membrane and distribution of the protein in some human tissues. *Biochem J.* 258(1):211-20.
- Wainwright SD, Mawby WJ, Tanner MJ. (1990). The membrane domain of the human erythrocyte anion transport protein. Epitope mapping of a monoclonal antibody defines the location of a cytoplasmic loop near the C-terminus of the protein. *Biochem J.* 272(1):265-8.
- Wang, D., Kuhlbrandt, W., Sarabia, V. and Reithmeier, R. (1993). Two-dimensional structure of the membrane domain of human band 3, the anion transport protein of the erythrocyte membrane. *EMBO J.* 12, 2233-2239.
- Waller KL, Cooke BM, Nunomura W, Mohandas N, Coppel RL. (1999). Mapping the binding domains involved in the interaction between the Plasmodium falciparum knob-associated histidine-rich protein (KAHRP) and the cytoadherence ligand P. falciparum erythrocyte membrane protein 1 (PfEMP1). *J Biol Chem.* 274(34):23808-13.
- Waller KL, Nunomura W, Cooke BM, Mohandas N, Coppel RL. (2002). Mapping the domains of the cytoadherence ligand Plasmodium falciparum erythrocyte membrane protein 1 (PfEMP1) that bind to the knob-associated histidine-rich protein (KAHRP). *Mol Biochem Parasitol.* 119(1):125-9.
- Waterkeyn JG, Wickham ME, Davern KM, Cooke BM, Coppel RL, Reeder JC, Culvenor JG, Waller RF, Cowman AF. (2000). Targeted mutagenesis of Plasmodium falciparum erythrocyte membrane protein 3 (PfEMP3) disrupts cytoadherence of malaria-infected red blood cells. *EMBO J.* 19(12):2813-23.
- Weatherall, D. J., Miller, L.H., Baruch, D.L., Marsh, K., Doumbo, O.K., Casals-Pascual, C., and Roberts, D.J. (2002). Malaria and the Red Cell, *Hematology Am Soc Hematol Educ Program.* 35-57.
- Wei X, Ding S, Jiang Y, Zeng XG, Zhou HM. (2006). Conformational changes and inactivation of bovine carbonic anhydrase II in 2,2,2-trifluoroethanol solutions. *Biochemistry (Mosc).* 71 Suppl 1:S77-82.
- Wetzel R, Becker M, Behlke J, Billwitz H, Böhm S, Ebert B, Hamann H, Krumbiegel J, Lassmann G. (1980). Temperature behaviour of human serum albumin. *Eur J Biochem.* 104 (2): 469-78.
- WHO. (2005). World Malaria Report.
- Wickham, ME., Rug, M., Ralph, SA., Klonis, N., McFadden, GI., Tilley, L., Cowman AF. (2001). Trafficking and assembly of the cytoadherence complex in Plasmodium falciparum-infected human erythrocytes. *EMBO Journal.* 20, 5636-5649.
- Winograd, E., Greenan, J.R.T., Sherman, I.W. (1987). Expression of senescent antigen on erythrocytes infected with a knobby variant of the human malaria parasite *Plasmodium falciparum*. *PNAS.* 84, 931-935.
- Winograd, E. and Sherman IW. (2004). Malaria infection induces a conformational change in erythrocyte band 3 protein. *Mol Biochem Parasitol.* 138:83-7.

5. Literature

- Winograd, E. and Eda S, Sherman IW. (2004). Chemical modifications of band 3 protein affect the adhesion of Plasmodium falciparum-infected erythrocytes to CD36. *Mol Biochem Parasitol.* 136(2):243-8.
- Winograd, E., Prudhomme, J., Sherman IW. (2005). Band 3 clustering promotes the exposure of neoantigens in Plasmodium falciparum-infected erythrocytes. *Molecular and Biochemical Parasitology* 142 ,98–105.
- Winter G, Chen Q, Flick K, Kremsner P, Fernandez V, Wahlgren M. (2003). The 3D7var5.2 (var COMMON) type var gene family is commonly expressed in non-placental Plasmodium falciparum malaria. *Mol Biochem Parasitol.* 127(2):179-91.
- Winter G, Kawai S, Haeggström M, Kaneko O, von Euler A, Kawazu S, Palm D, Fernandez V, Wahlgren M. (2005). SURFIN is a polymorphic antigen expressed on Plasmodium falciparum merozoites and infected erythrocytes. *J Exp Med.* 201(11):1853-63.
- Wilchek M and Bayer EA. (1988). The avidin-biotin complex in bioanalytical applications. *Analytic Biochemistry.* 171, 1-32.
- Wilchek M, and Bayer EA. (1990). Applications of avidin-biotin technology: literature survey. *Methods in Enzymology.* 184, 14-45.
- Wright AK, Thompson MR. (1975). Hydrodynamic structure of bovine serum albumin determined by transient electric birefringence. *Biophys J.* 15(2 Pt 1):137-41.
- Wong KP, Tanford C. (1973). Denaturation of bovine carbonic anhydrase B by guanidine hydrochloride. A process involving separable sequential conformational transitions. *J Biol Chem.* 248(24): 8518-23.
- Yazgan A, Henkens RW. (1972). Role of zinc (II) in the refolding of guanidine hydrochloride denatured bovine carbonic anhydrase. *Biochemistry.* 11(7):1314-8.
- Yamashita, M., and Fenn JB; (1984). Electrospray ion source, another variation of free jet theme, *J. Phys. Chem.*, 88, 4451- 4671.
- Young MM, Tang N, Hempel JC, Oshiro CM, Taylor EW, Kuntz ID, Gibson BW, Dollinger G. (2000). High throughput protein fold identification by using experimental constraints derived from intramolecular cross-links and mass spectrometry. *Proc Natl Acad Sci U S A.* 97(11):5802-6.
- Yu, J, Steck, TL. (1975). Isolation and characterization of band 3, the predominant polypeptide of the human erythrocyte membrane. *J Biol Chem.* 250(23):9170-5.
- Zhang D., Kiyatkin A, Bolin J.T. and Low P.S. (2000). Crystallographic structure and functional interpretation of the cytoplasmic domain of erythrocyte membrane band 3. *Blood.* 96, 2925-2933.
- Zaki L. (1981). Inhibition of anion transport across red blood cells with 1,2-cyclohexanedione. *Biochem Biophys Res Commun.* 99(1):243-51.
- Zipser Y, Piade A, Kosower NS. (1997) Erythrocyte thiol status regulates band 3 phosphotyrosine level via oxidation/reduction of band 3-associated phosphotyrosine phosphatase. *FEBS Lett.* 406(1-2):126-30.
- Zhu, Q., Lee, D. and Casey, J. (2003). Novel Topology in C-terminal Region of the Human Plasma Membrane Anion Exchanger, AE1. *J Biol Chem,* 278, 3112-3120.

V Summary

The biotinylation patterns of two soluble model proteins (BSA and CA II) were analyzed under different conditions. In a first step these proteins were biotinylated with an increasing molar excess of a biotin derivative. In this case increases in biotin concentration led to an increase in the number of biotinylated lysine residues until a point of saturation was reached. A further increase in biotin concentration did not result in additional lysine residues being biotinylated. The biotinylation pattern was reproducible and under any given conditions, only specific lysine residues are biotinylated.

After showing that the biotinylation of proteins is specific and reproducible, the same approach was used to map artificially induced conformation changes in BSA and CA II. These proteins were subjected to elevated temperatures that induce conformation changes. The biotinylation pattern of these proteins at room temperature and after exposure to 80°C was compared. For BSA, heating results in the biotinylation of two additional lysine residues. This is most likely due to conformation changes in the protein structure induced by the high temperature. In the case of CA II there was no difference in the biotinylation pattern of the protein at room temperature and at 80°C.

Having established that biotinylation patterns can be used to reliably detect conformational changes in protein structure, the biotinylation pattern of Band III (a trans-membrane protein of the human erythrocyte plasma membrane) in infected and non-infected erythrocyte was analyzed. These experiments confirmed previous observations that this protein undergoes a conformational change upon infection. The biotinylation pattern was different between RBC and IRBC in respect to a single lysine residue which is biotinylated only in RBC. These results suggest that, upon invasion by *P. falciparum*, the Band III protein undergoes conformation changes which are probably important for the survival of the parasite within the host cell.

VI Zusammenfassung

Das Biotinylierungsmuster zweier löslicher Proteine (BSA und CA II), sowie das des Erythrozytenmembranproteins Bande III wurde unter unterschiedlichen Bedingungen analysiert. Im ersten Schritt wurden diese Proteine mit einem Überschuss an Biotin in einem molaren Verhältnis biotinyliert. Für die löslichen Proteine führt eine Erhöhung der Biotinkonzentration zu einer Zunahme der Anzahl an biotinylierten Lysinresten bis zu einem Punkt der Sättigung. Eine weitere Erhöhung der Biotinkonzentration führt nicht zu zusätzlich mit Biotin markierten Lysinresten. Das Biotinylierungsmuster dieser beiden löslichen Proteine ist reproduzierbar und zeigt unter allen gewählten Bedingungen eine Biotinylierung spezifischer Lysinreste.

Nachdem gezeigt war, dass die Biotinylierung der Proteine spezifisch und reproduzierbar ist, wurde die gleiche Methode gewählt, um künstlich verursachte Konformationsänderungen in BSA und CA II anhand eines veränderten Biotinylierungsmusters zu zeigen. Diese Proteine wurden erhöhten Temperaturen ausgesetzt, um eine Konformationsänderung hervorzurufen, und anschliessend wurden die Biotinylierungsmuster bei Raumtemperatur und 80 °C miteinander verglichen. Bei BSA führt die Erhitzung auf 80 °C zu einer Biotinylierung von zwei zusätzlichen Lysinresten. Dabei ist es wahrscheinlich, dass die durch die Erwärmung verursachte Konformationsänderung die beobachtete Änderung des Biotinylierungsmusters zur Folge hat. Im Fall von CA II gibt es keinen Unterschied des Biotinylierungsmusters zwischen Raumtemperatur und 80 °C.

Da es Hinweise dafür gibt, dass sich die Konformation des Bande III Proteins in der Plasmamembran von Erythrozyten nach einer Infektion mit *P. falciparum* verändert, wurden intakte infizierte und nichtinfizierte Erythrozyten biotinyliert, um etwaige Unterschiede in den Biotinylierungsmustern festzustellen. Das Biotinylierungsmuster des Proteins unterschied sich zwischen RBC und IRBC nur in einem einzelnen Lysinrest, der nur in RBC biotinyliert ist. Diese Beobachtung bestätigt die Annahme, dass Bande III nach der Infektion durch *P. falciparum* eine Konformationsänderung erfährt und erlaubt es, die Position dieser Veränderung einzugrenzen.

Acknowledgements

I am very grateful to the German Academic Exchange Service (DAAD) which awarded me the scholarship for my Doctoral thesis.

I am deeply grateful to Professor Dr. Klaus Lingelbach, Head of the Parasitology Department, for having accepted me to join his group and for his continued understanding and support throughout the period of my fellowship. I also thank him very much for introducing me to the proteomics research; I thank him for his guidance, constant advice and support without which the whole study would not be possible.

I thank Prof. Dr. Uwe Maier for his constant scientific advice and support during my scholarship and for serving as the external examiner of this work.

I am deeply indebted to members of my examination committee: Prof. Dr. Uwe Maier, Prof. Dr. Ralph Schwarz and Prof. Dr. Erhard Bremer.

I would like to particularly thank Dr. Julius Nyalwidhe for introducing me to mass spectrometry research; his tireless practical help and supervision which made this study doable and successful. I gratefully acknowledge the good information, technical advice and continuously support that I received from him throughout my fellowship.

I specially thank Dr. Jude Przyborski for his helpful suggestions and scientific discussion. I really appreciate his patience for the critical reading and editing of this work.

I sincerely thank Prof. Dr. Klebe and Dr. Hillebrecht at the Institut für Pharmazeutische Chemie, Philipps-Universität Marburg, for helping to perform some aspects of this study.

I specially thank Prof. Dr. Marahiel and Dr. Linne, at the Fachbereich Chemie/Biochemie, Philipps-Universität Marburg for access to the CD spectrometer used in this study.

I am very grateful to Dr. Stefan Baumeister and Prof. Dr. Seeber for the information and discussion during my work.

I am very grateful to all the members of the Department of Parasitology for the nice and friendly atmosphere, my appreciation goes to Dr. Burghaus; Dr. Charpian; Nina Gehde; Simone Külzer; Trang Chu; Simone Spork; Lothar Kremp; Kathrin Stelter; Sandra Marx; Elisabeth Schmitt-Nau; Silke Fröhlich; Galina Bauer; Sven Bietz; Irine Montilla and specially to Markus Winterberg because of his constant friendly help.

Last but not least I would like to thank my wife; without her help and patience I never would have reached this point. Maryam, thanks that you are always there for me.

Erklärung

Ich versichere, dass ich meine Dissertation:

“An experimental approach to probe conformational changes in protein structure using a biotin derivative followed by mass spectrometry”

selbständig, ohne unerlaubte Hilfe angefertigt und mich dabei keiner anderen als der von mir ausdrücklich bezeichneten Quellen und Hilfen bedient habe. Die Dissertation wurde in der jetzigen oder einer ähnlichen Form noch bei keiner anderen Hochschule eingereicht und hat noch keinen sonstigen Prüfungszwecken gedient.

(Ort/Datum)

(Unterschrift mit Vor- und Zunahme)

Curriculum Vitae

Personal Details

Name: Omid Azim-Zadeh

Address: Am Richtsberg 88
D-35039 Marburg, Germany

Birth: on 16.09.1973 in Teheran (Iran)

Nationality: Iranian

Family status: married, one child

Education

2004- 2008: PhD. Philipps-Universität Marburg, Parasitology.
Title of dissertation: "An experimental approach to probe conformational changes in protein structure using a biotin derivative followed by mass spectrometry".

1996-2000: Master of Science, in Medical Parasitology, at Shahid Beheshti University of Medical Sciences and Health Services in Tehran
Title of Thesis:"Purification of surface antigen of *Sarcocystis*".

1991-1996: Bachelor of Science, in Microbiology, at Azad University in Tehran

Publications

- The use of biotin derivatives to probe conformational changes in proteins; *Journal of biological chemistry*; 2007, 282(30), 21609-21617.
- Isolation of Sheep Sarcocystis 35 kD Protein Fragment by Ion Exchange Chromatography; *Asian network for scientific information,PJBC*; 2005,8(11),1620-1622

Use of Biotin Derivatives to Probe Conformational Changes in Proteins^{*S}

Received for publication, November 27, 2006, and in revised form, May 16, 2007 Published, JBC Papers in Press, June 1, 2007, DOI 10.1074/jbc.M610921200

Omid Azim-Zadeh^{†1}, Alexander Hillebrecht[§], Uwe Linne[¶], Mohamed A. Marahiel[¶], Gerhard Klebe[§], Klaus Lingelbach^{‡2}, and Julius Nyalwidhe[‡]

From the [†]Fachbereich Biologie, the [§]Institut für Pharmazeutische Chemie, and the [¶]Fachbereich Chemie/Biochemie, Philipps-Universität Marburg, D-35032 Marburg, Germany

Sulfosuccinimidyl-6-(biotinamido) hexanoate and derivatives thereof covalently bind to the ϵ -amino group of lysine residues. Our observation that access of the biotin derivative to specific lysine residues depends on conformational properties of the entire polypeptide chain prompted us to investigate whether differential biotinylation patterns of a protein can be used as indicators for conformational changes. Bovine serum albumin is a soluble protein with characteristic unfolding kinetics upon exposure to high temperature. First, we show that biotinylation patterns of proteins are highly reproducible. Second, we demonstrate by mass spectrometry and tandem mass spectrometry that unfolding of the protein correlates with the accessibility of the biotin derivative to specific lysine residues. We have applied this experimental strategy to the analysis of a cell-surface protein, *viz.* the human band 3 anion exchanger of erythrocytes infected with the malaria parasite *Plasmodium falciparum*. We found that Lys⁸²⁶ in a highly flexible loop can be biotinylated in non-infected (but not infected) erythrocytes, confirming earlier observations (Winograd, E., and Sherman, I. W. (2004) *Mol. Biochem. Parasitol.* 138, 83–87) based on epitope-specific monoclonal antibodies suggesting that this region undergoes a conformational change upon infection.

The biotinylation of proteins is a commonly used tool for the affinity purification of proteins (1). It takes advantage of the highly specific interaction between biotin and avidin or its bacterial homolog, streptavidin. Protein biotinylation utilizes biotin derivatives containing an active ester group that reacts with primary amines of proteins, particularly with the N terminus and the ϵ -amino group of lysine residues. A novel amide bond is thereby formed, and the biotin moiety is covalently attached to the respective amino group, often separated by a spacer of defined size. The biotin derivative sulfosuccinimidyl-6-(biotin-

namido) hexanoate (sulfo-NHS-LC-biotin)³ is a hydrophilic reagent that is excluded from most cells and is therefore used for the biotinylation and subsequent affinity purification of cell-surface proteins.

Recently, we used sulfo-NHS-LC-biotin to label proteins exposed on the surface of human red blood cells infected with the malaria parasite *Plasmodium falciparum* (iRBC) (2). In contrast to the non-infected erythrocyte (RBC), the plasma membrane of the infected erythrocyte was permeable for this biotin derivative (2). Uptake of the compound occurs through the so-called novel permeability pathways, which are parasite-induced and have a broad specificity with a preference for anions (3–6). Biotinylation of internal proteins can be minimized if the reaction occurs in the presence of novel permeability pathway inhibitors such as furosemide. The proteins that constitute the novel permeability pathway are still unknown. The band 3 anion exchanger AE1 is the most abundant anion transporter in RBC (7). The reactivity of an epitope-specific monoclonal antibody with band 3, which differs between infected and non-infected erythrocytes, has been interpreted as a conformational change in the protein in at least one of the extracellular domains (8). Although band 3 itself does not appear to be the actual channel protein mediating the novel permeability pathway (5), its conformational change as a consequence of the infection may nevertheless play an important role in the survival of the parasite within its host cell. Therefore, we sought an experimental strategy to more precisely define the position within the band 3 molecule where this conformational change could possibly occur.

In a recent proteome analysis, we used *in situ* biotinylation of permeabilized iRBC to specifically label soluble parasite proteins contained in the parasitophorous vacuole (9). Peptide mass fingerprinting of 27 different biotinylated proteins revealed a high reproducibility of the biotinylation patterns of individual proteins in different experiments. These observations prompted us to investigate whether changes in protein conformation are reflected by changes in biotinylation patterns and whether this mapping can be exploited as an experimental strategy to detect conformational changes in cell-surface proteins. Although amino acid residue modifications by specific tags and cross-linkers in combination with mass spectrometry

^{*} This work was supported in part by Deutsche Forschungsgemeinschaft Grant SFB 593 (to K. L.). The costs of publication of this article were defrayed in part by the payment of page charges. This article must therefore be hereby marked "advertisement" in accordance with 18 U.S.C. Section 1734 solely to indicate this fact.

^S The on-line version of this article (available at <http://www.jbc.org>) contains supplemental Figs. 1 and 2 and Tables 1–3.

[†] Recipient of a scholarship from the German Academic Exchange Service.

[‡] To whom correspondence should be addressed: Fachbereich Biologie, Philipps-Universität Marburg, Karl von Frisch Str. 8, D-35032 Marburg, Germany. Tel.: 49-6421-282-3404; Fax: 49-6421-282-1531; E-mail: lingelba@Staff.Uni-Marburg.de.

³ The abbreviations used are: sulfo-NHS-LC-biotin, sulfosuccinimidyl-6-(biotinamido) hexanoate; iRBC, infected red blood cells; RBC, non-infected red blood cells; BSA, bovine serum albumin; PBS, phosphate-buffered saline; MS, mass spectrometry; MALDI, matrix-assisted laser desorption/ionization; MS/MS, tandem mass spectrometry.

Protein Biotinylation

have been used as tools for probing the tertiary structure of proteins (10–12), the use of biotin derivatives has additional advantages: (i) labeled proteins can be readily visualized before analysis; (ii) labeled peptides can be affinity-enriched; and (iii) several membrane-impermeant derivatives exist, allowing the selective labeling of cell-surface proteins. As a case study, we have used bovine serum albumin (BSA) as a soluble model protein to show that specific, experimentally induced, conformational changes result in a highly reproducible biotinylation pattern of lysine residues. Using this method, a comparison of the biotinylation patterns of band 3 allowed us to identify a distinct difference between iRBC and RBC.

EXPERIMENTAL PROCEDURES

Biotinylation of BSA and Carbonic Anhydrase—Fatty acid-free BSA (Roth, Karlsruhe, Germany) was dissolved in phosphate-buffered saline (PBS) to a final concentration of 10 mg/ml. For analysis of the biotinylation pattern of BSA, 1 ml of the solution (containing 1.4×10^{-4} mol of BSA) was biotinylated with 1-, 10-, 20-, 40-, and 60-fold molar eq (taking into account 60 lysine residues/BSA molecule) of sulfo-NHS-LC-biotin (Pierce) at 4 °C for 30 min. The reaction was stopped by the addition of glycine to a final concentration of 100 mM. The unreacted biotin derivative was removed from the sample by centrifugation at $3000 \times g$ using a Millipore microconcentrator with a size exclusion of 5 kDa. This step was repeated twice after dilution with PBS before determining the protein concentration using the BCA assay (Pierce). For bovine carbonic anhydrase, 1.2×10^{-4} mol of carbonic anhydrase were biotinylated using a 40-fold molar excess of biotin derivative and processed as described for BSA. For analysis of the artificially induced conformational changes, BSA and carbonic anhydrase were dissolved in PBS as described above and subjected to an elevated temperature of either 56 or 80 °C for 30 min before cooling to room temperature and biotinylation with a 40-fold molar excess of biotin derivative. For affinity purification of the biotinylated proteins, 72 μ l of streptavidin-Sepharose beads (Pierce) were washed extensively with PBS containing 1% (v/v) Nonidet P-40 before mixing the beads with 100 μ g (1.44×10^{-6} mol) of biotinylated proteins. After overnight incubation at 4 °C, the unbound non-biotinylated protein fraction was obtained as a supernatant after centrifugation at $10,000 \times g$ for 10 min. The beads containing bound biotinylated protein were washed consecutively in 10 mM Tris-HCl (pH 7.5), 0.2% Nonidet P-40, 2 mM EDTA, and 150 mM NaCl; in 10 mM Tris-HCl (pH 7.5), 0.2% Nonidet P-40, 2 mM EDTA, and 500 mM NaCl; and finally in 10 mM Tris-HCl (pH 7.5). The bound protein fraction was eluted from the beads by boiling in 500 μ l of denaturing SDS-PAGE sample buffer and separated by 12% SDS-PAGE.

Biotinylation of Erythrocyte Membrane Proteins—RBC were obtained from blood group A⁺ donors and infected with the human malaria parasite *P. falciparum* using standard conditions. RBC and iRBC were cultured separately in RPMI 1640 medium in the presence of 10% human plasma under standard conditions (13). Erythrocytes infected with mature stage parasites were isolated from culture by plasmagel flotation, resulting in >90% iRBC (14). Biotinylation of intact erythrocytes

(either infected or non-infected) was performed as described (4). Briefly, 2×10^8 RBC or iRBC were washed with PBS (pH 7.6), incubated in the same buffer containing different concentrations of the biotin derivative (2, 1, and 0.5 mg/ml) for 1 h at 4 °C in the presence of 100 μ M furosemide, and subsequently sedimented at $1300 \times g$ for 5 min at 4 °C. To block and remove unreacted biotin derivative molecules, cells were washed three times with PBS (pH 7.6) containing 100 mM glycine and then with PBS. To enrich for membrane proteins, cells were resuspended in distilled water supplemented with a protease inhibitor mixture containing antipain, chymostatin, aprotinin, trypsin inhibitor, Na-EDTA, pepstatin, leupeptin, and elastatinal (each at a concentration of 1 μ g/ml) and lysed by three cycles of freezing and thawing. The membrane fraction was sedimented by centrifugation at $18,000 \times g$ for 20 min, solubilized in SDS-PAGE sample buffer, and separated by 7.5% SDS-PAGE.

Western Blot Analysis—Proteins separated by SDS-PAGE were transferred to nitrocellulose membranes using standard procedures. To detect biotin-labeled proteins, the membranes were blocked with 3% BSA in PBS (pH 7.4) for 1 h at room temperature before incubation for 20 min with alkaline phosphatase-conjugated streptavidin (1:10,000/3% BSA in PBS (pH 7.4); Pharmingen). The membranes were washed three times with 10 mM Tris-HCl (pH 7.4) and 150 mM NaCl, and the biotin-labeled proteins were visualized after staining with nitro blue tetrazolium and 5-bromo-4-chloro-3-indolyl phosphate.

Sample Preparation for Mass Spectrometry (MS)—Protein bands were excised from polyacrylamide gels and subjected to in-gel trypsin digestion before MS analysis (15). Briefly, the excised spots were washed with 50% (v/v) acetonitrile in 200 mM ammonium bicarbonate, and the destained protein was in-gel-reduced with 10 mM dithiothreitol in 100 mM ammonium bicarbonate for 1 h at 56 °C and alkylated with 50 mM iodoacetamide in the same buffer for 45 min at room temperature in darkness. The gel pieces were washed with 100 mM ammonium bicarbonate, dehydrated in acetonitrile, and dried. The gels were re-swollen in 15 μ l of 40 mM ammonium bicarbonate containing 20 μ g/ml sequencing-grade trypsin (Promega Corp.) for 45 min at 4 °C. Excess protease-containing solution was discarded, and 5 μ l of 5 mM ammonium bicarbonate were added to keep the gel pieces wet during the 18-h proteolytic cleavage step at 37 °C. To extract the peptides, 15 μ l of diffusion solution (10% acetonitrile and 1% trifluoroacetic acid) were added, and the samples were sonicated for 45 min at 37 °C. The soluble portion of the sample was evaporated to dryness. For MS measurements, the samples were redissolved in 15 μ l of 0.1% (v/v) trifluoroacetic acid and 5% (v/v) acetonitrile in water. The peptides were purified and concentrated using ZipTip™ columns made from the reverse chromatography resins POROS R2 and Oligo R3 (Applied Biosystems). The bound peptides were washed with a solution of 0.5% formic acid and eluted from the ZipTip™ columns with 2 μ l of 33% (v/v) acetonitrile and 0.1% trifluoroacetic acid saturated with α -cyano-4-hydroxycinnamic acid directly onto a matrix-assisted laser desorption ionization (MALDI) sample plate and air-dried before analysis in the mass spectrometer.

Alternatively, for affinity enrichment of biotinylated tryptic peptides, SDS-PAGE-separated proteins were transferred to

nitrocellulose membranes and visualized by Ponceau staining. The stained membranes were cut into 2 × 2-mm square pieces, thoroughly destained with water, treated with 10 mM dithiothreitol in 100 mM ammonium bicarbonate for 1 h at 56 °C, and alkylated with 50 mM iodoacetamide in the same buffer for 45 min at room temperature in darkness. The nitrocellulose pieces were washed with 100 mM ammonium bicarbonate and dried. The membranes were incubated in a minimal volume of 40 mM ammonium bicarbonate containing 20 μg/ml sequencing-grade trypsin and incubated at 37 °C for 18 h. The tryptic peptides were extracted from the membrane pieces twice using 20% acetonitrile in 1% trifluoroacetic acid, with sonication at 37 °C for 45 min. The eluted peptides were resuspended in 500 μl of 100 mM ammonium bicarbonate and incubated overnight with 72 μl of washed streptavidin-Sepharose beads to affinity purify the biotinylated peptides. The unbound non-biotinylated peptide fraction was obtained as a supernatant after centrifugation at 10,000 × *g* for 10 min. This fraction was evaporated to dryness and resuspended in 0.1% trifluoroacetic acid before processing for MS. The Sepharose beads containing bound biotinylated peptides were washed three times with 100 mM ammonium bicarbonate and 1% octyl glucoside. The bound peptides were eluted with 70% acetonitrile, 5% trifluoroacetic acid, and 1 mM D-biotin in 100 mM ammonium bicarbonate at room temperature for 2 h. The solution was evaporated to dryness and resuspended in 0.1% trifluoroacetic acid before processing for MS.

MS Analysis—MS was performed using a Bruker Daltonics UltraflexTM mass spectrometer equipped with a nitrogen laser (337 nm laser, 3-ns pulse width, and 50-Hz repetition rate) and panoramic mass range focusing (PANTM) technology and high precision calibration (HPCTM) for high mass accuracy. For analysis of intact protein, mass spectra were acquired after an external calibration using the reference protein standards trypsinogen, protein A, bovine albumin, protein A²⁺, and bovine albumin²⁺ (protein calibration standard II, Bruker Daltonics). Mass spectra were acquired in the linear positive mode with a pulsed extraction using ~100 laser shots, and the masses were assigned and processed using BioToolsTM and flexAnalysisTM software (Bruker Daltonics). For the trypsin digests, peptide mass fingerprint spectra were acquired in the reflectron positive mode with a pulsed extraction using an average of 100 laser shots. The spectra were acquired after an external calibration using reference peptides (peptide mixture II, Bruker Daltonics). The spectra were further internally calibrated using trypsin autolysis peaks (842.5100 and 2211.1046 Da). Monoisotopic masses were assigned and processed using BioToolsTM and flexAnalysisTM software before submission to the Mascot program (www.matrixscience.com) for searches against the non-redundant NCBI Database. The following variable modifications were used in the searches: methionine oxidation, lysine sulfo-NHS-LC-biotin-labeled, pyroglutamic acid from Glu at the N terminus, pyroglutamic acid from Gln, and a fixed cysteine carbamidomethylation modification. To analyze the effect of missed proteolytic cleavage of peptides on the identification of the proteins and biotinylated lysine residues, the searches were done allowing complete cleavage (0 missed cleav-

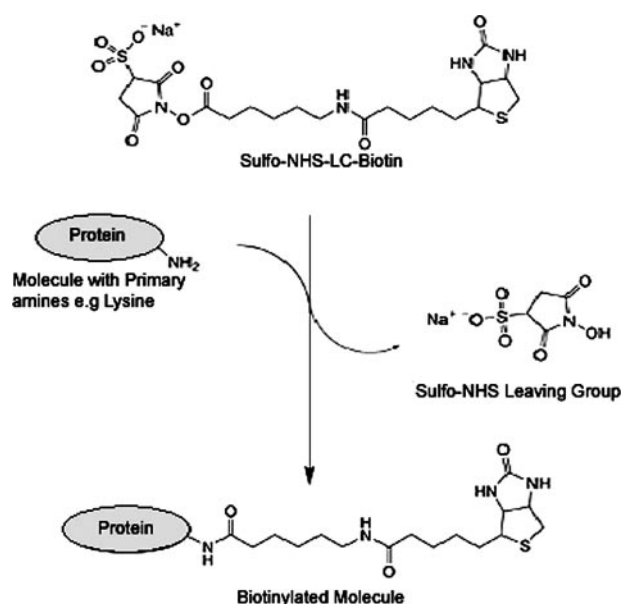


FIGURE 1. The sulfo-NHS-LC-biotin derivative reacts with primary amines to form a stable amide bond. The primary amine may be the N-terminal amino group or the ϵ -amino group of lysine residues. The figure was modified from that supplied by Pierce.

age sites) and allowing one or two missed cleavage sites. A mass accuracy of 50 ppm or better was used in all identifications.

Tandem mass spectrometry (MS/MS) analysis was done using the LIFTTM mode to provide i, a, b, and y ions. The masses of the fragmented ions were submitted to the Mascot program for data base searching using the following parameters: peptide mass tolerance of 100 ppm, MS/MS tolerance of 0.7 Da, and two missed cleavage sites. The variable and fixed modifications of amino acid residues were used as described for the peptide mass fingerprint analyses.

To analyze the spatial distribution of lysine residues across the structures of BSA and carbonic anhydrase II, the crystal structure of the latter enzyme (Protein Data Bank code 1V9E) was examined. As no crystal structure of BSA has been deposited in the Protein Data Bank, a homology model was obtained from the SWISS-MODEL Repository (17) based on the crystal structure of human serum albumin as a template (Protein Data Bank code 1N5U). To detect possible correlations between the degree of biotinylation, the local environment of lysine residues, and the solvent-accessible surface (18), their involvement in hydrogen bonding, the hydrogen bond energy, and the local electrostatic potential were studied. The latter was computed and visualized using the MOLCAD module of SYBYL 7.1 (19); hydrogen bond energies were calculated using the MAB force field implemented in MOLOC (20).

RESULTS AND DISCUSSION

Biotinylation of BSA Is Saturable but Incomplete—Sulfo-NHS-LC-biotin derivatives possess an active ester group that reacts with the primary amines of proteins and/or the ϵ -amino group of lysine residues, thereby forming an amide bond (Fig. 1). For each lysine residue, this reaction results in an increase in mass of 339.161 Da. If all 60 lysine residues of the BSA molecule were biotinylated, the calculated mass shift of the protein would

TABLE 1

Effect of an increase in the molar ratio of sulfo-NHS-LC-biotin to BSA on the mass of BSA

BSA was biotinylated with increasing molar ratios of sulfo-NHS-LC-biotin to protein. The mass of the protein was determined by MALDI time-of-flight MS. ND, not detectable.

Sulfo-LC-biotin/BSA molar ratio	Mass of BSA by MS	Approximate no. of incorporated biotin residues ^a
	<i>Da</i>	
0	66,525.3	None
1	66,598.0	ND
10	68,269.0	5
20	69,853.9	10
40	72,271.4	17
60	72,599.5	18

^a Each modified lysine residue resulted in an increase in mass of ~339 Da.

be 20.34 kDa. BSA was biotinylated with increasing molar ratios of sulfo-NHS-LC-biotin to protein and analyzed by time-of-flight MS in linear mode. The mass of the protein increased in an almost linear correlation with the molar excess of the biotin derivative, up to a 40-fold molar excess of the derivative (Table 1). The maximal increase we observed was 6.1 kDa, accounting for ~18 biotinylated lysine residues. Thus, the biotinylation of lysine residues in the BSA molecule is incomplete. Analysis of the biotinylated protein by SDS-PAGE confirmed the increase in molecular mass of Coomassie Blue-stained protein, which was verified by biotin detection with streptavidin (supplemental Fig. 1).

To investigate whether biotinylation occurs randomly or whether specific lysine residues are preferentially labeled, biotinylated BSA was analyzed by peptide mass fingerprinting. Trypsin, the most commonly used protease to generate peptides for peptide mass fingerprinting, cleaves peptides at the C termini of the basic amino acid residues arginine and lysine. Because biotinylation occurs at the protonated ϵ -amino group of the lysine residue, the modification is likely to affect tryptic cleavage, leading to the generation of peptides containing a missed cleavage site. To analyze biotinylated peptides, BSA was first transferred to nitrocellulose filters and trypsinized. Subsequently, the peptides were affinity-purified and subjected to MS using the reflectron mode. Data base searches assuming complete cleavage were unable to identify BSA-derived peptides, indicating that the peptides contained cleavage sites that were not recognized by the protease. Allowing for one or two missed cleavage sites led to an increased number of identifiable peptides, with only one additional peptide having two missed cleavage sites (supplemental Fig. 2). In the subsequent bioinformatics analyses, we therefore allowed for two missed cleavage sites. BSA biotinylated with different molar ratios of sulfo-NHS-LC-biotin was excised from polyacrylamide gels, cleaved with trypsin, and subjected to MS in the reflectron mode. Together, the peptides identified contained 34 of the total 60 lysine residues and covered 56% of the BSA sequence. This coverage was the same as obtained for non-biotinylated BSA (data not shown). With increasing concentrations of the biotin derivative in the biotinylation reaction, the numbers of biotinylated peptides increased. Each of these peptides was then analyzed by MS/MS, allowing the identification of individual biotinylated lysine residues. The samples treated with higher concentrations of the biotin derivative contained more biotinylated residues. As in

TABLE 2

Biotinylation of individual lysine residues follows a concentration-dependent specific order

BSA was biotinylated with sulfo-NHS-LC-biotin at a molar excess of 1-, 10-, 20-, 40-, and 60-fold. Tryptic peptides were analyzed by MS/MS to identify biotinylated lysine residues. All lysine residues listed as biotinylated were detected in five of five analyses.

	Sulfo-NHS-LC-biotin/BSA molar ratio					Hydrogen bond formation	
	ϕ	1	10	20	40		60
Lys ³⁶				+	+	+	
Lys ¹⁰⁰					+	+	+
Lys ¹⁵⁶				+	+	+	
Lys ¹⁶⁰				+	+	+	+
Lys ²⁰⁴				+	+	+	
Lys ²¹¹			+	+	+	+	
Lys ²²⁸					+	+	+
Lys ²³⁵		+	+	+	+	+	
Lys ²⁴⁵					+	+	+
Lys ²⁶⁶					+	+	
Lys ³⁷⁴					+	+	+
Lys ⁴⁰¹			+	+	+	+	
Lys ⁴¹²					+	+	
Lys ⁴²⁰					+	+	
Lys ⁴⁵⁵		+	+	+	+	+	+
Lys ⁴⁶³					+	+	
Lys ⁴⁹⁸					+	+	
Lys ⁵⁵⁹					+	+	
Total	0	2	4	8	18	18	6

the analysis of the intact protein, the correlation between the numbers of biotinylated lysines and biotin concentration was almost linear (Table 2). The numbers of the modified lysine residues identified by MS/MS correlated with the predicted numbers after MS of the intact protein in the linear mode (Table 1). More important, when biotin concentrations below the point of maximal incorporation were used, labeling of lysine residues did not occur randomly, but at specific sites. Residues that were biotinylated with lower concentrations of the derivative were also labeled when higher concentrations were used. These observations indicate a concentration-dependent, preferential accessibility of individual residues.

Recently, Huang *et al.* (21) used hydrophilic and hydrophobic cross-linkers and subsequent MS to probe the tertiary structure of BSA. One of the cross-linkers was bis(sulfosuccinimidyl) suberate, which has a reaction mechanism similar to that of sulfo-NHS-LC-biotin. They identified a total of 20 modified lysine residues, 13 of which were also labeled with sulfo-NHS-LC-biotin in our experiments. Three of the modified residues (Lys¹³⁸, Lys¹⁴⁰, and Lys⁴⁹⁵) identified in the previous study were detected in all of our experiments, although they were non-biotinylated. One residue (Lys⁸⁸) was not detected at all in our experiments, and one residue (Lys³⁹⁹) was detected only once in its biotinylated form. Two residues (Lys⁴³⁷ and Lys⁵²³) were also biotinylated in our study, but only after exposure of BSA to high temperature (see below). We also identified five additional lysine residues (Lys³⁶, Lys¹⁰⁰, Lys²⁶⁶, Lys⁴⁹⁸, and Lys⁵⁵⁹) that had not been detected by Huang *et al.* (21), and it is therefore not possible to directly compare the labeling status in the two experiments. In conclusion, different ionization conditions (electrospray *versus* MALDI) revealed almost identical peptides, and despite the use of different modifying reagents (bis(sulfosuccinimidyl) suberate *versus* sulfo-NHS-LC-biotin), the majority of the modified residues were identical in both

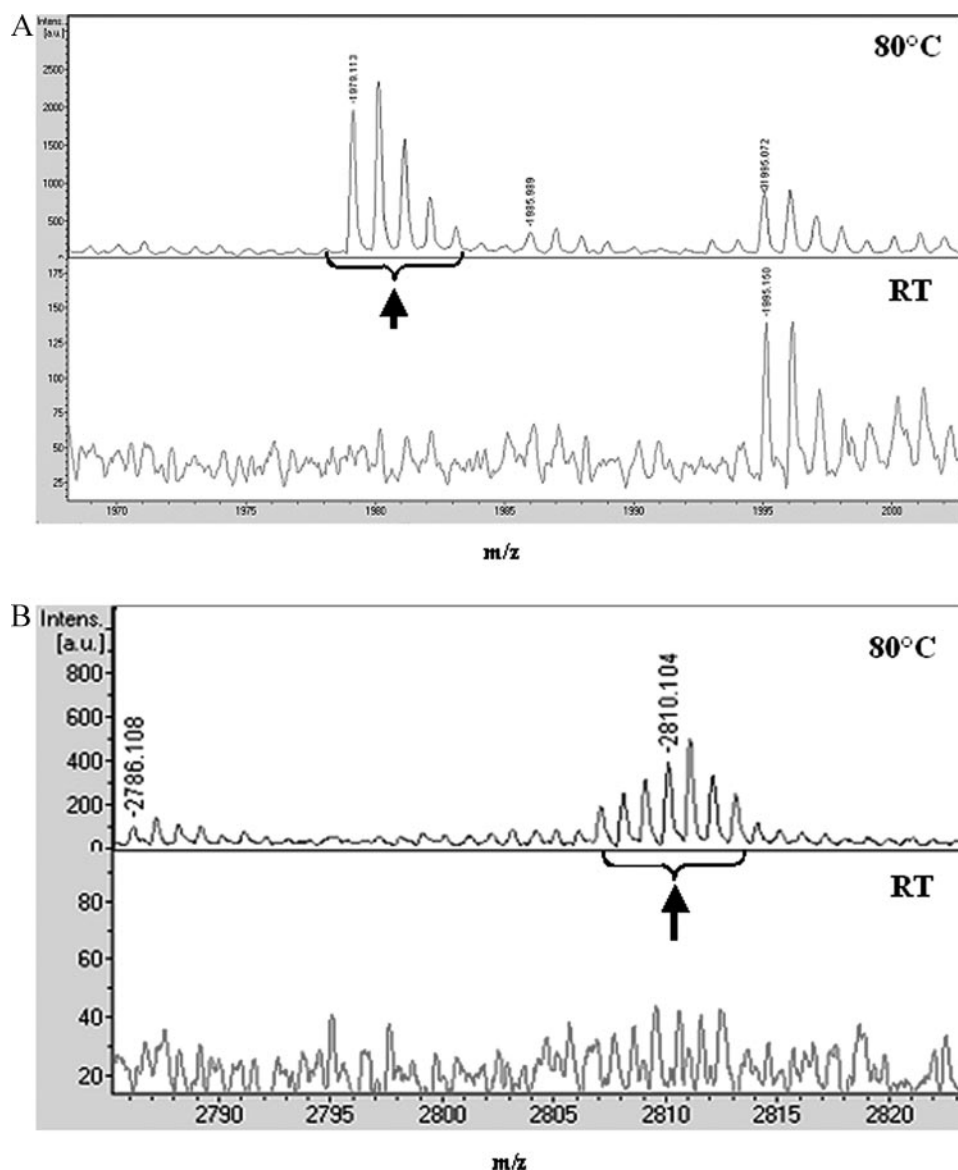


FIGURE 2. Sections of the MALDI mass spectra for BSA biotinylated with sulfo-NHS-LC-biotin after exposure to an elevated temperature of 80 °C compared with BSA biotinylated at room temperature (RT). In A, the peak at m/z 1979.113 corresponds to peptide 437–451 of BSA with sequence KVPQVSTPTLVEVSR, in which Lys⁴³⁷ is biotinylated. The arrow indicates the monoisotopic peak cluster corresponding to the biotinylated peptide. Lys⁴³⁷ is biotinylated only after BSA is exposed to 80 °C. In B, the peak at m/z 2810.100 corresponds to peptide 508–528 of BSA with sequence RPCFSALTPDETYVPKAFDEK, in which Lys⁵²³ is biotinylated. The arrow indicates the monoisotopic peak cluster corresponding to the biotinylated peptide. Lys⁵²³ is biotinylated only after BSA is exposed to 80 °C. Intens., intensity; a.u., arbitrary units.

studies, underscoring the reproducibility of the biotinylation reaction described above.

In light of a recent report (22) that lysine modification by *N*-succinimidyl propionate lacking the biotin moiety may induce conformational changes in a low molecular mass protein that is detectable by CD measurements, we investigated the possibility that the reaction between sulfo-NHS-LC-biotin and the lysine residues induces structural changes in the BSA molecule. CD spectroscopy was used to monitor changes in the structures of untreated BSA and BSA reacted with increasing molar ratios of the biotin derivative as described above. Far-UV (180–300 nm) measurements were performed at room temperature with a Jasco 810 spectrometer using 50 mM BSA in HEPES. The observed protein CD spectrum is an average of CD

signals from all structures and reflects the geometric variability in the secondary structure. There was no significant difference in the spectra of untreated BSA and BSA reacted with the biotin derivative at different molar ratios (data not shown). In all the cases, the BSA structure is predominantly composed of α -helices, and the biotinylation reaction did not induce structural changes that were detectable by CD. In comparison with the protein of the light-harvesting complex that has been analyzed in a previous study (22) and that has a maximum of two disulfide bonds, the BSA molecule forms 17 intramolecular disulfide bonds (23). We anticipate that the structural compactness of BSA is the reason why this protein does not undergo a conformational change upon biotinylation.

To obtain some structural insight into the accessibility of the lysine residues of BSA, a homology model of BSA (NCBI accession number P02769) based on the crystal structure of human serum albumin as a template was consulted (sequence identity of 76%). All lysine residues of BSA were examined with respect to a possible correlation with the following structural descriptors: (i) spatial accessibility (visual inspection and calculation of the solvent-accessible surface), (ii) involvement in a hydrogen bond along with the associated energy of these hydrogen bonds, and (iii) electrostatic potential in the close environment of the considered residues. For descriptors i and iii, no clearly evident correlation could be discovered, whereas

the involvement of a lysine residue in a hydrogen bond seems to significantly decrease the probability of biotinylation (supplemental Table 1). For BSA, only 7 of 24 lysine residues involved in a hydrogen bond reacted with sulfo-NHS-LC-biotin. However, it has to be taken into account that two of these seven lysines that do not fit the correlation are mutated in the homology model with respect to the crystallographically characterized template, thus increasing the uncertainty about their actual involvement in hydrogen bonds. To seek additional descriptors that might explain the deviating reactivity of the lysine residues involved in hydrogen bonding, we calculated the average energy of the hydrogen bonds separately for those lysines that become biotinylated and those that remain non-biotinylated. The mean energy for the non-biotinylated resi-

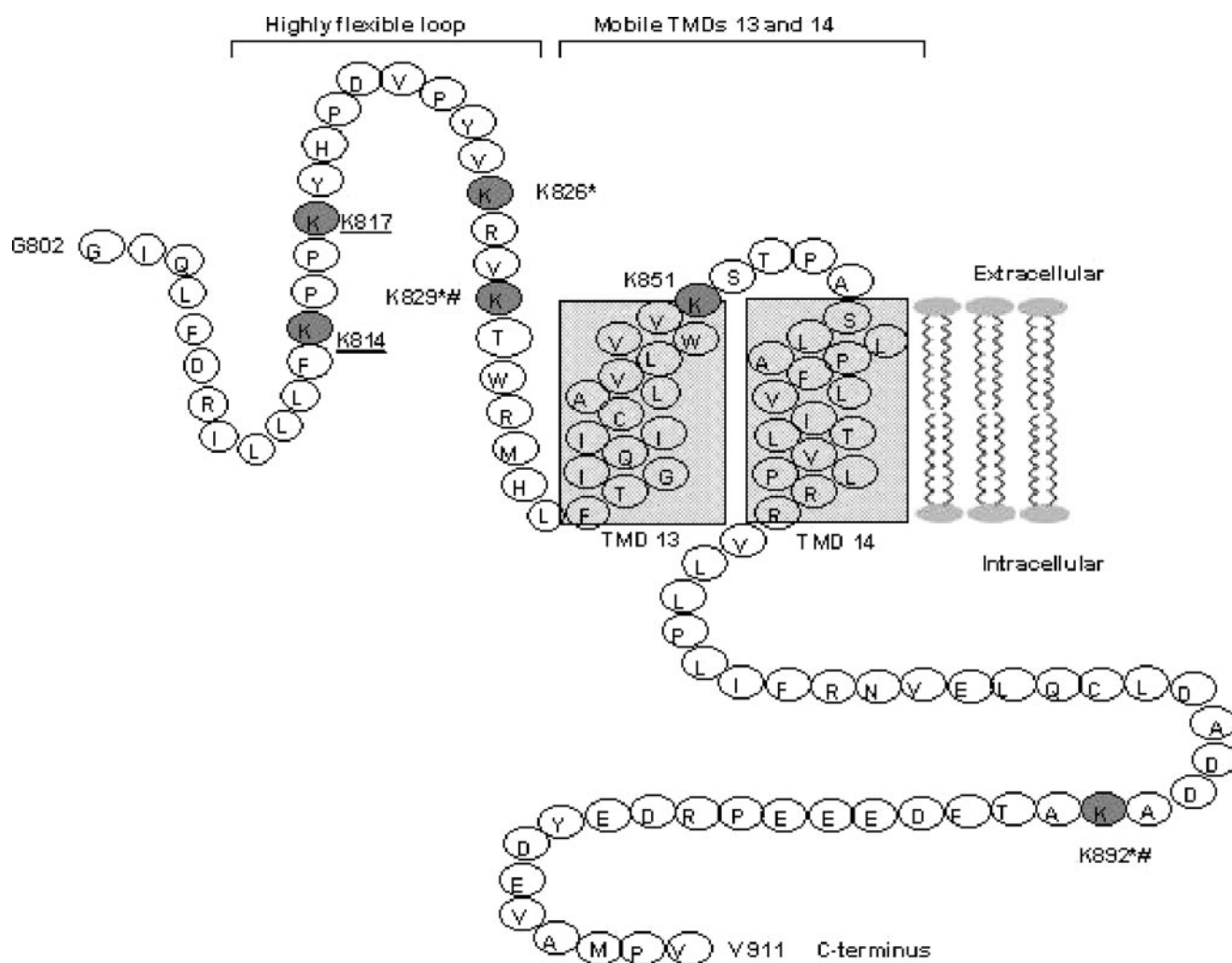


FIGURE 3. **Biotinylation pattern of the highly flexible domain of the band 3 molecule (modified from Zhu *et al.* (29)).** The underlined lysine residues Lys⁸¹⁴ and Lys⁸¹⁷ were detected in both infected and non-infected erythrocytes and were not biotinylated. Lys⁸⁵¹ was detected only in RBC and was not biotinylated. Lys⁸²⁹ and Lys⁸⁹² were detected in both RBC and iRBC and were biotinylated. Lys⁸²⁶ was detected in both RBC and iRBC but was biotinylated only in RBC, indicating that, in iRBC, this residue is not accessible to the external media. *, biotinylated lysine residue in RBC; #, biotinylated lysine residue in iRBC. TMDs, transmembrane domains.

dues is more favorable by a factor of 3 than that for those that become biotinylated (excluding Lys¹⁰⁰ and Lys²⁴⁵, which are mutated in the model with respect to the template). This rather pronounced discrimination based on the residue geometries found in the experimental structures suggests that those of the originally hydrogen-bonded lysines that are biotinylated have been involved in significantly weaker hydrogen bonds. Obviously, the participation in sufficiently strong hydrogen bonds prevents reaction with sulfo-NHS-LC-biotin, which is in accordance with previous notions that the involvement in hydrogen bonding may reduce the reactivity of lysine residues (22, 24).

Elevated Temperatures Expose Novel Lysine Residues—The highly reproducible biotinylation pattern of BSA and the obviously highly ordered accessibility of individual lysine residues prompted us to investigate whether treatments that result in conformational changes in the protein affect biotinylation patterns. BSA has a heart-shaped structure of three homologous domains that are divided into nine loops by 17 disulfide bonds (23). Heat-treated serum albumin undergoes a conformational

change that is reversible as long as the temperature does not exceed 65 °C. The conformational change induced by higher temperatures is irreversible, but does not necessarily result in the complete destruction of the ordered structure (25). In our experiments, BSA was biotinylated at room temperature and after heating at 56 or 80 °C. For BSA treated at 56 °C, MS analysis revealed the identical biotinylated peptides as detected at room temperature. At 80 °C, two additional lysine residues (Lys⁴³⁷ and Lys⁵²³) were found biotinylated by MS/MS. As both of these residues were identified as non-biotinylated in the samples treated at the lower temperatures (Fig. 2, A and B), we conclude that heating, leading to an irreversible conformational change in the protein, allows access of biotin to these residues. Lys⁵²³ is in helix 2 of subdomain IIIb of BSA (23), and we suggest that this domain undergoes a considerable and irreversible conformational change upon heating to 80 °C. It is noteworthy that both Lys⁴³⁷ and Lys⁵²³ were identified as labeled residues in the study by Huang *et al.* (21), who performed the reaction at room temperature. Although the molecular masses of sulfo-NHS-LC-biotin and bis(sulfosuccinimidyl)

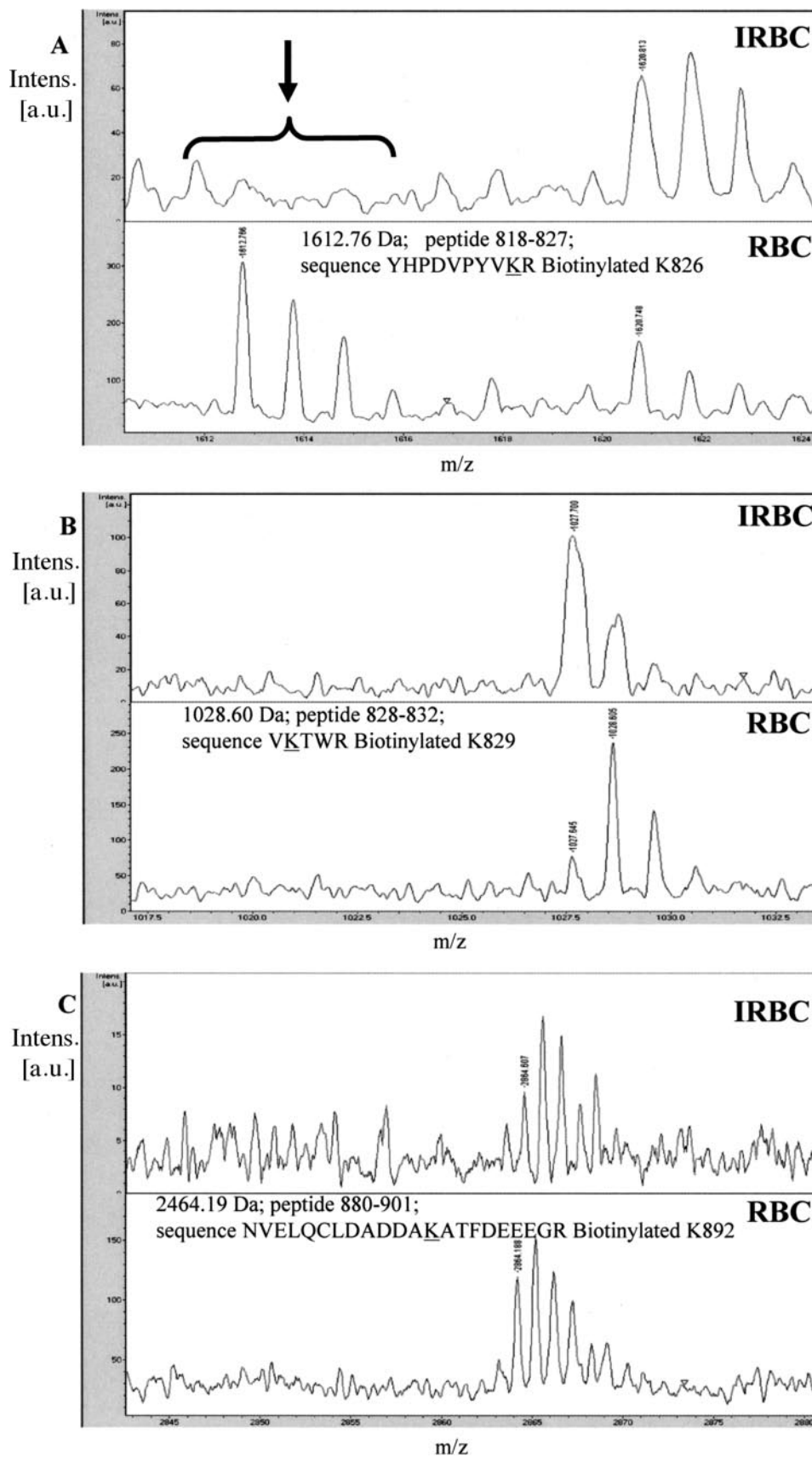


FIGURE 4. **Differential biotinylation of lysine residues of band 3 in iRBC and RBC.** Shown are enlarged sections of the MALDI mass spectra for band 3 from *P. falciparum*-infected erythrocytes and non-infected erythrocytes. In non-infected erythrocytes (RBC), Lys⁸²⁶, Lys⁸²⁹, and Lys⁸⁹² in peptides with masses 1612.76, 1027.700, and 2864.19 Da, respectively, were biotinylated. In infected erythrocytes, Lys⁸²⁹ and Lys⁸⁹² were biotinylated, but Lys⁸²⁶ was not. The arrow in A shows the absence of the biotinylated peptide in the spectra for band 3 from infected erythrocytes. *a.u.*, arbitrary units. *Intens.*, intensity.

suberate are similar (556 and 572 Da, respectively), the lengths of the spacer arms differ by ~ 2 -fold, which may explain the differential accessibility of these residues to the two compounds.

We also carried out a similar analysis on carbonic anhydrase, a 28-kDa single-domain protein with a dominating β -sheet that extends throughout the entire molecule (26). The thermal denaturation curve of carbonic anhydrase has a classical sigmoid shape with a melting temperature at 64.2 °C (27). Only minor structural changes, if any, are to be expected at this pre-transition temperature (27). Carbonic anhydrase has a total of 18 lysine residues. After biotinylation with a 40-fold molar excess of the biotin derivative at either room temperature or 56 °C, 15 lysine residues were detectable by MS, seven of which were biotinylated (supplemental Table 2). Heating the protein to 80 °C and cooling to room temperature prior to biotinylation had no effect on this pattern because of the rapid refolding of the protein.

Also in the case of bovine carbonic anhydrase II, we examined the available crystal structure for the putative accessibility of the lysine residues. The same descriptors as described above were studied. Similarly, analysis suggested a correlation between the involvement in hydrogen bonding and the decreased probability of biotinylation (supplemental Table 3). Only one of eight lysine residues involved in a hydrogen bond is biotinylated.

As shown for BSA, heating the protein increased the number of biotinylatable lysine residues without the loss of biotinylation sites accessible at low temperature. Presumably, the higher temperature resulted in a generally more open, possibly partially unfolded or denatured structure of the BSA molecule. This observation is supported by our CD spectrometry measurements showing a change in the conformation of BSA with a shift from a predominantly α -helix structure to the more open β -sheet conformation after exposure to an elevated temperature of 80 °C. However, we anticipate that conformational changes, others than those induced by elevated temperature, do not necessarily result in a gain of biotinylatable sites. Depending on the experimental circumstances, a loss of such sites, e.g. as a result of steric hindrance, is equally possible.

Comparison of the Biotinylation Patterns of Band 3 in RBC and iRBC—Biotinylation of BSA revealed a linear correlation between the molar ratio of the biotin derivative and biotinylated lysine residues until all sufficiently reactive residues were saturated. The band 3 protein is present on the erythrocyte surface at 10^6 copies/cell (28). To ensure excess of the biotin derivative, standardized numbers of either infected or non-infected cells were biotinylated using concentrations of sulfo-NHS-LC-biotin ranging from 0.5 to 2 mg/ml. The reactions were carried out in the presence of furosemide to minimize internal labeling of infected erythrocytes (4). Proteins contained in membrane fractions of erythrocytes were separated by SDS-PAGE and stained with Coomassie Blue, and the band corresponding to band 3 was excised and analyzed. As described above, in the data base searches, two missed cleavage sites per peptide were allowed. Within the chosen range, the concentration of the biotin derivative did not have an effect on the biotinylation status of individual lysine residues (data not shown).

Band 3 is a multimembrane-spanning protein with 11–14 transmembrane domains (16, 29). According to the predicted topology, five domains are exposed extracellularly. Whereas three domains are composed of fewer than 10 amino acid residues, two domains (Phe⁵⁴³–Pro⁵⁶⁸ and Glu⁶²⁶–Met⁶⁶³) are composed of 26 and 38 amino acids, respectively. One additional domain (Gly⁸⁰²–Leu⁸³⁵) is predicted to exhibit enhanced flexibility, which can vary between an extracellular and intracellular topology. Although the various models differ in details, they are consistent in that, of the total 29 lysine residues, nine residues reside in the extracellular loops, four of which are located in one of two large loops. Four additional lysine residues are found in the flexible loop.

After surface biotinylation of RBC, three lysine residues were found to be biotinylated (Fig. 3). Two of these residues (Lys⁸²⁶ and Lys⁸²⁹) are located in the prominent flexible loop, and one (Lys⁸⁹²) in a predicted intracellular domain. In contrast, in iRBC, only two lysine residues (Lys⁸²⁹ and Lys⁸⁹²) were biotinylated. Although it is conceivable that conformational changes take place only in a certain percentage of the band 3 molecules, we were unable to detect biotinylated Lys⁸²⁶ in iRBC, and conversely, peptides from RBC containing Lys⁸²⁶ were always biotinylated (Fig. 4, A–C). These results suggest that all band 3 molecules undergo a conformational change in iRBC. We have no explanation why Lys⁸⁹², which is predicted to be intracellular, was found biotinylated in both samples. The overall low sequence coverage for band 3 (30%) can be attributed to the high proportion of hydrophobic domains present in this molecule.

In conclusion, biotinylation of proteins is highly reproducible and appears to be dependent on protein conformation. Possibly the involvement of the ϵ -amino group of lysine in hydrogen bonding provides an explanation for the gradual reactivity observed for the various residues. Thus, conformational changes or alternative structural transformations in proteins lead to alternative biotinylation patterns. As shown for the band 3 molecule in non-infected and malaria parasite-infected erythrocytes, this approach allowed us to identify a differentially biotinylated lysine residue. This residue is positioned in the extracellular flexible loop in a region that is also differentially recognized in non-infected and infected erythrocytes by a monoclonal antibody (8). We suggest that surface biotinylation of intact cells followed by MS is a rapid method for identifying putative conformational changes in surface proteins, for example, following pathogen infection or under varying physiological conditions.

Acknowledgment—We thank Sandra Marx for expert technical assistance.

REFERENCES

1. Wilchek, M., and Bayer, E. A. (1990) *Methods Enzymol.* **184**, 14–45
2. Nyalwidhe, J., Baumeister, S., Hibbs, A. R., Tawill, S., Papakrivovs, J., Volker, U., and Lingelbach, K. (2002) *J. Biol. Chem.* **277**, 40005–40011
3. Kirk, K. (2001) *Physiol. Rev.* **81**, 495–537
4. Baumeister, S., Endermann, T., Charpian, S., Nyalwidhe, J., Duranton, C., Huber, S., Kirk, K., Lang, F., and Lingelbach, K. (2003) *Mol. Biochem. Parasitol.* **132**, 35–45

5. Baumeister, S., Winterberg, M., Duranton, C., Huber, S. M., Lang, F., Kirk, K., and Lingelbach, K. (2006) *Mol. Microbiol.* **60**, 493–504
6. Cohn, J. V., Alkhalil, A., Wagner, M. A., Rajapandi, T., and Desai, S. A. (2003) *Mol. Biochem. Parasitol.* **132**, 27–34
7. Frazar, T. F., Weisbein, J. L., Anderson, S. M., Cline, A. P., Garrett, L. J., Felsenfeld, G., Gallagher, P. G., and Bodine, D. M. (2003) *Mol. Cell. Biol.* **23**, 4753–4763
8. Winograd, E., and Sherman, I. W. (2004) *Mol. Biochem. Parasitol.* **138**, 83–87
9. Nyalwidhe, J., and Lingelbach, K. (2006) *Proteomics* **6**, 1563–1573
10. Bennett, K. L., Kussmann, M., Bjork, P., Godzwon, M., Mikkelsen, M., Sorensen, P., and Roepstorff, P. (2000) *Protein Sci.* **9**, 1503–1518
11. Young, M. M., Tang, N., Hempel, J. C., Oshiro, C. M., Taylor, E. W., Kuntz, I. D., Gilson, B. W., and Dollinger, G. (2000) *Proc. Natl. Acad. Sci. U. S. A.* **97**, 5802–5806
12. Back, J. W., Notenboom, V., Koning, L. J., Muijsers, A. O., Sixma, T. K., Koster, C. G., and Jong, L. (2002) *Anal. Chem.* **74**, 4417–4422
13. Trager, W., and Jensen, J. B. (1976) *Science* **193**, 673–675
14. Pasvol, G., Wilson, R. J., Smalley, M. E., and Brown, J. (1978) *Ann. Trop. Med. Parasitol.* **72**, 87–88
15. Hellman, U., Wernstedt, C., Gonez, J., and Heldin, C. H. (1995) *Anal. Biochem.* **224**, 451–455
16. Popov, M., Li, J., and Reithmeier, R. A. (1999) *Biochem. J.* **339**, 269–279
17. Kopp, J., and Schwede, T. (2004) *Nucleic Acids Res.* **32**, D230–D234
18. Ahmad, S., Gromiha, M., Fawareh, H., and Sarai, A. (2004) *BMC Bioinformatics* **5**, 51
19. Tripos Inc. (2005) *SYBYL Molecular Modeling Package*, Tripos Inc., St. Louis, MO
20. Gerber, P. R., and Muller, K. (1995) *J. Comput. Aided Mol. Des.* **9**, 251–268
21. Huang, B. X., Kim, H. Y., and Dass, C. (2004) *J. Am. Soc. Mass Spectrom.* **15**, 1237–1247
22. Gao, J.-P., Zhang, F., Zhang, L., Guo, Y. L., Ruan, K.-C., Jiang, D., and Xu, C.-H. (2006) *Acta Biochim. Biophys. Sin.* **38**, 611–619
23. Carter, D. C., and Ho, J. X. (1994) *Adv. Protein Chem.* **45**, 153–203
24. Baker, E. N., and Hubbard R. E. (1984) *Prog. Biophys. Mol. Biol.* **44**, 97–179
25. Wetzel, R., Becker, M., Behlke, J., Billwitz, H., Bohm, S., Ebert, B., Hamann, H., Krumbiegel, J., and Lassmann, G. (1980) *Eur. J. Biochem.* **104**, 469–478
26. Hakansson, K., Carlsson, M., Svensson, L. A., and Liljas, A. (1992) *J. Mol. Biol.* **227**, 1192–1204
27. Sarraf, N. S., Saboury, A. A., Ranjbar, B., and Moosavi-Movahedi, A. A. (2004) *Acta Biochim. Pol.* **51**, 665–671
28. Fairbanks, G., Steck, T. L., and Wallach, D. F. (1971) *Biochemistry* **10**, 2606–2617
29. Zhu, Q., Lee, D. W., and Casey, J. R. (2003) *J. Biol. Chem.* **278**, 3112–3120